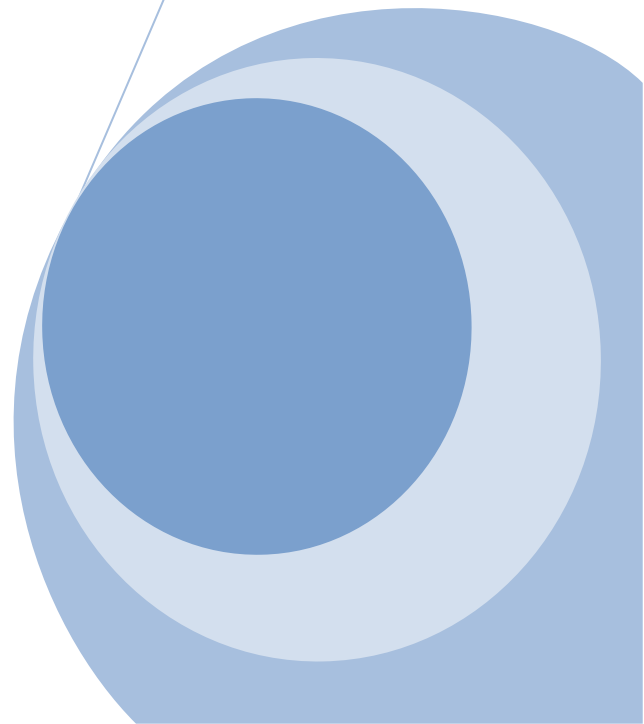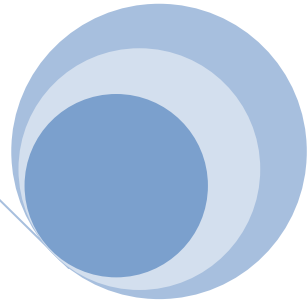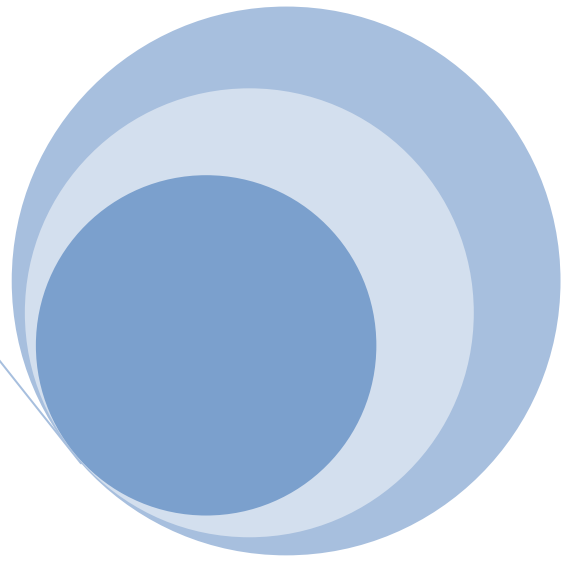# CHAPTER # 1

Introduction

1.1 __Composites__

A composite is commonly defined as a combination of two or more distinct materials, each of which retains its own distinctive properties, to create a new material with properties that cannot be achieved by any of the components acting alone. Using this definition, it can be determined that a wide range of engineering materials fall into this category. For example, concrete is a composite because it is a mixture of Portland cement and aggregate. Fiberglass sheet is a composite since it is made of glass fibers imbedded in a polymer.

Composite materials are said to have two phases. The reinforcing phase is the fibers, sheets, or particles that are embedded in the matrix phase. The reinforcing material and the matrix material can be metal, ceramic, or polymer. Typically, reinforcing materials are strong with low densities while the matrix is usually a ductile, or tough, material.

Figure 1.1   Applications of composite material

Some of the common classifications of composites are:
- Reinforced plastics
- Metal-matrix composites
- Ceramic-matrix composites
- Sandwich structures
- Concrete

Composite materials can take many forms but they can be separated into three categories based on the strengthening mechanism. These categories are dispersion strengthened, particle reinforced and fiber reinforced. Dispersion strengthened composites have a fine distribution of secondary particles in the matrix of the material. These particles impede the mechanisms that allow a material to deform. (These mechanisms include dislocation movement and slip, which will be discussed later). Many metal-matrix composites would fall into the dispersion strengthened composite category. Particle reinforced composites have a large volume fraction of particle dispersed in the matrix and the load is shared by the particles and the matrix. Most commercial ceramics and many filled polymers are particle-reinforced composites. In fiber-reinforced composites, the fiber is the primary load-bearing component. Fiberglass and carbon fiber composites are examples of fiber-reinforced composites.(1,2,11)

If the composite is designed and fabricated correctly, it combines the strength of the reinforcement with the toughness of the matrix to achieve a combination of desirable properties not available in any single conventional material. Some composites also offer the advantage of being tailor able so that properties, such as strength and stiffness, can easily be changed by changing amount or orientation of the reinforcement material. The downside is that such composites are often more expensive than conventional materials.

Composite material is a material composed of two or more distinct <u>phases</u> (matrix and dispersed phase) and having bulk properties significantly different form those of any of the constituents.

- <u>Matrix phase:</u>

The primary phase, having a continuous character, is called matrix. Matrix is usually more <u>ductile</u> and less hard phase. It holds the dispersed phase and shares a load with it.

- <u>Dispersed (reinforcing) phase:</u>

The second phase (or phases) is embedded in the matrix in a discontinuous form. This secondary phase is called dispersed phase. Dispersed phase is usually stronger than the matrix, therefore it is sometimes called reinforcing phase.

Many of common materials (<u>metal</u> <u>alloys</u>, doped <u>Ceramics</u> and <u>Polymers</u> mixed with additives) also have a small amount of dispersed phases in their structures, however they are not considered as composite materials since their properties are similar to those of their base constituents (<u>physical properties</u> of <u>steel</u> are similar to those of pure iron).

There are two classification systems of composite materials. One of them is based on the matrix material (metal, ceramic, polymer) and the second is based on the material structure. (1)

1.1.1 Classification of composites Based on Matrix

- *Metal Matrix Composites (MMC):*

<u>Metal Matrix Composites</u> are composed of a metallic matrix (<u>aluminum</u>, magnesium, iron, cobalt, <u>copper</u>) and a dispersed ceramic (<u>oxides</u>, <u>carbides</u>) or metallic (lead, tungsten, molybdenum) phase.

- *Ceramic Matrix Composites (CMC):*

<u>Ceramic Matrix Composites</u> are composed of a ceramic matrix and embedded fibers of other ceramic material (dispersed phase).

- *Polymer Matrix Composites (PMC):*

<u>Polymer Matrix Composites</u> are composed of a matrix from <u>thermoset</u> (<u>Unsaturated Polyester (UP)</u>, <u>Epoxiy (EP)</u>) or <u>thermoplastic</u> (<u>Polycarbonate (PC)</u>, <u>Polyvinylchloride</u>, <u>Nylon</u>, Polysterene) and embedded glass, <u>carbon</u>, steel or Kevlar fibers (dispersed phase).

1.1.2 Classification of composite materials based on reinforcment

- <u>Particulate Composites</u>

Particulate Composites consist of a matrix reinforced by a dispersed phase in form of particles.
1. Composites with random orientation of particles.
2. Composites with preferred orientation of particles.

Dispersed phase of these materials consists of two-dimensional flat platelets (flakes), laid parallel to each other.

- • Fibrous Composites
1. Short-fiber reinforced composites. Short-fiber reinforced composites consist of a matrix reinforced by a dispersed phase in form of discontinuous fibers (length < 100*diameter).
    a) Composites with random orientation of fibers.
    b) Composites with preferred orientation of fibers.
2. Long-fiber reinforced composites. Long-fiber reinforced composites consist of a matrix reinforced by a dispersed phase in form of continuous fibers.
    a) Unidirectional orientation of fibers.
    b) Bidirectional orientation of fibers (woven).
- • Laminate Composites

When a fiber reinforced composite consists of several layers with different fiber orientations, it is called multilayer (angle-ply) composite.(2,11)

1.2 **Stress and Strain**

1.2.1 Stress

The term stress (s) is used to express the loading in terms of force applied to a certain cross-sectional area of an object. From the perspective of loading, stress is the applied force or system of forces that tends to deform a body. From the perspective of what is happening within a material, stress is the internal distribution of forces within a body that balance and react to the loads applied to it. The stress distribution may or may not be uniform, depending on the nature of the loading condition. For example, a bar loaded in pure tension will essentially have a uniform tensile stress distribution. However, a bar loaded in bending will have a stress distribution that changes with distance perpendicular to the normal axis.

Simplifying assumptions are often used to represent stress as a vector quantity for many engineering calculations and for material property determination. The word *"vector"* typically refers to a quantity that has a "magnitude" and a "direction". For example, the stress in an axially loaded bar is simply equal to the applied force divided by the bar's cross-sectional area.
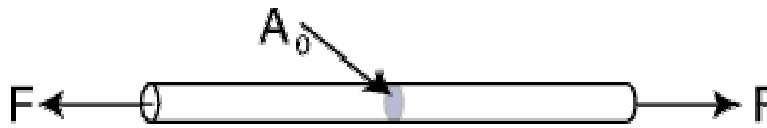

$$\text{Stress, } \sigma = \frac{\text{Force}}{\text{Cross-Sectional Area}} = \frac{F}{A_0}$$

Figure 1.2   Measurement of stress

Some common measurements of stress are:

- Psi = lbs/in^2 (pounds per square inch)
- ksi or kpsi = kilopounds/in^2 (one thousand or 10^3 pounds per square inch)
- Pa = N/m 2 (Pascals or Newtons per square meter)
- kPa = Kilopascals (one thousand or 10^3 Newtons per square meter)
- GPa = Gigapascals (one million or 10^6 Newtons per square meter)

Any metric prefix can be added in front of psi or Pa to indicate the multiplication factor It must be noted that the stresses in most 2-D or 3-D solids are actually more complex and need be defined more methodically. The internal force acting on a small area of a plane can be resolved into three components: one normal to the plane and two parallel to the plane.
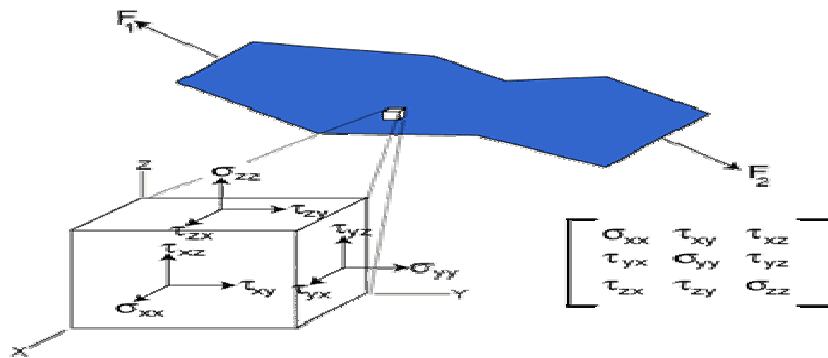

Figure1.3   Three dimensional stress

The normal force component divided by the area gives the normal stress (s), and parallel force components divided by the area give the shear stress (t). These stresses are average stresses as the area is finite, but when the area is allowed to approach zero, the stresses become stresses at a point. Since stresses are defined in relation to the plane that passes through the point under consideration, and the number of such planes is infinite, there appear an infinite set of stresses at a point. Fortunately, it can be proven that the stresses on any plane can be computed from the stresses on three orthogonal planes passing through the point. As each plane has three stresses, the stress tensor has nine stress components, which completely describe the state of stress at a point. (6,7)

1.2.2 Strain

Strain is the response of a system to an applied stress. When a material is loaded with a force, it produces a stress, which then causes a material to deform. Engineering strain is defined as the amount of deformation in the direction of the applied force divided by the initial length of the material. This results in a unitless number, although it is often left in the unsimplified form, such as inches per inch or meters per meter. For example, the strain in a bar that is being stretched in tension is the amount of elongation or change in length divided by its original length. As in the case of stress, the strain distribution may or may not be uniform in a complex structural element, depending on the nature of the loading condition.

$$\text{Strain} = \frac{\text{Elongation}}{\text{Orininal Length}} = \frac{\Delta L}{L_0}$$
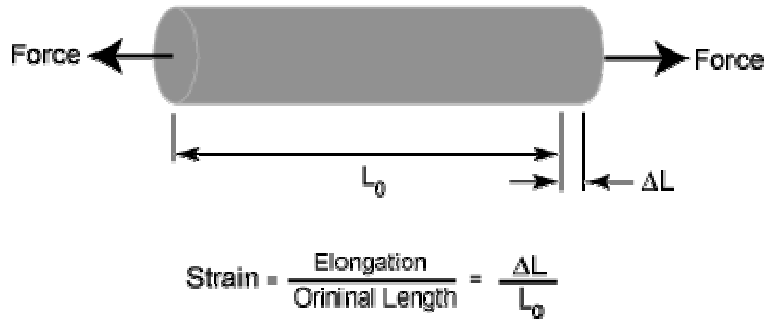
Figure 1.4   Measurement of strain

If the stress is small, the material may only strain a small amount and the material will return to its original size after the stress is released. This is called elastic deformation, because like elastic it returns to its unstressed state. Elastic deformation only occurs in a material when stresses are lower than a critical stress called the yield strength. If a material is loaded beyond it elastic limit, the material will remain in a deformed condition after the load is removed. This is called plastic deformation. (1,2,6,7)

1.2.3 Engineering and True Stress and Strain

The discussion above focused on engineering stress and strain, which use the fixed, undeformed cross-sectional area in the calculations. True stress and strain measures account for changes in cross-sectional area by using the instantaneous values for the area. The engineering stress-strain curve does not give a true indication of the deformation characteristics of a metal because it is based entirely on the original dimensions of the specimen, and these dimensions change continuously during the testing used to generate the data.
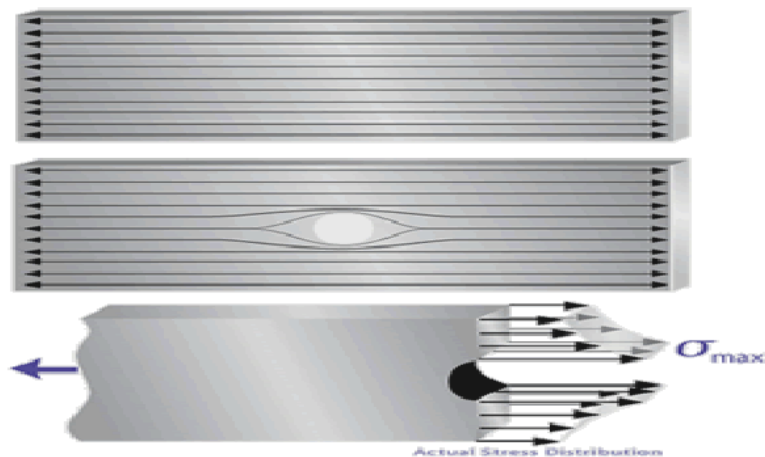

Figure 1.5   Stress concentration due to cavity

Engineering stress and strain data is commonly used because it is easier to generate the data and the tensile properties are adequate for engineering calculations. When considering the stress-strain curves in the next section, however, it should be understood that metals and other materials continues to strain-harden until they fracture and the stress required to produce further deformation also increase. (7,2)

1.2.4 Stress Concentration

When an axial load is applied to a piece of material with a uniform cross-section, the norm al stress will be uniformly distributed over the cross-section. However, if a hole is drilled in the material, the stress distribution will no longer be uniform. Since the material that has been removed from the hole is no longer available to carry any load, the load must be redistributed over the remaining material. It is not redistributed evenly over the entire remaining cross-sectional area but instead will be redistributed in an uneven pattern that is highest at the edges of the hole as shown in the image. This phenomenon is known as stress concentration. (6,1)

1.2.5 Tensile Properties

Tensile properties indicate how the material will react to forces being applied in tension. A tensile test is a fundamental mechanical test where a carefully prepared specimen is loaded in a very controlled manner while measuring the applied load and the elongation of the specimen over some distance. Tensile tests are used to determine the modulus of elasticity, elastic limit, elongation, proportional limit, reduction in area, tensile strength, yield point, yield strength and other tensile properties.

The main product of a tensile test is a load versus elongation curve which is then converted into a stress versus strain curve. Since both the engineering stress and the engineering strain are obtained by dividing the load and elongation by constant values (specimen geometry information), the load-elongation curve will have the same shape as the engineering stress-strain curve. The stress-strain curve relates the applied stress to the resulting strain and each material has its own unique stress-strain curve. A typical engineering stress-strain curve is shown below. If the true stress, based on the actual cross-sectional area of the specimen, is used, it is found that the stress-strain curve increases continuously up to fracture.
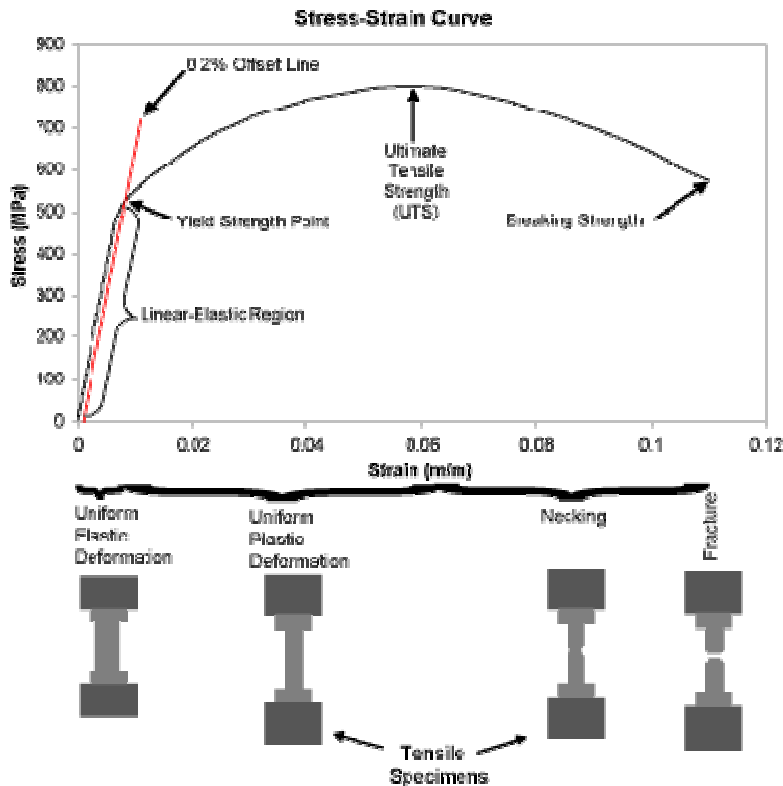
Figure 1.6   Stress strain curve behaviour

1.2.6 Linear-Elastic Region and Elastic Constants

As can be seen in the figure, the stress and strain initially increase with a linear relationship. This is the linear-elastic portion of the curve and it indicates that no plastic deformation has occurred. In this region of the curve, when the stress is reduced, the material will return to its original shape. In this linear region, the line obeys the relationship defined as Hooke's Law where the ratio of stress to strain is a constant.

The slope of the line in this region where stress is proportional to strain and is called the modulus of elasticity *or* Young's modulus. The modulus of elasticity (E) defines the properties of a material as it undergoes stress, deforms, and then returns to its original shape after the stress is removed. It is a measure of the stiffness of a given material. To compute the modulus of elastic , simply divide the stress by the strain in the material. Since strain is unitless, the modulus will have the same units as the stress, such as kpi or MPa. The modulus of elasticity applies specifically to the situation of a component being stretched with a tensile force. This modulus is of interest when it is necessary to compute how much a rod or wire stretches under a tensile load. There are several different kinds of moduli depending on the way the material is being stretched, bent, or otherwise distorted. When a component is subjected to pure shear, for instance, a cylindrical bar under torsion, the shear modulus describes the linear-elastic stress-strain relationship. (7,14)

8

Axial strain is always accompanied by lateral strains of opposite sign in the two directions mutually perpendicular to the axial strain. Strains that result from an increase in length are designated as positive (+) and those that result in a decrease in length are designated as negative (-). Poisson's ratio is defined as the negative of the ratio of the lateral strain to the axial strain for a uniaxial stress state.

$$v = -\frac{\varepsilon_{lateral}}{\varepsilon_{axial}}$$

Poisson's ratio is sometimes also defined as the ratio of the absolute values of lateral and axial strain. This ratio, like strain, is unitless since both strains are unitless. For stresses within the elastic range, this ratio is approximately constant. For a perfectly isotropic elastic material, Poisson's Ratio is 0.25, but for most materials the value lies in the range of 0.28 to 0.33. Generally for steels, Poisson's ratio will have a value of approximately 0.3. This means that if there is one inch per inch of deformation in the direction that stress is applied, there will be 0.3 inches per inch of deformation perpendicular to the direction that force is applied.

Only two of the elastic constants are independent so if two constants are known, the third can be calculated using the following formula:

$$E = 2 (1 + n) G.$$

Where: E = modulus of elasticity (Young's modulus)

n = Poisson's ratio

G = modulus of rigidity (shear modulus).

A couple of additional elastic constants that may be encountered include the bulk modulus (K), and Lame's constants (m and l). The bulk modulus is used describe the situation where a piece of material is subjected to a pressure increase on all sides. The relationship between the change in pressure and the resulting strain produced is the bulk modulus. Lame's constants are derived from modulus of elasticity and Poisson's ratio. (2,7,16)

1.2.7 Yield Point

In ductile materials, at some point, the stress-strain curve deviates from the straight-line relationship and Law no longer applies as the strain increases faster than the stress. From this point on in the tensile test, some permanent deformation occurs in the specimen and the material is said to react plastically to any further increase in load or stress. The material will not return to its original, unstressed condition when the load is removed. In brittle materials, little or no plastic deformation occurs and the material fractures near the end of the linear-elastic portion of the curve.

With most materials there is a gradual transition from elastic to plastic behavior, and the exact point at which plastic deformation begins to occur is hard to determine. Therefore, various criteria for the initiation of yielding are used depending on the sensitivity of the strain

measurements and the intended use of the data. For most engineering design and specification applications, the yield strength is used. The yield strength is defined as the stress required to produce a small, amount of plastic deformation. The offset yield strength is the stress corresponding to the intersection of the stress-strain curve and a line parallel to the elastic part of the curve offset by a specified strain (in the US the offset is typically 0.2% for metals and 2% for plastics).

To determine the yield strength using this offset, the point is found on the strain axis (x-axis) of 0.002, and then a line parallel to the stress-strain line is drawn. This line will intersect the stress-strain line slightly after it begins to curve, and that intersection is defined as the yield strength with a 0.2% offset. A good way of looking at offset yield strength is that after a specimen has been loaded to its 0.2 percent offset yield strength and then unloaded it will be 0.2 percent longer than before the test. Even though the yield strength is meant to represent the exact point at which the material becomes permanently deformed, 0.2% elongation is considered to be a tolerable amount of sacrifice for the ease it creates in defining the yield strength.

Some materials such as gray cast iron or soft copper exhibit essentially no linear-elastic behavior. For these materials the usual practice is to define the yield strength as the stress required to produce some total amount of strain. (6,17)

- True elastic limit is a very low value and is related to the motion of a few hundred dislocations. Micro strain measurements are required to detect strain on order of 2 x 10 -6 in/in.
- Proportional limit is the highest stress at which stress is directly proportional to strain. It is obtained by observing the deviation from the straight-line portion of the stress-strain curve.
- Elastic limit is the greatest stress the material can withstand without any measurable permanent strain remaining on the complete release of load. It is determined using a tedious incremental loading-unloading test procedure. With the sensitivity of strain measurements usually employed in engineering studies (10 -4in/in), the elastic limit is greater than the proportional limit. With increasing sensitivity of strain measurement, the value of the elastic limit decreases until it eventually equals the true elastic limit determined from micro strain measurements.
- Yield strength is the stress required to produce a small-specified amount of plastic deformation. The yield strength obtained by an offset method is commonly used for engineering purposes because it avoids the practical difficulties of measuring the elastic limit or proportional limit.

1.3   Ultimate Tensile Strength

The ultimate tensile strength (UTS) or, more simply, the tensile strength, is the maximum engineering stress level reached in a tension test. The strength of a material is its ability to withstand external forces without breaking. In brittle materials, the UTS will at the end of the linear-elastic portion of the stress-strain curve or close to the elastic limit. In ductile materials, the UTS will be well outside of the elastic portion into the plastic portion of the stress-strain curve.

On the stress-strain curve above, the UTS is the highest point where the line is momentarily flat. Since the UTS is based on the engineering stress, it is often not the same as the

breaking strength. In ductile materials strain hardening occurs and the stress will continue to increase until fracture occurs, but the engineering stress-strain curve may show a decline in the stress level before fracture occurs.
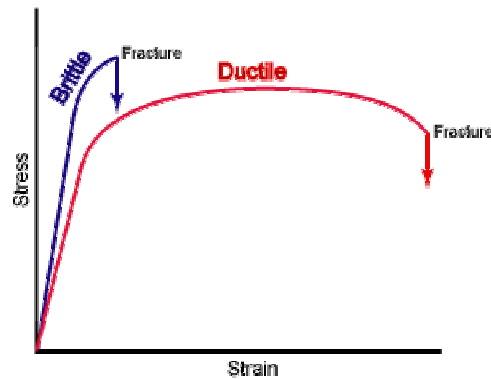

Figure 1.7   Deformation behaviors of ductile and brittle materials

This is the result of engineering stress being based on the original cross-section area and not accounting for the necking that commonly occurs in the test specimen. The UTS may not be completely representative of the highest level of stress that a material can support, but the value is not typically used in the design of components anyway. For ductile metals the current design practice is to use the yield strength for sizing static components. However, since the UTS is easy to determine and quite reproducible, it is useful for the purposes of specifying a material and for quality control purposes. On the other hand, for brittle materials the design of a component may be based on the tensile strength of the material. (2,7,16)

1.4   Measures of Ductility (Elongation and Reduction of Area)

The ductility of a material is a measure of the extent to which a material will deform before fracture. The amount of ductility is an important factor when considering forming operations such as rolling and extrusion. It also provides an indication of how visible overload damage to a component might become before the component fractures. Ductility is also used a quality control measure to assess the level of impurities and proper processing of a material.

The conventional measures of ductility are the engineering strain at fracture (usually called the elongation) and the reduction of area at fracture. Both of these properties are obtained by fitting the specimen back together after fracture and measuring the change in length and cross-sectional area. Elongation is the change in axial length divided by the original length of the specimen or portion of the specimen. It is expressed as a percentage. Because an appreciable fraction of the plastic deformation will be concentrated in the necked region of the tensile specimen, the value of elongation will depend on the gage length over which the measurement is taken. The smaller the gage length the greater the large localized strain in the necked region will factor into the calculation. Therefore, when reporting values of elongation , the gage length should be given.

One way to avoid the complication from necking is to base the elongation measurement on the uniform strain out to the point at which necking begins. This works well at times but some

engineering stress-strain curve are often quite flat in the vicinity of maximum loading and it is difficult to precisely establish the strain when necking starts to occur.

Reduction of area is the change in cross-sectional area divided by the original cross-sectional area. This change is measured in the necked down region of the specimen. Like elongation, it is usually expressed as a percentage.

As previously discussed, tension is just one of the way that a material can be loaded. Other ways of loading a material include compression, bending, shear and torsion, and there are a number of standard tests that have been established to characterize how a material performs under these other loading conditions.(7)

1.5   Notch-Toughness

Notch toughness is the ability that a material possesses to absorb energy in the presence of a flaw. As mentioned previously, in the presence of a flaw, such as a notch or crack, a material will likely exhibit a lower level of toughness. When a flaw is present in a material, loading induces a triaxial tension stress state adjacent to the flaw. The material develops plastic strains as the yield stress is exceeded in the region near the crack tip. However, the amount of plastic deformation is restricted by the surrounding material, which remains elastic. When a material is prevented from deforming plastically, it fails in a brittle manner.

Notch-toughness is measured with a variety of specimens such as the Charpy V-notch impact specimen or the dynamic tear test specimen. As with regular impact testing the tests are often repeated numerous times with specimens tested at a different temperature. With these specimens and by varying the loading speed and the temperature, it is possible to generate curves such as those shown in the graph. Typically only static and impact testing is conducted but it should be recognized that many components in service see intermediate loading rates in the range of the dashed red line.(6)
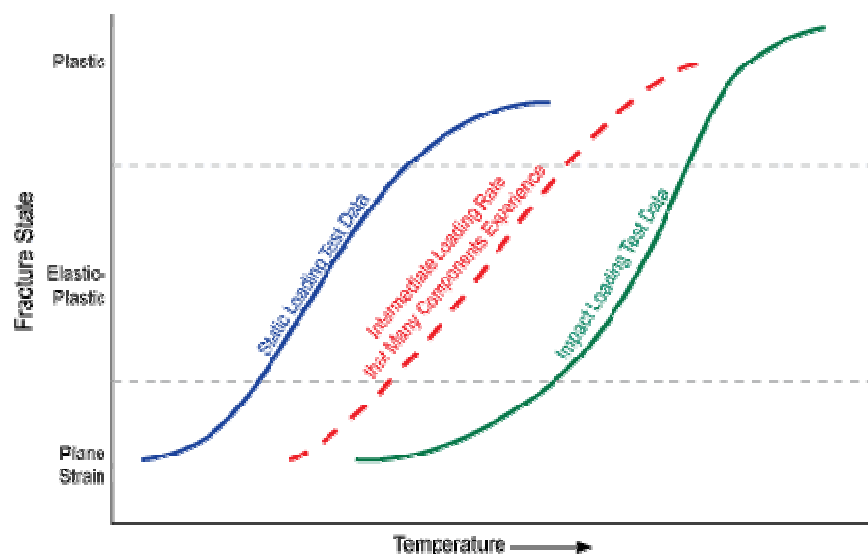

Figure 1.8   Fracture test versus temperature plot of different loading regimes

12

CHAPTER # 2

Literature review

2.1 Mechanical Properties of Materials

2.1.1 The Tensile Test:

In this chapter we will discuss the methods of analyzing the stress distribution produced by various kinds of force on structures. Knowing the stresses, the designer must then select the material and te dimensions of the structure in such a way that it will safely withstand various loading conditions in service. For this purpose it is necessary to have information regarding the elastic properties and strength characteristics of structural materials under various stress conditions. The designer must know the limits under which the material can be considered as perfectly elastic for various stress conditions and also the behaviour of the material beyond those limits . informations of this type can be obtained only by experimental investigations. Materials-testing laboratories are equipped with testing machines which produce certain typical deformation of test specimens, such as tension , compressed , torsion and bending.(16,18)

Expriements show that test result are sometimes affected by the size and shape of the test specimen. Thus to mae the result of tests compareable ,certain proportion for test specimens have been established and are recognized as standard. The most widely used of all mechanical tests of structural materials is undoubtedly the tension test . the standard tensile test . the standard tensile test specimen in the united states is circular , with 1.5 in. diameter and 2 in. gage length, so that .

$$L\,/d = 4 \ \ or \ l \ = 4.51\sqrt{A} \hspace{2cm} (a)$$

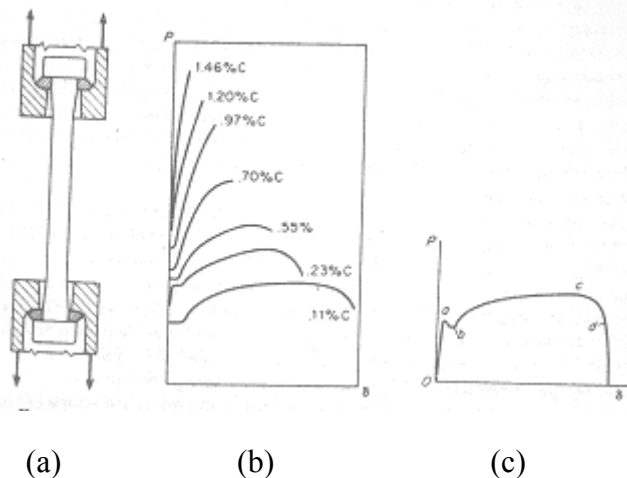Where $A = \Pi d2\,/4$ is cross sectional area of the specimen.

(a) (b) (c)

Figure 2.1 (a) A cylindrical specimen grip in machine show central load application (b) series of tensile diagramsof carbon steel with various contents of carbons (c) tensile test diagram of mild steel

The length of the cylindrical portion of the specimen is always somewhat greater than the gage length l and is usually at least l+d. The ends of the specimen are generally made with a large cross-section in order to prevent the specimen from breaking in the grips of the testing machine , where stress condition arc more serve because of local irregularities in stress distribution. A cylindrical specimen with l = 10d is shown in figure 2.1(a) which also shows the spherical seats in the grips of the machine , used to insure central application of the load.

Tensile test machines are usually provided with a device which automatically draws a tensile test diagram representing the relation between the load P and the extension δ of the specimen. Such a diagram exhibits important characteristic of material. Figure 2.1(b) for example shows a series of tensile test diagrams for carbon steel with various contents of carbon. It can be seen that as the carbon content increases, but at the same time the elongation before fracture decreases and the material has less ductility. High carbon steel is relative brittle. It follows Hook's law up to the high value of stress and then fractures at a very small elongation. On the other hand, mild steel with small carbon content is ductile and stretches considerably before fracture.(21)

Figure 2.1(c) represents the tensile test diagram for mild structural steel. From this diagram the important characteristics such as yield point, ultimate strength, and amount of plastic elongation can be obtained.

In determining the proportional limit, sensitive extensometers are necessary in order to detect the slightest deviation from a straight line in the tensile test diagram. Obviously the position found for this limit depends considerably on sensitivity of the instruments. In order to obtain greater uniformity in results, a specified amount of permanent set or a certain deviation from proportionality is often taken as the basis for determining the proportional limit as the tensile stress at which the permanent set is 0.001 percent.

The yield point is a very important characteristic for structural steel .At the yield point stress, the specimen elongates a considerable amount with out any increase in load. In the case of mild steel this elongation may be more than 2 percent. Sometime yielding is accompanied by an abrupt decrease in load , and the tensile test diagram has the shape shown in figure 2.1(c) .In such a case the upper and lower limits of the load at a and b , divided by the initial cross sectional area ,are called the upper and lower yield points respectively. The position of the upper yield point is affected by the speed of testing, by the form of the specimen and by the shape of the cross section. The lower yield point is usually considered a true characteristic of the material and therefore is used as a basis for determining working stresses.

Owning to the relatively large stretching of the material at the yield point it is not necessary to use sensitive extensometers to determine this point. It can be determine with the simplest instruments or can be taken directly from the tensile test diagram. For structural carbon steel the stress at the yield point is about 55 – 60 percent of the ultimate strength. Structural steel with about 1 percent silicon has a yield point stress about 70 -8- percent of ultimate strength. The

ultimate strength of silicon steel is about the same as for the carbon steel. Such a high value for the yield point justifies the usual practice of taking higher working stresses for silicon steel.

A sharply defined yield point is a characteristic not only of structural steel but also of material such as bronze and brass. There are other materials, however, which do not have a pronounced yield point. For these materials stress at which the permanent set reaches the values 0.2 percent is sometimes arbitrarily called the yield point. It must be kept in mind that the yield point defined in this manner does not represent a definite physical characteristic of the material but depends upon the arbitrarily chosen permanent set.(24,25)

The ultimate strength is usually defined as the stress obtained by dividing the maximum load on the specimen (point c in figure 2.1(c)) by the initial cross-sectional area. This quantity also is often taken as a basis for determining the working stresses.

The area under the tensile test diagram Oacde figure 2.1 (c) represents the work required to produce fracture. This quantity is also used as characteristics properties of the material and depends not only on the strength but also on the ductility of the material.

The ductility of the metal is usually considered to be characterized by the elongation of the gage length of the specimen during a tensile test and by the reduction in area of the cross-section where fracture occurs. In the first stage of plastic elongation, from a to c in figure 2.1(c), the specimen remains practically constant. This uniform elongation is accompanied by a uniform lateral contraction, so that the volume of the specimen remains practically constant. At point c the tensile force reaches a maximum value, and further extension of the specimen is accompanied by a decrease in the load. At this stage of plastic elongation the deformation becomes localized and necking begins, the specimen taking the shape shown in figure 2.2.
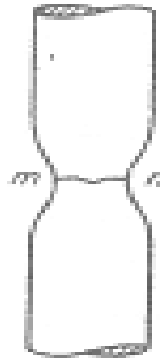
Figure 2.2 In plastic elongation deformation start by necking formation in sample

It is difficult to determine accurately the amount when necking begins and thereby establish separately the magnitudes of the uniform stretching and the magnitude of the elongation due to necking. It is therefore customary to measure the total increase in the gage length after the specimen has fractured. The elongation is then defined as the ratio of this total elongation of the gage length to initial length. In practice the elongation at fracture is usually

given in percentage. If l is the original gage length and δ the total elongation at failure in percentage is

$$\epsilon = \delta/l \cdot 100 \qquad\qquad (a)$$

This elongation is usually taken as a measure of the ductility of the material. Elongation obtained in the manner depends on the proportions of the specimen. The increase in the gage length due to necking is a large part of the total increase and is practically the same for a short gage length. Hence the elongation defined with above equation.11.1becomes larger as the gage length decrease. For steel , the elongation obtained for specimens with l=5d is about 1.22 times the elongation for a specimen of the same material with $l = 10$ d.

Experiment also shows that the shape of the cross-section affects the elongation of the specimen. This shows that comparable result with respect to elongation can be obtained only by using geometrically similar specimen.(21.23,24)

The reduction in area at the cross-section of fracture is expressed as follows:

$$q = (A_o - A_1)/ A_o \qquad\qquad (b)$$

In which A_o is the initial cross-sectional area and A_1 is the final cross-sectional area at the section where fracture occurs.

2.1.2 Yield point

The early portion of the tensile test diagram figure 2.2is shown to a larger scale in figure 2.3 ,as a stress – strain diagram . the shape of this diagram at the yield point depends noticeably on the mechanical arrangement of the testing machine.

If extension of the specimen is produced by an increase of distance between the grips of the machine moving at a uniform speed , the sudden motion ,and small vibration may appear on the diagram.

In order to study in more detail the deformation which occur at the yield point , specimen with polished surface have been used. Such experiments show that at the time the ten Ạ dislike stress drops from point A to point B fig 2.3 fine , dull lines begins to appear on the surface of the specimen.
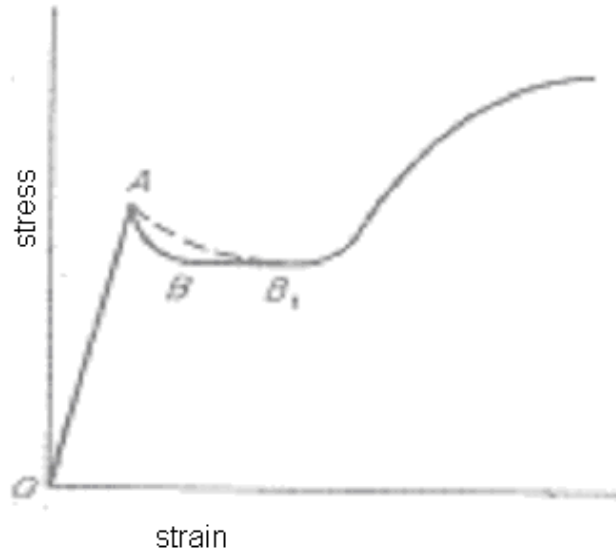
Figure 2.3   plot σ Vs ε

These lines are inclined about 45 to the direction of tension and are called lueder's lines. With further stretching , the lines increase in width and in number, and during stretching from B to B 1 , they cover the entire surface of the specimen. Instead of polishing , sometimes special paints are brittle and cannot sustain large deformations hence they crack during loading and indicate the pattern of lueder's lines.

Studies with a microscope show that lueder's lines represent the intersection with the lateral surface of the specimen of thin layers of material in which plastic deformation has occur while the adjacent portions of the material remain perfectly elastic. By cutting the specimen and using a special etching the thin plastic layers in the interior of the specimen can be mad visible. Under a microscope it is seen that these layers consist of crystals which have been distorted by sliding.

Experiments shows that the values of the yield point stress and the yield point strain depends upon the rate of strain. The curves in figure 2.4 show stress-strain diagrams for mild steel for a wide range of rates of strain (u = de/dt = 9.5 x 10^{-7}). It is seen that not only the yield point but also the ultimate strength and the total elongation depend greatly upon the rate of strain increases.
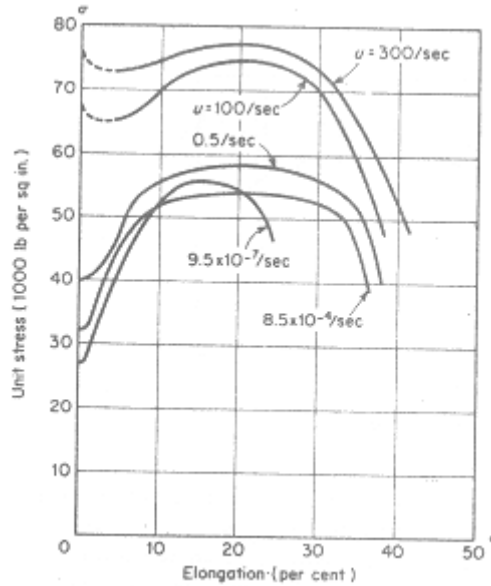
Figure 2.4   Unit stress Vs elongation for mild steel

To explain the sudden stretching of steel at its yield point , it has been suggested that the boundaries of the grains consist of a brittle material and form a rigid skeleton which prevents plastic deformation of the grains at low stress. Without such a skeleton the tensile test diagram would be like that indicated in figure 2.5by the broken line.(17)
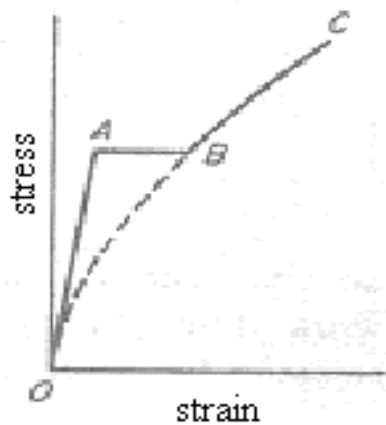
Figure 2.5Simple stress strain diagram

Owing to the presence of the rigid skeleton .the material remains perfectly elastic and follows Hook's law up to point A, where the skeleton breaks down. Then the plastic grain material suddenly obtains the permanent strain AB, after which the material follows the usual curve BC for the plastic material. This theory explains the condition of instability of the material at the upper yield point. It also accounts for the fact that materials with small grain size usually show

19

higher values for the yield stress. As a result ,such materials undergo more stretching at the yield point , as defined by the length of the horizontal line AB in figure 2.5 in addition , the theory explains the fact that in high speed tests the increase in yield point stress is accompanied by an increase in the amount of stretching at yielding as shown by curve in figure 2.4.

2.1.3 Stretching of steel beyond the yield point

During stretching of a steel specimen beyond the yield point , the material hardness and stress required for stretching the bar increase as shown by the portion BC of the stress and strain diagram in fig 2.6. elongation of the specimen is combined with uniform reduction of the cross-sectional area so that the volume of the specimen remains practically constant.
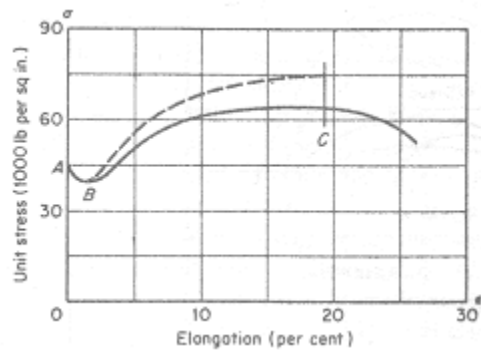

Figure 2.6Unit stress VS elongation in % of mild steel

The work done during stretching is transformed largely into heat, and the specimen becomes hot. Calorimetric measurements show that not all of the mechanical energy is transformed into heat, however part of it remains in the specimen in the form of strain energy. Owing to difference in orientation of the crystal, the stresses are not uniformly distributed over the cross sections, and after unloading, some residual stress and a certain amount of strain energy remains in the specimen.(16,17)

In after unloading we load the specimen a second time; we will find that its yield point is raised. This characteristic is shown in figure 2.6 which represents a tensile test diagram for mild steel. After stretching the bar to the point C it was unloaded. During unloading, the material followed approximately a straight –line law, as shown by the line CD on the diagram. When the load was applied to the bar a second time, the material again followed approximately Hook's law and the line DF was obtained. At point F which corresponds to the previous loading at C, the curve abruptly changed character and traced the portion FG, which can be considered a prolongation of the curve BC.
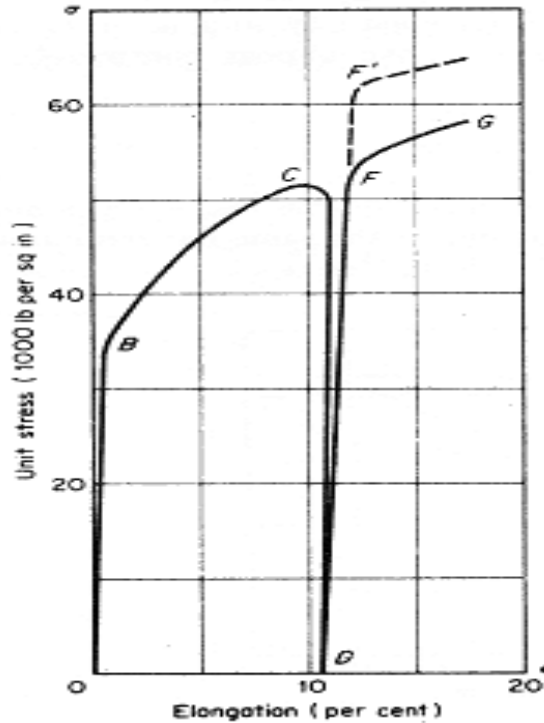
Figure 2.7Tensile test diagram for mild steel

This represents a rising of the yield point due to previous stretching of the material. If several days are allowed to elapse after the first unloading , then upon reloading a still higher yield point may be obtained ,as indicated by the dotted line at F '. Figure 2.7 shows the result of a tensile test of die –cast aluminum.
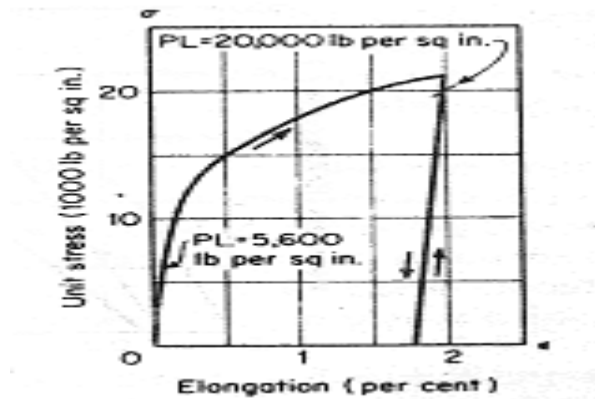
Figure 2.8tensile test diagram for Die cast Aluminium

The initial proportional limits of the material were 5600psi. After stretching the specimen 2 percent, the proportional limit upon reloading was found to be 20,000 psi and the yield point about 21,000psi.(17)

More complete investigation show that the time which elapses between unloading and reloading has a great influence on the stress-strain curve during reloading. If reloading begins immediately after unloading accurate measurements show that there is deviation from the straight –line law at very low stress and the proportional limit is greatly lowered. But if a considerable interval of time elapses between unloading and reloading, the material recovers its elastic properties completely.
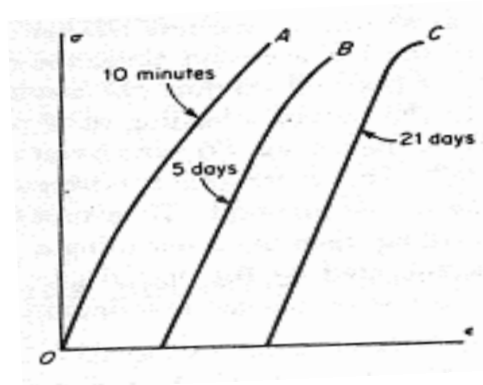
Figure 2.9Stress VS time diagram for mild steel

Figure 2.9 shows that curve obtained for mild steel which indicates that if reloading follow in ten minutes after over strain , the material does not follow hook's law , but after five days it has partially recovered its elasticity and after twenty one days it has almost completely recovered it.

Experiments also show that if the material is subjected to heat treatment after unloading ,say in a bath of 100 C the recovery of elastic properties occurs in a much shorter interval of time. Figure tensile test is represented by the curve A. Curve B represents reloading of the same bar ten minutes after unloading and considerable deviation from Hooke's law is noticeable.
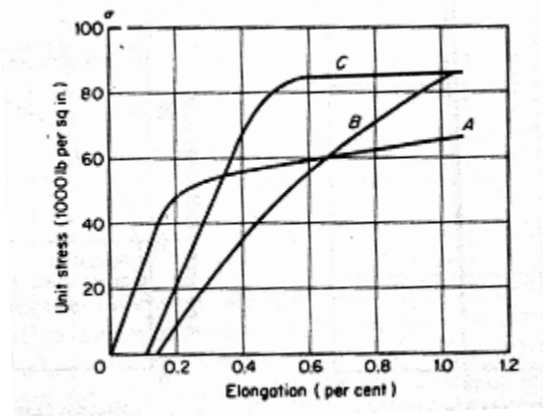
Figure 2.10Unit stress Vs Elongation in % of steel bar

Curve C is the diagram obtained with the same bar after a second unloading and after heat treating at 100C for four minutes. In this case the material has completely recovered its elastic properties.(17)

The phenomena of strain hardening due to plastic deformation is encountered in many technological processes such as rolling bars and drawing tubes and wires at low temperature, cutting sheet metal by shear and drawing and punching holes. In all these cases the part of the material which under go plastic deformation becomes harder and its ductility is greatly reduced.

To eliminate this undesirable effect of strain hardening, it is customary to anneal the material, which restores the initial ductility.

Sometimes the strain hardening of ductile material is of practical use in manufacturing. It is common practice to subject the chains and cables of hoisting machines to certain amount of over strain in order to eliminate undesirable stretching of these parts in service. The cylinders of hydraulic presses are sometime subjected to an initial internal pressure sufficient to produce permanent deformation of the walls. The strain hardening and residual stresses produced by this pressure prevent any permanent set in service. Overstraining of the material is sometime used in the manufacturing of guns. By stretching the metal in the wall of a gun beyond the initial yield point and afterwards subjecting it to a mild heat treatment, the elastic properties of the material are improve some times initial stresses are produced which combine with the stress produced by the explosive to give a more favorable stress distribution. Turbine disc and rotors are sometimes given an analogous treatment. By running these subjected to overstrain at the bore to prevent any possibility of their loosening and the shaft in service. Considerable plastic flow of the metal is sometimes produced in pressing the hubs of locomotive wheels onto their axels, and this has proved a favorable effect. Copper bars in the commutators of electric machinery are subjected to considerable cold work by drawing in order to give them the required strength.

In using overstrain in this manner to raise the yield point and improve the elastic properties of a structure, it is necessary to keep in mind
  a) That the hardening disappears if the structure is subjected to annealing temperature
  b) That stretching the metal in a certain direction, while making it stronger with respect to tension in that direction does not proportionality improve the mechanical properties with respect to compression in the same direction.

The fact that stretching a metal in a certain direction dose not improve the mechanical properties in compression in the same proportion as it dose in tension must not be overlooked in cases in which the material is subjected to reversal of stresses. It should also be mentioned that there are indication that material which has yielding in a particular region is more sensitive in that region to chemical action ,and there is a tendency for corrosion to enter the melt along the surface of sliding. This phenomenon is of particular importance in the case of boiler and other containers subjected simultaneously to stress and to chemical action.

In construction a tensile test diagram such as curve ABC in figure 2.10 the tensile load usually divided by the initial cross-sectional area A of the specimen in order to obtain the

conventional unit stress . but for large stretching there will be a considerable reduction in cross-sectional area and to obtain the true stress the actual area A ,instead of A_o should be used .

From the constancy of the actual volume of the specimen ,we have,

$$l_o\, A_o = lA$$
$$A = (A_o l_o)/l = A_o/(1 + C) \qquad \dots\dots\dots\dots\dots\dots\text{(a)}$$

And the true stress is

$$\sigma = P/A = P(1 + \varepsilon)/A_o \qquad \dots\dots\dots\dots\dots\dots\text{(b)}$$

To obtain the true stress diagram the ordinates of the conventional diagram must be multiplied by $1 + \varepsilon$. in fig 11.8 such a diagram is shown by the broken line . it extends as far as a vertical through point C, where the load reaches its maximum value . on further stretching of the specimen ,load reduction of the cross-section (necking) begins and ε is no longer constant along the specimen. then eq (b) is no longer applicable ,since the stress over the minimum cross-section are not uniformly distributed.

In such a case ,eq (b) gives only an average value of σ. The avargae unit elongation ε

At the minimum section may be found from eq (a) , which gives

$$\varepsilon = \underline{A_o} - 1 \qquad \dots\dots\dots\dots\dots\dots\text{..(c)}$$
$$A$$

Using the symbol q for the unit reduction of the cross-sectional area, we obtain,

$$q = (A_o - A_1)/A_o$$

or,

$$A = A(1-q)$$

And eq .(c) gives

$$\varepsilon = q/(1-q) \qquad \dots\dots\dots\dots\dots\text{..} \quad \text{(d)}$$

From eq .(d) the unit elongation at the minimum section can be readily calculated if the reduction in area of that section is measured. This quantity is called the effective elongation and is much larger than the elongation $\varepsilon = \delta/l$ determined from the total elongation δ of the gage length.(14,25)

2.2   **Types of fractures in tension**

In discussing fractures , we distinguish between (1) brittle fracture , a in the case of cast iron or glass and (2) shear fracture ,as in the case of mild steel ,aluminum and other metals . in the first case ,fracture occurs practically without plastic deformation over a cross-section perpendicular to the axis of the specimen. In the second case fracture occurs after considerable plastic stretching and has the familiar cup- cone form ,shown in fig 2.11
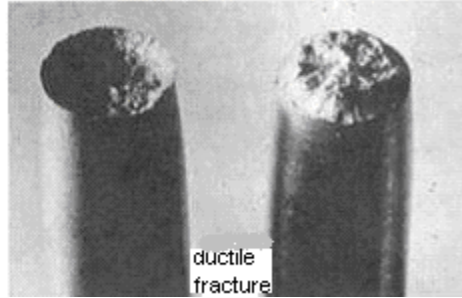
Figure 2.11Cup – Cone fracture

In discussing these two kinds of fracture , the theory has again been forward that the strength of the material can be descried by two characteristics, the resistance to separation and the resistance to sliding. If the resistance to sliding is greater than the resistance to separation , we have a brittle material , and fracture will occur as a result of overcoming the cohesive forces without any appreciable deformation.

In Mode I fracture , a tensile force acting normal to the crack surface severs to open up the crack and propagate it in a direction normal to tensile stress.

In Mode II fracture , a shear component of stress is applied normal to the leading edge of the crack, which propagates in the direction parallel to the senses of the applied stress.

Anti strain or Mode III fracture ,takes place when a shear component of stress is applied parallel to the leading edge crack. The displacement of the crack surfaces parallels that of the applied stress, but the crack propagates normal to this direction.(24)

Figure 2.12 Modes of fracture

Table 2.1 Table Between δ & Ultimate strength(lb per sq in.)

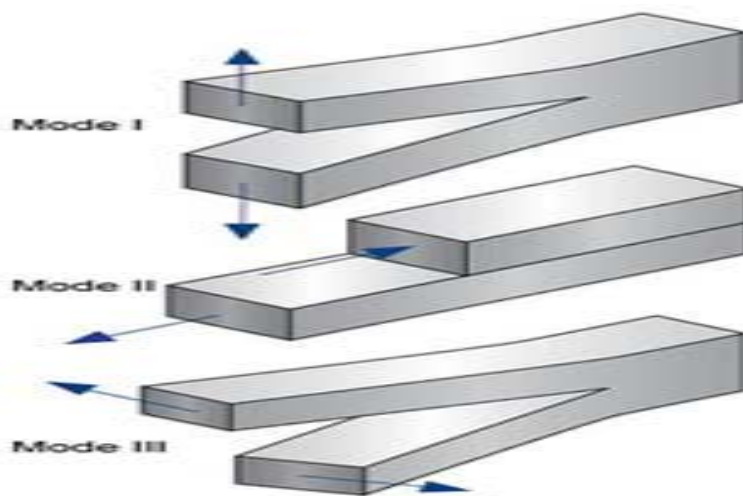| δ (inches)	Ultimate strength(lb per sq in.)			
	Carbon steel		Nikel chorme steel	
	Computed from original area	Computed from reduced area	Computed from original area	Computed from reduced area
1/32	163,000	176,000	193,000	237,000
1/16	164,000	177,000	184,000	232,000
1/8	143,000	158,000	154,000	199,000
Normal specimen	102,000	227,000	108,000	348,000

If the resistance to separation is larger than the resistance to sliding, we have a ductile material .then sliding along inclined planes begins first and the cup – cone fracture occurs only after considerable uniform stretching and subsequent local reduction of the cross-sectional are necking) of the specimen.

The preceding discussion refers only to tensile tests of standard circular specimen are quite different.

As illustrated by the grooved specimen shown in fig 2.12 during a tensile test, reduction of the cross- sectional area at the grooved section is partially prevented by the presence of the portions of larger diameter D. it is natural that this action should increase as the width δ of the groove decreases.

Table 2.1 gives the result of tests obtained with two different material(25)

(1)   carbon steel with proportional limit 56000psi yield point 64,500psi , ultimate strength 102,000psi ,elongation 26.5 percent, reduction in area 55 percent
(2)   nickel chrome steel with proportional limit 80,000psi yield point 85,000psi , ultimate strength 108,000psi ,elongation 27 percent, reduction in area 60 percent

These figures were obtained from ordinary tensile test on normal cylindrical specimen with ½ - in diameter and 2-in-gage length. The original cross –sectional are was used in calculating the stresses. The grooved specimen of the type shown in fig 2.13 had d = 0.5 in. and D 1.5 in.
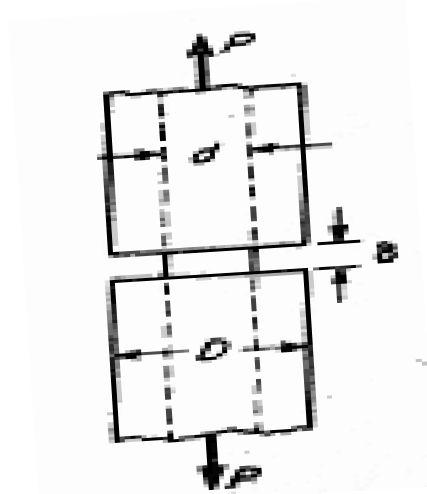
Figure 2.13Rectangular shape specimen in machine

The table shows that in all cases the breaking load for the grooved specimen was larger than for the corresponding cylindrical specimens.

With the grooved specimen only a small reduction in area took place, and the appearance of the fracture was like that of brittle materials. The ultimate strength of the cylindrical specimens was larger than for the grooved specimen because fracture of the cylindrical specimen occurs after considerable plastic flow. This resulted strain hardening and increased not only the resistance to sliding but also the resistance to separation.

Similar conditions are sometimes encountered in engineering practice. An effect analogous to that of the narrow groove in figure 2.13 may be produced by internal cavities in large forgings, such as turbo rotors.

Thermal stresses and residual stresses may combine with the effect of the stress concentration at the cavity to produce a crack. The resulting fracture will have the characteristics of a brittle failure without appreciable plastics flow, although the material may prove ductile in the usual tensile tests.

Because most of the grooved specimen remains elastic during a tensile test to failure, it will have a very small elongation, and hence only a small amount of work is required to produce fracture. A small impact force can supply the work required for failure. The specimen is brittle because of its shapes, not because of any mechanical property of the material. In machine parts subjected to impact all sharp changes in cross-section are dangerous and should be avoided.

2.3   **Compression tests**

The compression test is commonly used for testing brittle material such as stone, concrete and cast-iron. The specimens used in the tests are usually made in either cubic or cylindrical shapes in the compressing the specimen between the plane surface of the testing machine it is

27

normally assumed that the compressive force is uniformly distributed over the cross-section .the actual stress distribution is much more complicated ,even if the surface are in prefect contact and the load is centrally applied. Owing to friction on the surfaces of contact between the specimen and the heads of the machine. The lateral expansion which accompanies compression is prevented at these surfaces and the material in this region is in a more favor able stress condition. As a result, the type of fracture obtained in a compression test of a cubical specimen of concrete is as shown in figure 2.13 the material in contact with the machine remains unaffected while the material at the sides is crushed out.

In order to obtain the true resistance to compression of a material such as concrete, the influence of friction at the surface of contact must be eliminated or minimized. For this purpose A .Foppl covered the surfaces of contact with paraffin and found that the ultimate strength was then greatly reduced. The type of failure was completely different and cubic specimens failed by subdividing into plates parallel to one of the lateral sides. Another method of eliminating the effect of friction forces is to use specimen in the form of prisms having a length in the direction of compression several times larger than the lateral dimensions. The middle portion of the prisms then approaches the condition of uniform compression.

A very interesting method of producing uniform compression on cylindrical specimens as developed in the Kaiser – Wilhelm institute is shown in figure 2.14.
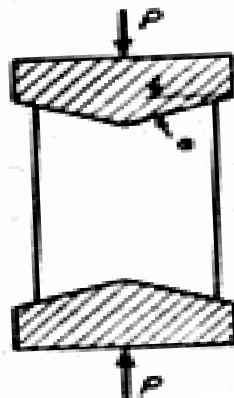
Figure 2.14 Method developed in Kaiser Wilhelm for producing uniform compression on cylindrical specimen.

The head pieces of the testing machine and the ends of the cylindrical specimen are machined to conical surfaces with the angle α equal to the angle of friction. Thus the effect of friction is compensated for by the wedging action and uniform compression results.(24,25)

Compression tests of materials such as concrete, stone and cast-iron show these material have a very low proportional limits. Beyond the proportional limit the deformation increase at a faster rate relative to the load and compression test diagram has the shape shown in figure 2.15.
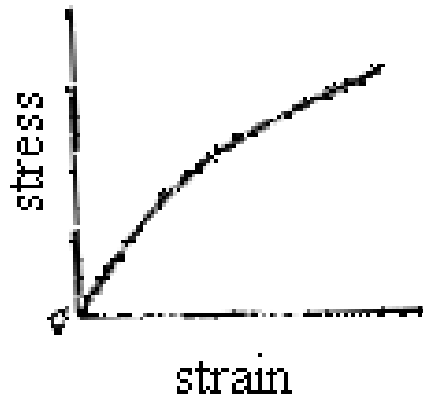
Figure 2.15stress- strain curve for specimen in figure 2.14

Sometimes it is desirable to have an analytical expression for such a diagram. For these cases Bach proposed an exponential law given the equation.

$$\varepsilon = \sigma^n / E \qquad \ldots\ldots\ldots\ldots\ldots \text{(a)}$$

In which n is a number depending on the properties of the material. Bach fond the values n = 1.09 for pure cement and n = 1.13 for granite.

Compression tests of ductile materials show that the shape of the diagram depends on the proportions of the specimen. As the dimension in the direction of compressing decreases, the effect of friction at the ends becomes more pronounced and the compression test diagram becomes steeper.
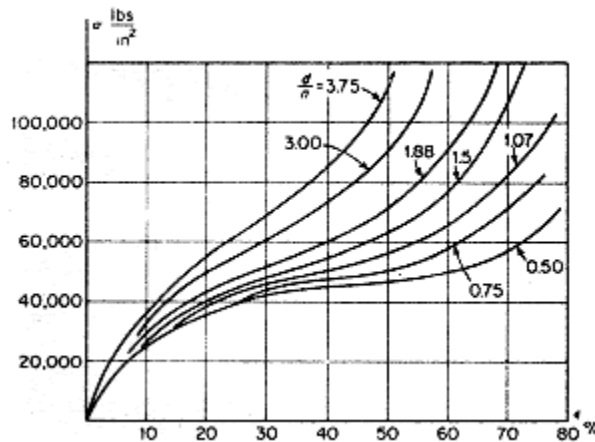
Figure 2.16 the result of compression tests on copper cylinders

For example, figure 2.16 shows the result of compression tests on copper cylinders with various ratios d/h of the diameter to the height of the specimen. In the compression of such ductile material; as copper. Fracture is seldom obtained. Compression is accompanied by lateral expansion and a compression cylinder ultimately assumes the shapes of a flat disc.

2.4 **Tests of material under combined stresses**

Leaving the discussion of simple tension and compression tests lets us now consider cases in which the materials are tested under combined stresses. We begin with a discussion of materials tested under uniform hydrostatic pressure. Such tests show that under uniform pressure, homogeneous materials can sustain enormous compressive stresses and remains elastic. Tests also show that large pressure produces only small changes in volume.

Several attempts have been made to produce uniform hydrostatic tension of material, but up to now there has not been a satisfactory solution to this interesting problem.

Tensile tests of various steels combined with lateral pressure have shown that the pressure has a great effect on the shape of the neck and on the reduction in area at the minimum cross-section. Figure 2.17 shows the yoke arrangement by which tension was applied to specimens within the pressure vessel.
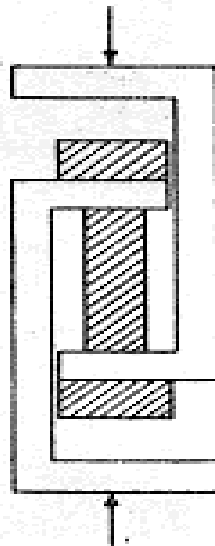
Figure 2.17 shows the yoke arrangement by which tension was applied to a specimen within the pressure vessel.

Figure 2.18 a and b illustrate fractures of medium carbon steel (0.45percent carbon) at atmosphere pressure and at a lateral pressure of 145,000psi. In first case the average true stress was 114,000psi. In the second case the corresponding value was 474,000psi. It was also found that with an increase in lateral pressure the relative extent of the flat part at the bottom of the cup-cone fracture becomes entirely shear fracture.
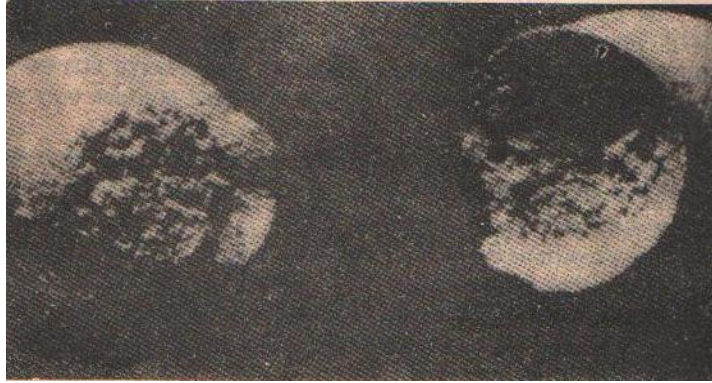
Figure 2.18 (a)Fracture of medium carbon steel (0.45% of carbon) with true stress 114,000psi

Figure 2.18 (b) Fracture of medium carbon steel (0.45% of carbon) with true stress 474,000psi

The combination of axial compression and lateral pressure was used by Th. V. Kerman in compression tests of marble. These test showed that with increasing lateral pressure marble becomes more and more plastic ,and initial cylindrical specimen may obtain barreled forms , as shown in figure 2.19
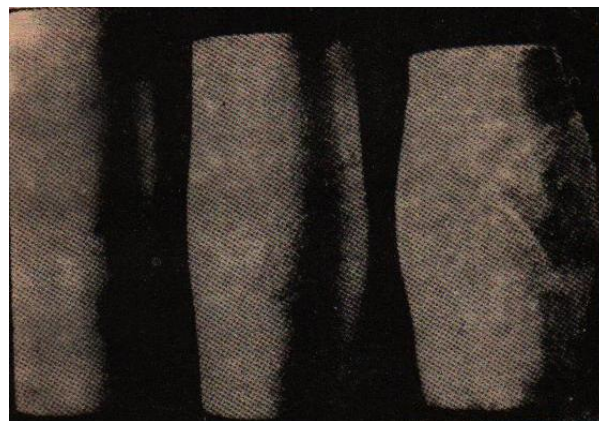
Figure 2.19The combined axial compression and lateral pressure on marble specimen

In studying two –dimensional stress conditions, thin –walled cylindrical tubes have been tested. By subjecting a tube to axial tension combined with internal pressure , the yield point stresses for various ratios of the two principal stresses was established for several material , including iron, copper, and nickel. The results obtained in way were in satisfactory agreement with the maximum distortion energy theory.

In practice application not only the yield point stressed but also the ductility and strain hardening are of great importance in cases of combined stresses. Unusual cases of failure, such as explosive of large spherical storage tanks and sudden cracks in the hulls of welded cargo ships, have recently called attention to these subjects. In both these types of failure, low –carbon steel plates were used which showed satisfactory strength and ductility in ordinary tensile testes. But the fractured surfaces of the plates in the exploded pressure vessel and in the damaged ships did no show plastic deformation and had a brittle character. Most of these failures occurred at low atmospheric temperature and under two –dimensional stress conditions.(17)

In order to determine the influence of temperature and two – dimensional stress on the strength and ductility of low –carbon steel, a considerable amount of experimental work has been done in recent times in various laboratories. Thin –walled tubes were used to produce two-dimensional stress conditions. These tubes were subjected simultaneously to axial tension and internal hydrostatic pressure, so that tensile stresses σ_t in the circumferential direction and σ ain the axial direction could be produced in any desired ratio n = σ_t / σ_a .

Using tubes of medium –carbon steel (0.23 percent carbon) with 1.450-in. outside diameter and 0.100-in. wall thickness, E.A. Davis made test with five different values of the ratio n. Figure 2.20 shows the types of fracture obtained.

Figure 2.20 If n= σ_t / σ_a then for different values of n different type of fracture.

For the small values of the ratio n the cracks were circumferential, and for the larger values they were longitudinal. By making an additional series of test it was established that the

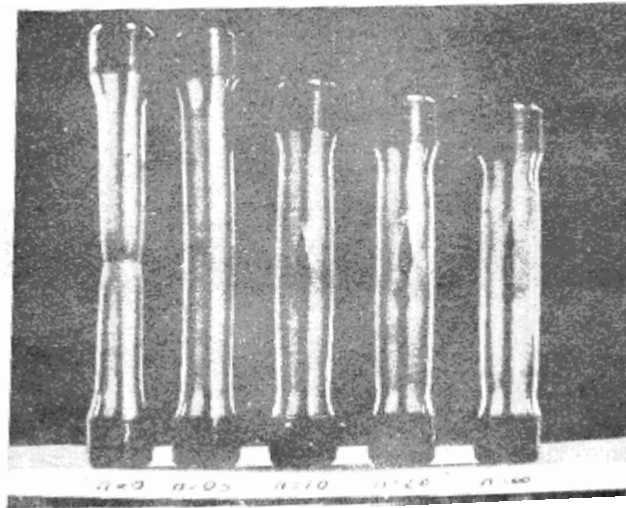transition from one type of failure to the other occurred at the value n = 0.76. it was found that in the case of circumferential cracks the fracture occurred along the planes of maximum shearing stress and at true stresses of about the same magnitude as in the case of flat specimen prepared from the same material as the tubes. In the case of the longitudinal cracks, rupture appeared to be more brittle. Failure usually started along the planes of maximum shearing stress, but owing to high stress concentration at r=the crack ends, it continued as brittle fracture in the axial plane without substantial plastic deformation. The maximum shearing stress at which the longitudinal cracks began was always much smaller than in the case of circumferential cracks. It seems that the difference in the two fractures were due largely to the shape of the specimens.

In the case of circumferential cracks the material was much more free to neck down than in the case of longitudinal cracks and therefore the latter occurred with smaller local deformation and smaller decrease in load beyond the ultimate strength.

In the experiments at the university of California test were made at two different temperature using thin walled tubes of low –carbon steel. The diameter of the tubes was 5.25in. and the temperature were 70° F and -138° F . the test at room temperature always gave a shear type of fracture with considerable plastics deformation. The result at low temperature (with n= 1) showed brittle fracture with very small plastic deformation. This brittleness was attributed to the local stresses at the welded junctions of the tubes with the end connections.

After these tests with small tubes, large-size tubular specimens of 20in.outside diameter and 10-ft length , made of 0.75in. ship plat , were tested at 70° F and -40° F. The tests at low temperature, especially with the ratio n=1, showed brittle fracture at stress much smaller than those obtained from tensile tests of ordinary cylindrical specimens made of the same material.

2.5 Basic principles of Composite materials

2.51 Introduction

Unlike the case of the two-phase materials considered in chap.5, the strengths of composite materials are not defined by microscopic interactions between phases. Rather, their strengths, as well as their other mechanical characteristics are some appropriate average of the properties of the individual materials comprising the composite. Composites are useful materials, because they contain a reinforcing phase in which high tensile strengths are realized when they are processed to fine filaments, wire, or whiskers (hereinafter called fibers). Such fibers typically have diameters ranging from ca. 1 µm to 0.025cm. The inherently high strengths of the fibers are utilized in monolithic materials by their incorporation into a suitable matrix. In such fibrous composites, the matrix serves as a "glue" to hold the fibers together and also a means to transfer applied stress to them. In many cases the matrix also functions to protect the strong fiber from deleterious interactions with the environment, such as oxidation and corrosion. Thus, many fiber-

reinforced materials consist of a high-strength material in fiber from imbedded in a much less string matrix that serves the purposes described above.

Strong, yet brittle, materials can also be reinforced if fibers of reasonable ductility are incorporated within them. In this case the term "reinforced" in something of a misnomer, for the function if the fiber is to toughen the matrix; i.e., the fibers serve to resist brittle crack propagation rather then to improve the material strength.

As mentioned, in most cases the strengths of composites are unrelated to microscopic interaction effects, because the phase "scale" of most composites is large compared to that at which interaction effects become important. However, in some cases both the size and separation of the reinforcing phase is on the order off micrometers or less and, when this is so, description of the mechanical behavior of composites must also consider aspects of deformation.(26,27)

2.52 Basic Principles

The appropriate "average" of the individual phase properties to be used in describing composite behavior can be elucidated with reference to fig. 2.21. The two-phase material considered consists of N slabs (lamellae) of α and β phases of thicknesses ι_α and ι_β, respectively. Thus, the volume fractions v_α , v_β) of the phases are

$$\left.\begin{array}{l} V_\alpha = l_\alpha /(l_\alpha + l_\beta) \\[2mm] V_\beta = l_\beta /(l_\alpha + l_\beta) \end{array}\right\} \qquad\qquad \textbf{2.1}$$

In fig. 2.21 a, a tensile force f is applied normal to the broad faces (of dimensions L x L) of the phases. In this arrangement the stress borne by each of the phases (= F/L^2) is the same, but the strains experienced by them are different. Provided ι is not so small in comparison to L that the "brazed joint"
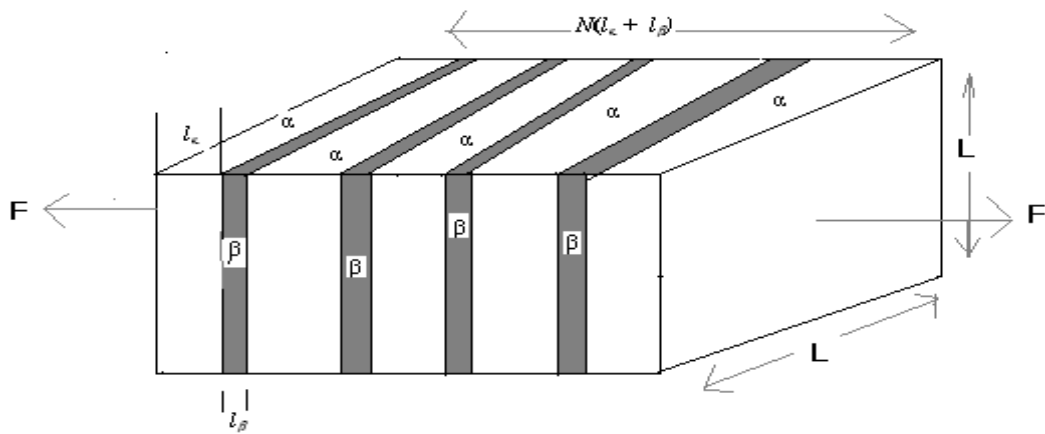
(a)
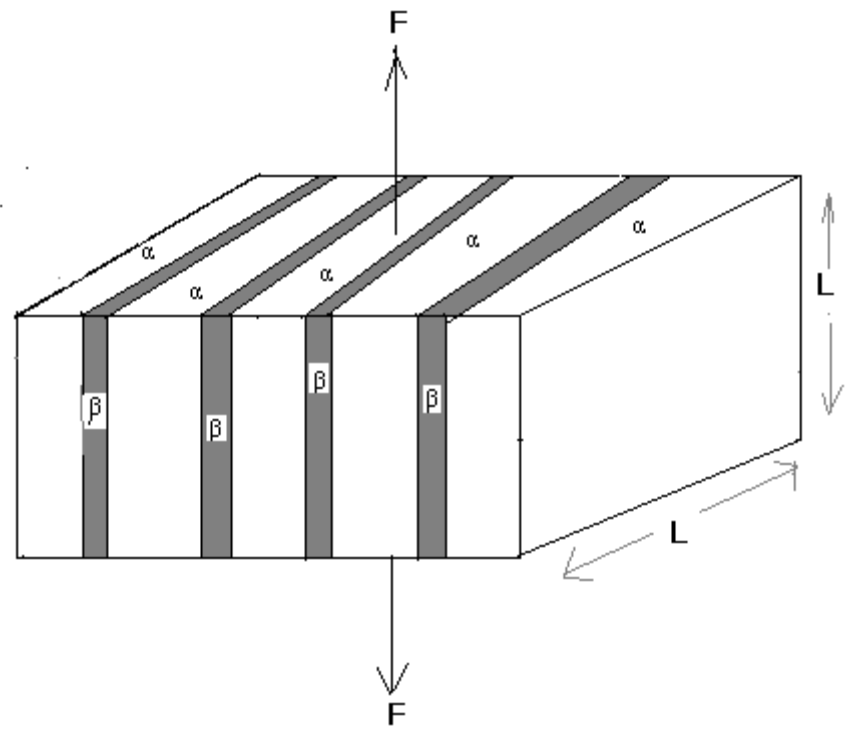
(b)

FIGURE 2.21 Lamellar arrangements of two phases (α and β) having different properties. In (a) a tensile force is applied in a direction such that the stress borne by both phases is the same, but they experience different strains. In (b), the force is applied in a direction that results in the

phases experiencing the same strain but different stresses. This is the arrangement that utilizes the strong phases to the best advantage.

Effect must be considered, we can assume that the strains in both phases $(\varepsilon_\alpha, \varepsilon_\beta)$ are equivalent to those that would be found in tension tests of the individual components. Thus, the elongation in one slab of the phase α $(=\Delta\iota_\alpha)$ is

$$\Delta\iota_\alpha = \varepsilon_\alpha \iota_\alpha \qquad\qquad 2.2$$

With a corresponding expression for $\Delta\iota_\beta$. the total elongation of the composite, $\Delta\iota_c$, is obtained as

$$\Delta\iota_c = N\,\Delta\iota_\alpha + N\,\Delta\iota_\beta \qquad\qquad 2.3$$

And the composite strain (ε_c) is

$$\varepsilon_c = \Delta l_c / [N(l_\alpha + l_\beta)] = (\Delta l_\alpha + \Delta l_\beta)/(l_\alpha + l_\beta) \qquad\qquad 2.4$$

Substitution of Eq. 2.1) into Eq. (2..4) gives

$$\varepsilon_c = \mathbf{v}_\alpha \varepsilon_\alpha + \mathbf{v}_\beta \varepsilon_\beta \qquad\qquad 2.5$$

That is , the composite strain is a volumetric weighted average of the strains of the individual phases.

If the deformation in both phases is elastic (i.e. $\varepsilon_\alpha = \sigma_\alpha / E_\alpha$ etc.), Eqq.6.5

$$\varepsilon_c = \alpha\,[(V_\alpha / E_\alpha) + (V_\beta / E_\beta)] \qquad\qquad 2.6$$

And the composite modulus E_c $(=\sigma/\varepsilon_c)$ is found from

$$1/E_c = [(V_\alpha / E_\alpha) + (V_\beta / E_\beta)] \qquad\qquad 2.7$$

Or

$$E_c = E_\alpha E_\beta / (V_\alpha E_\beta + V_\beta E_\alpha) \qquad\qquad 2.8$$

Equation (2.5) is one from of a volume-fraction rule, and is appropriate for a phase geometry d in which both phases experience equal stress. However, in most composite the arrangement of the phases with respect to an applied external force is similar to that shown in fig. 2.21b. Here the strain in both phases are equal (and the same as the composite strain), but the external force is partitioned unequally between the phases. The force division can be determined by realizing that the sum if the forces ($F_\alpha + F_\beta$) borne by the individual phases is equal to the total external force F. Each α lamella is assumed to carry a stress σ_α; thus F_α is obtained as

$$F_\alpha = \quad \sigma_\alpha N \iota_\alpha L \qquad\qquad 2.9$$

With a corresponding expression for F_β. Hence

$$F = NL(\sigma_\alpha \iota_\alpha + \sigma_\beta \iota_\beta) \qquad\qquad 2.10$$

And division of Eq. (2.10) by the cross-sectional area $(= NL(\iota_\alpha + \iota_\beta)$

$$\sigma_c = \sigma_\alpha l_\alpha / (l_\alpha + l_\beta) + \sigma_\beta l_\beta / (l_\alpha + l_\beta) = \sigma_\alpha V_\alpha + \sigma_\beta V_\beta \qquad\qquad 2.11$$

The volume-fraction rule **(VFR)** of Eq. (2.11) is the one most closely followed by composites, as the phase geometry is usually close to that for which the equal-strain approximation is valid. That the equal-strain condition is useful for providing reinforcement can be illustrated for the simple case in which both phases are elastic (i.e., $E_c = \sigma_c / \varepsilon$, $E_\alpha = \sigma_\alpha / \varepsilon$, $E_\beta = \sigma_\beta / \varepsilon$). For this condition the composite modulus is given as

$$E_c = V_\alpha \, E_\alpha + V_\beta \, E_\beta \hspace{4cm} 2.12$$

The ration of the forces borne by the α and β phases in the elastic regime is

$V_\alpha \, E_\alpha / V_\beta$ (cf.Eq.(2.9) . This ratio is plotted in fig. 2.22 as a
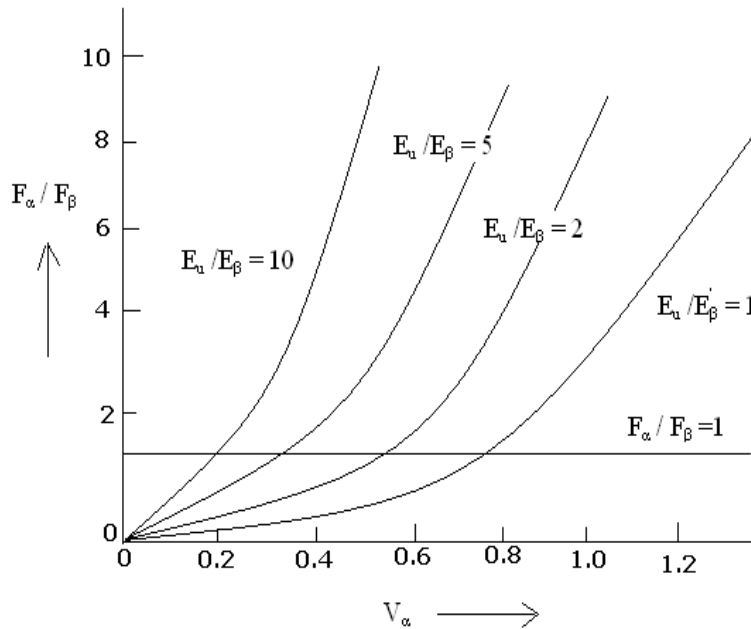
FIGURE 2.22   The ratio of the force carried by the (strong) α phase to that of the β

Phase for the two geometries shown in fig. 2.21. For the equal-stress condition (fig.2.21a), $F_\alpha / F_\beta = 1$, and the ratio is independent of V_α , the α phase volume fraction . for the equal-strain condition F_α / F_β increases with both V_α and the stiffness ration (E_α / E_β) of the phases. The results shown in this figure apply when both phases deform by linear elastic deformation.

Function of V_α (α is presumed the stiffer of the phases) for several values of E_α / E_β and compared to the equal stress condition (for which $F_\alpha / F_\beta = 1$). It can be seen that provided E_α is sufficiently large in comparison to E_β , the α phase is utilized more efficiently in the equal-strain condition . However, and as we shall see, for this to be true, a certain volume fraction o the

stronger phase must be incorporated into the matrix. This us the case for most useful composite materials. (25,26)

2.6 REINFORCEMENT WITH CONTINUOUS FIBERS

Various phase arrangements can be obtained in composite and other two-phase materials. As shown in the previous section m the phases may be arranged in a lamellar or platelike array or, as in the case of TRIP or dual-phase steels, the phase morphology

May be described approximately as equiaxed arrays of the particles. However, the most widely utilized phase geometry in composites is one in which the reinforcing, strong phase is in the form of a fiber. In part this results from the extraordinary strengths attainable in many materials when they are in fibrous form. Table 6.1 lists the properties of a number of such

Table : 2.2 Properties of selected fibers

Material class	Material	E (GN/m^2)	T.S (GN/m^2)	P(Mg/m^3)	E/ρ(MNm/Kg)	T.S/ρ(MNm/Kg)
Metals	Be	315	1.3	1.8	175	0.72
	Peralite Steel	210	4.2	7.9	27	0.53
	Stainless steel	203	2.1	7.9	26	0.27
	Mo	34	2.1	10.3	33	0.20
	β – Ti	119	2.3	4.6	26	0.50
	W	350	3.9	19.3	18	0.20
Inorganics	Al_2O_3	470	2.0	3.96	119	0.51
	Al_2O_3 whiskers	470	2.0 – 20.0	3.96	119	—
	B	385	7.0	2.6	148	2.69
	BN	90	1.4	1.9	47	0.74

	Graphite	490	3.2	1.9	258	1.68
	Graphite(Kevlar)	133	2.8	1.5	89	1.87
	E Glass	84	4.6	2.55	33	1.80
	S Glass	72	6.0	2.5	29	2.40
	Mica	231	3.2	2.7	86	1.19
	SiC	380	2.8	2.7	141	1.04
	SiC whiskers	470	2.0 -20.0	3.17	148	___
	Si_3N_4	380	1.0 – 10.0	3.8	100	___
Polymers	Nylon 66	4.9	1.05	1.1	4	0.95

Nonmetallic and metallic fibers . Nonmetallic fibers demonstrate not only high strengths nut also very high strength -to- density ratios, which render them attractive candidates for aerospace structural materials. This is true despite their relatively high costs; however, economies of manufacture attendant on large-scale production should improve this situation. Morever, the strengths realizable in a given fiber have, as a result of improved production techniques, increased substantially in the last twenty years, and it is expected that such quality improvement will continue.

Useful composites require not only high-strength fibers but a processing technique whereby they can be incorporated into a (usually much weaker) matrix, incorporation of fibers into polymeric matrices (typically) epoxy or polyester resins) is comparatively inexpensive vis-à-vis their incorporation into metallic matrices. Polymeric matrix composites, however, are limited in their use at elevated temperature owing to degradation of properties and/or polymer decomposition, whereas this is not so true for metal matrices. Nonetheless, the economics of production is such that current use of polymeric matrix composites in recreational (e.g., golf clubs) and aerospace applications far exceeds that of metal-matrix composites.

The deformation behavior of fiber-reinforced composites is frequently adequately described by a VFR appropriate for the equal-strain condition (Eq., (2.11)). For fiber composites we alter the subscripts of Eq. (2.11) so that α, the "hard" phase corresponds to the fiber (f) and the softer phase corresponds to the matrix (m). Thus for a fiber-reinforced material with a tensile force applied parallel to the ling axis of the fiber (fig.2.23),

$$\sigma_c = V_f \sigma_f + V_m \sigma_m \qquad\qquad 2.13$$

As mentioned, it is implicit in Eq. (2.13) that the stress-strain behavior of the composite constituents (the fiber and the matrix) are ascertained by tensile testing them individually.

The uniaxial stress-strain response of a fiber composite can be divided into several stages. In the first (Stage I), the strain is so small that both the fiber and matrix deform elastically. If this strain is linearly elastic, we have

$$\sigma_c = E_c \varepsilon_c = \varepsilon_c [V_f E_f + V_m E_m] \qquad \text{(stage 1)} \qquad 2.14$$
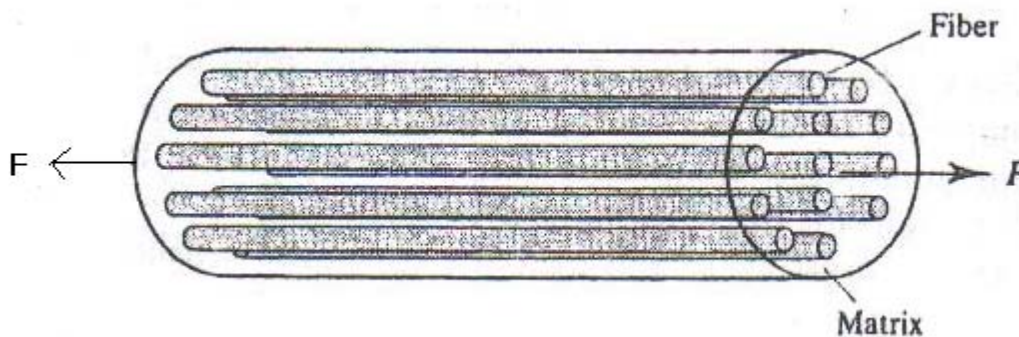

FIGURE 2.23 A fiber composite consisting of strong fibers imbedded in a (presumably) weaker matrix. When the force is applied in the direction shown, the equal-strain condition holds.

In typical fiber-reinforced materials the matrix begins to deform permanently at a strain at which the fiber remains elastic. This constitutes the onset of stage II deformation. For which

$$\sigma_c = V_f E_f \varepsilon_c + V_m \sigma_m (\varepsilon_c) \qquad \text{(stage II)} \qquad 2.15$$

Where, as mentioned $\sigma_m (\varepsilon_c)$ is assumed to be the stress carried by the matrix

(at strain ε_c) as determined from a uniaxial stress-strain test of the matrix. The stage II "modulus," E'_c, is defined as the instantaneous slope of the composite stress-strain curve during Stage II deformation. That is,

$$E'_c = \qquad \text{stage II} \qquad 2.16$$

In most cases the second term of Eq. (2.16) is small in comparison to the first, so that

$$E'_c = V_f E \qquad 2.17$$

Although $d\sigma_m / d\varepsilon_c$ is presumed to be the slope of the stress-strain curve of the matrix tested in monolithic form, this is not always the case during stage II deformation strains during stage II deformation. In the absence of fiber-matrix interactions, the lateral strain is - $V\varepsilon_c$ for the fiber (where V is Poisson's ratio of the fiber) and - $\varepsilon_c / 2$ for the plastically deforming matrix. Compatibility of lateral deformation in the composite is provided ht introduction of internally generated stresses. These affect this stress state of both fiber and matrix, but alter the behavior of the latter to a greater extent. The magnitude of the internal stress depends directly on the incompatibility that would exist in the unconstrained state i.e., the stress is proportional to (1/2-v). Thus, the matrix work-hardening coefficient of stage II is that of a constrained matrix, and is invariably

greater than that for the unconstrained, matrix and is invariably grater than that for the unconstrained matrix, the adequacy of the approximation of Eq. (2.17) depends on the value of $V_f E_f$ relative to the second term of Eq. (2.16) provided V_f is sufficiently large, Eq. (2.17) remains a reasonable approximation for the secondary modulus.

Many high-strength fibers do not exhibit permanent deformation prior to fracture. Thus, the tensile strengths of composite containing them are usually defined in the second stage of composite deformation. On the other hand, metallic fibers frequently deform plastically before fracture, and composites containing permanently deforming fibers exhibit a third stage in their uniaxial stress-strain curve. During this stage III, the VFR is expressed as

$$\sigma_c(\varepsilon_c) = V_f\sigma_f(\varepsilon_c) + V_m\sigma_m(\varepsilon_c) \qquad\qquad 2.18$$

Where $\sigma_f(\varepsilon_c)$ and $\sigma_m(\varepsilon_c)$ are the respective fiber and matrix flow stresses at the composite strain ε_c. During stage III deformation the lateral strains in the constituents are compatible (the effective plastic Poisson's ratio for each is (1/2), and this the constraints present in stage II deformation are absent. This is true at least up to and near the composite tensile strength. As the necking strain of one of the phases is approached, the other phase acts on it in such a manner as to delay necking. Thus, the uniform or necking strain of the composite lies between the necking stains of the individual constituents. For example, if $V_f(T.S)_f$ is much greater than $V_m(T.S)_m$, the composite necking strain is nearly the fiber necking strain. When the converse holds, the composite necking strain is approximately the matrix necking strain. When neither of the above conditions apply, the composite necking strain is intermediate between those of the constituents.

The stages of composite behavior described above are illustrated schematically in figs. 2.24a and b illustrates composite stress-strain behavior manifesting all three deformation stages. The fracture event illustrated in fig. 2.24a is appropriate when all of the fibers fail at the same strain. As is also shown in fig. 2.24a, composite failure is not necessarily concurrent with fiber fracture; that is, although for the composite whose behavior is illustrated, the matrix is still able to

(a)

STAGE II

σ_c

$V_f(T.S.)_f + V_m\sigma_m(\varepsilon_f)$

STAGE III

$$\frac{d\sigma_c}{d\varepsilon} = V_f \frac{d\sigma_f}{d\varepsilon} + V_m \frac{d\sigma_m}{d\varepsilon}$$

$V_m(T.S.)_m$

ε_f

$(\varepsilon_c)_f$

STAGE I

ε_c
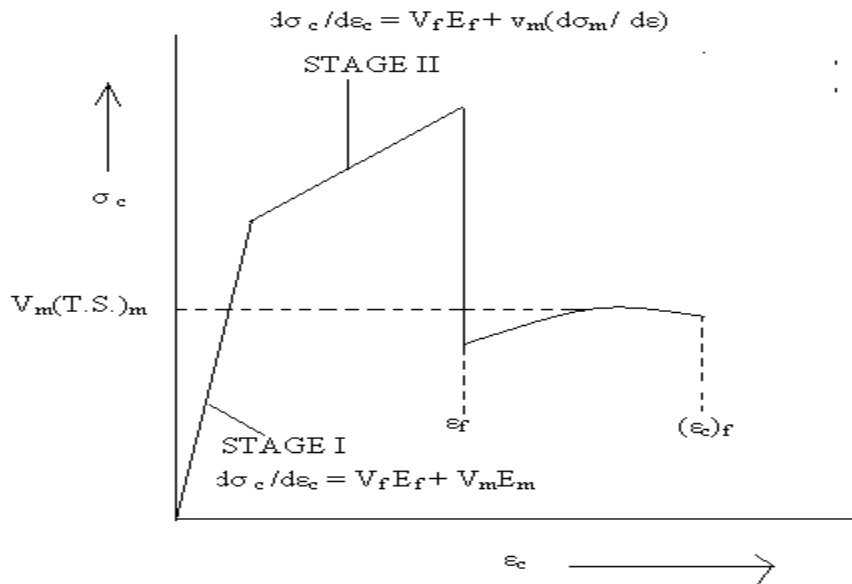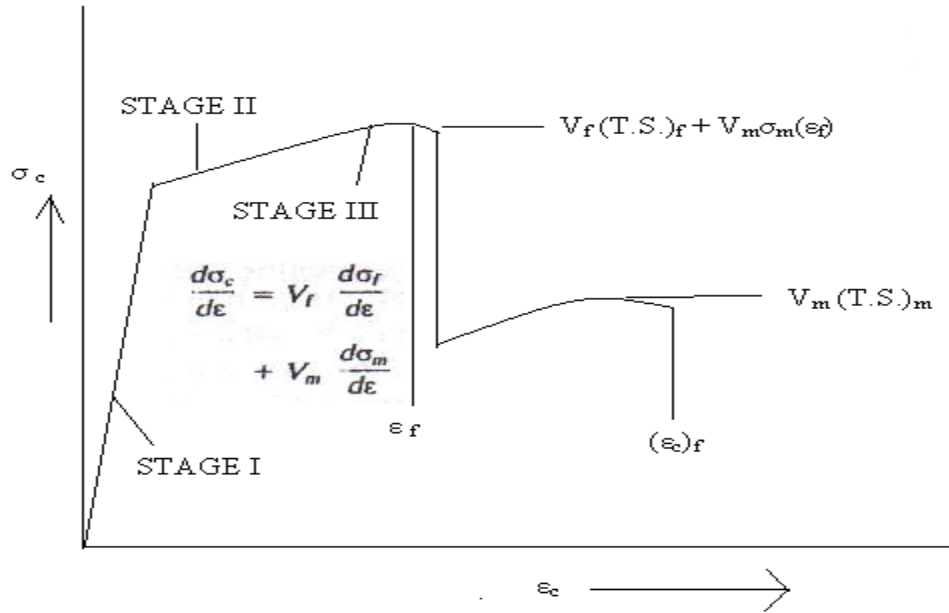
(b)

FIGURE 2.24 composite stress-strain curves are predicted by the volume fraction rule, in both (a) and (b), stages I and II are shown. In stage I, the fiber and matrix deform elastically and the modulus is the volumetrically weighted modulus of both phases. In stage II the matrix deforms plastically and the fiber elastically. Thus, the "secondary" modulus, i.e., the slope of the stress-strain curve, is reduced. In (b), a third stage, in which both the matrix and fiber deform plastically, is shown. The fiber failure strain (ε_c) is assumed less than that of the matrix. Matrix failure is not necessarily concurrent with fiber failure. Thus, a secondary tensile strength V_m $(T.S)_m$ is observed following fiber failure.
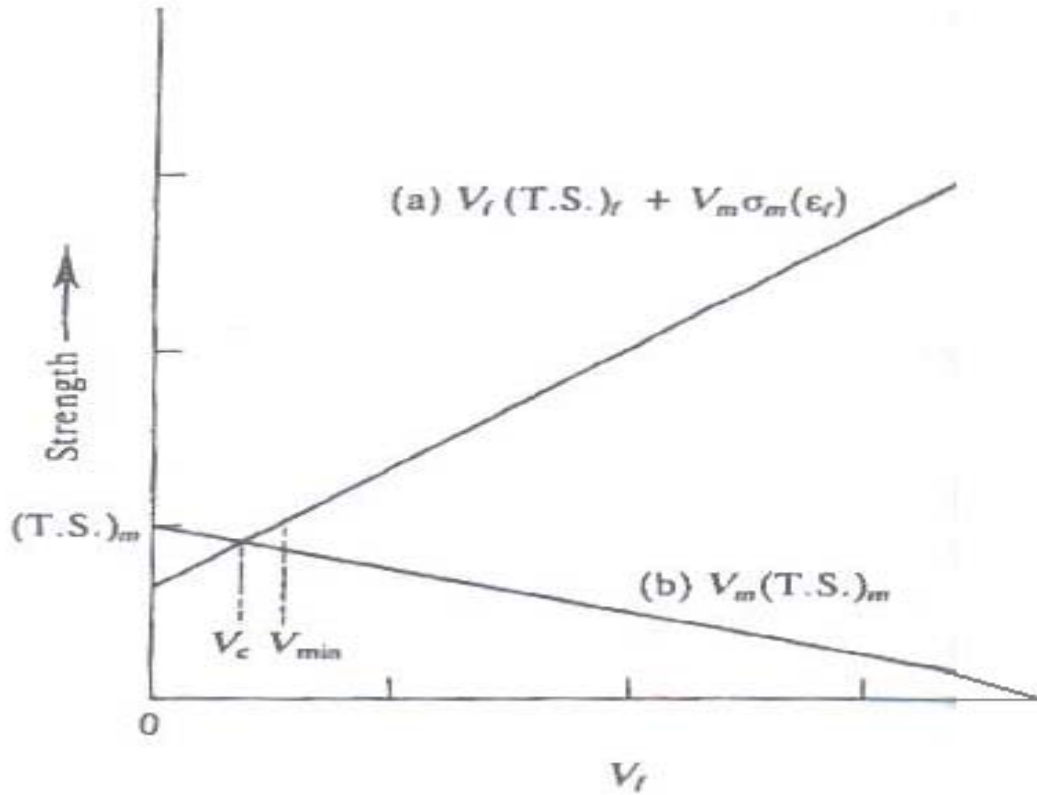
FIGURE 2.25 composite tensile strength as predicted by the volume fraction rule (curve (a)) and the "secondary" tensile strength (curve (b)) as function of fiber volume fraction, V_f. Observed composite tensile is the greater of these two values. For $V_f < V_c$, the secondary tensile strength is greater than the VFR strength and composite strength decrease with V_f. In order for composite tensile strength to exceed that of the matrix, a minimum volume fraction (V_{min}) of the fiber must be present.

Sustain load and to deform subsequent to fiber fraction. Thus a "secondary" tensile strength ($= V_m (T.S.)_m$ is observed.

Provided composite tensile strength is coincident with the fiber failure strain, it can be expressed as

$$(\textbf{T.S.})_c = V_f(\textbf{T.S.})_f + V_m \sigma_m (\varepsilon_f) \qquad\qquad 2.19$$

Where $(\mathbf{T.S.})_f$ is the fiber tensile strength and $\sigma_m(\varepsilon_f)$ is the flow stress of the matrix at the fiber failure strain ε_f. The VFR applied to composite tensile strength, as given by Eq. (2.19), is shown by the curve marked (a) in fig. 2.25, which plots $(\mathbf{T.S.})_c$ vs $\mathbf{V}_f$. on the other hand, if $\mathbf{V}_f$ is low, the secondary tensile strength may be greater than that given by Eq. (2.19). This possibility is illustrated in fig. 2.26, which shows composite stress-strain curves for both "low" and "high" values of $\mathbf{V}_f$. The secondary tensile strength is plotted against $\mathbf{V}_f$ as the curve marked (b) in fig. 2.25 as can be seen, the secondary tensile strength exceeds that predicted by Eq. (2.19) for values for $\mathbf{V}_f$ less than some critical value $\mathbf{V}_c$. Thus composite tensile strength is given as

$$(\mathbf{T.S.})_c = V_m(\mathbf{T.S.})_m \quad V_f \leq V_c \tag{2.20a}$$

Or

$$(\mathbf{T.S.})_c = V_f(\mathbf{T.S.})_f + V_m\sigma_m(\varepsilon_f) \quad V_f \geq V_c \tag{2.20b}$$

The critical volume fraction is found by equation Eqs. (2.20a) and (2.20b); thus,

$$V_c = [(T.S)_m - \sigma_m(\varepsilon_f)] / [(T.S)_f + (T.S)_m - \sigma_m(\varepsilon_f)] \tag{2.21}$$
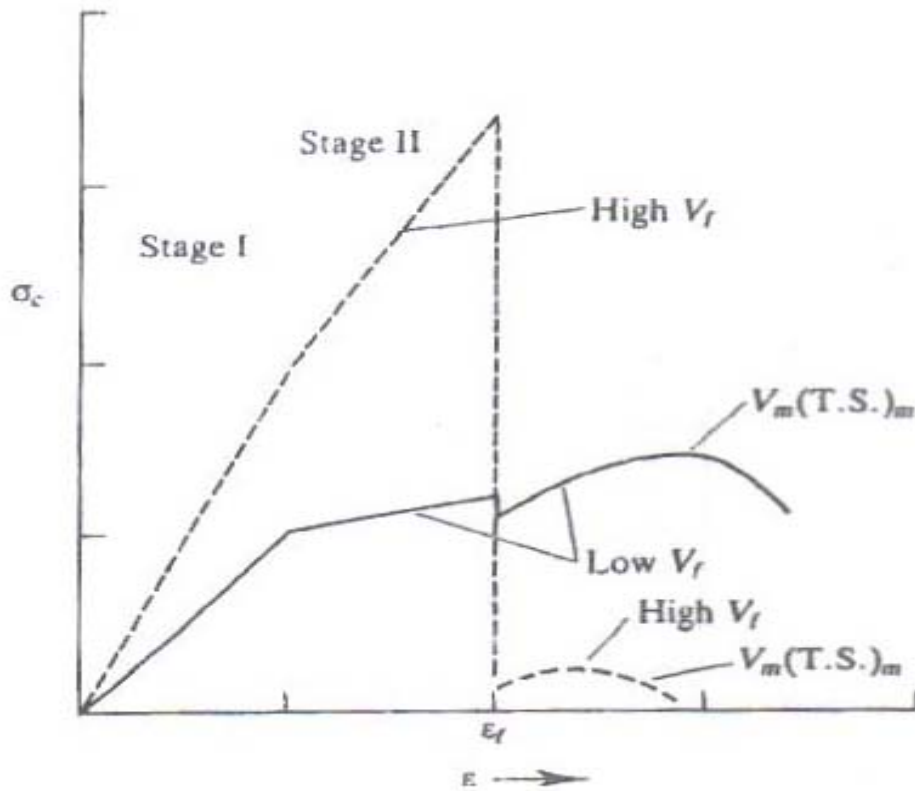
FIGURE 2.26 composite stress-strain curves (stage I and II) for two different fiber volume fraction. The curve marked "low V_f" has $V_f < V_c$ and composite tensile strength is the secondary tensile strength. For the curve marked "high V_f" ($V_f > V_c$), composite tensile strength is given by the volume-fraction rule.

As can also be seen in fig. 2.25, composite tensile strength exceeds that of the matrix only if Eq. (2.19) is greater than $(T.S.)_m$. Thus a certain minimum fiber volume fraction, V_{min}, must be incorporated into the matrix for composite tensile strength to exceed matrix tensile strength. The value of V_{min} is

$$V_{min} = [(T.S.)_m - \sigma_m(\varepsilon_f)] / [(T.S.)_f - \sigma_m(\varepsilon_f)] \qquad 2.22$$

47

For typical matrix –fiber combination, both V_c and V_{min} are on the order of 0.02-0.10, and these values are readily exceeded in most fiber composite. Thus, Eq. (2.19) provides reasonable approximation to the tensile strength of most aligned fiber composite.

The discussion so far has been appropriate to the case in which the long axis of the fiber is aligned parallel to the applied tensile force. When this is not so, composite strength may be much less than predicted by eq (2.19) , as the equal strain condition no longer applies. Hence the fiber composites are intrinsically anisotropic, with their strengths begun greater when the applied force is parallel to the fiber long axis. An estimate of the "critical" misorientation of the fiber and tensile axes, below which Eq.(2.19) is expected to apply and above which composite strength falls rapidly with increasing misorientation, can be obtained with reference to fig 2.27a.
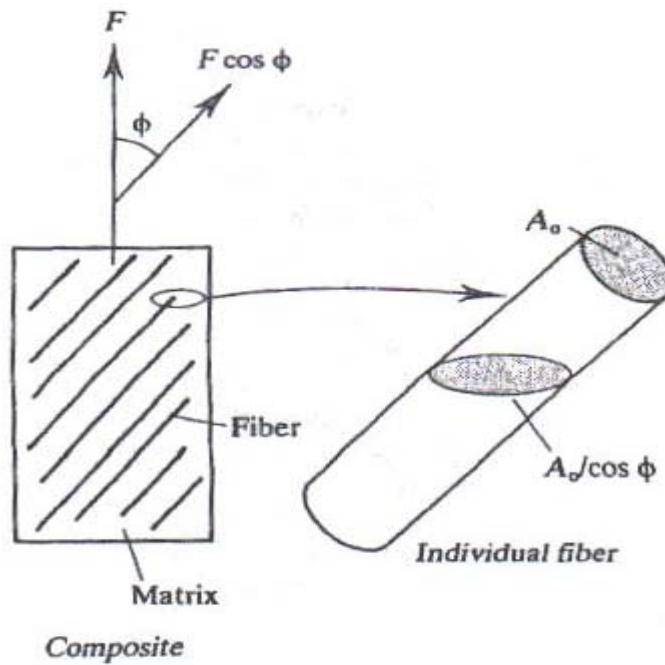
(a)
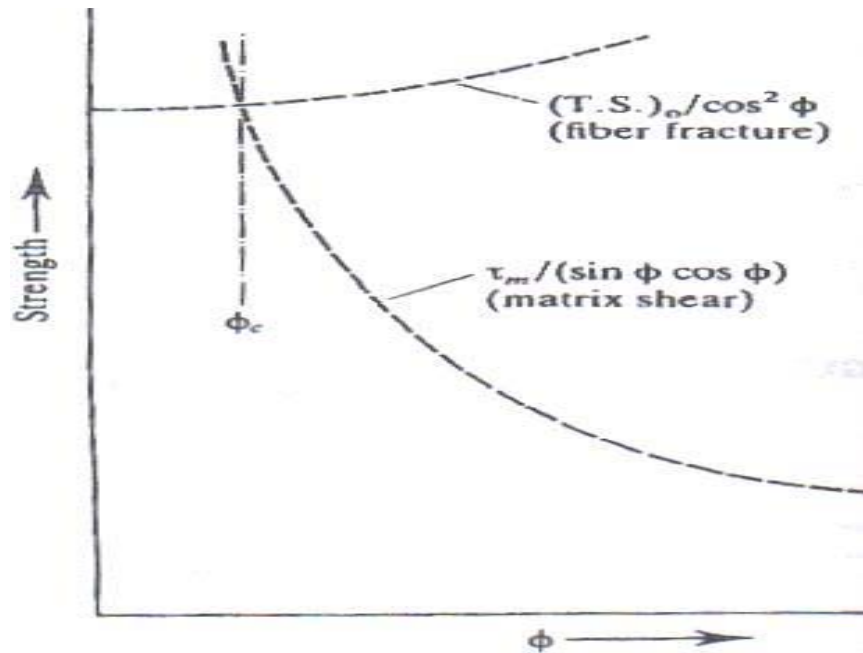
(b)

Fig 2.27: (a) The effect of fiber mis-orientation on fiber tensile fracture. (b) curve between strength and Φ.

Here the resolved tensile force, F_R , on the fiber resulting from the applied force F is $F_R = F \cos \Phi$, where Φ is the angle between the fiber and tensile axes. Likewise , the effective cross sectional area of the fiber is

$A_o/ \cos \Phi$, where A_o is their nominal cross sectional area. Thus, the tensile stress acting on the fibers is $\sigma_o \cos^2 \Phi$, where σ_o is the stress that would act if the fiber rand tensile axes were coincident (i.e. if $\Phi = 0^o$).

Fibers will fracture at an observed tensile strength, $(T.S.)_c{}'$, such that $(T.S.)'_c \cos^2 \Phi = (T.S.)_{c0,}$ where $(T.S.)_{c0}$ is the tensile strength for $\Phi = 0^o$.

Thus,

$$(T.S.)'_c = (T.S.)_{c0} / \cos^2 \Phi \qquad\qquad 2.23$$

Equation (2.23) predicts that composite strength should increase with increasing misorientation, provided the composite failure mode is fiber fracture.

However as the misorientation angle increases, composite failure can occur bby matrix shear. The resolved force on the matrix including shear flow is equal to $F\sin\Phi$; the area on which the shear force acts is $A_m/\cos\Phi$, where A_m is the matrux area at zero misorientation. Thus if τ_m is the matrix shear strength, failure by shear will take place at an applied tensile stress $(T.S.)_c$, such that

$$(T.S.)_c \sin\Phi \cos\Phi = \tau_m \qquad\qquad 2.24$$

Equations (2.23) and (2.24) are plotted against Φ in fig 6.7b. Composite failure will take place by the fiber fracture for $\Phi \leq \Phi_c$, where Φ_c is obtained by equating Eqs. (2.23) and (2.24). This critical angle is

$$\Phi_c = \tan^{-1}\left[\tau_m / (T.S.)_{c0}\right] \qquad\qquad 2.25$$

Values of Φ_c are typically small ($\leq 10^o$) so that only small misorienatations are sufficient to negate the high strength capabilities of composites. This adds complexity to engineering design for composites subjected, for example, to biaxial loading .
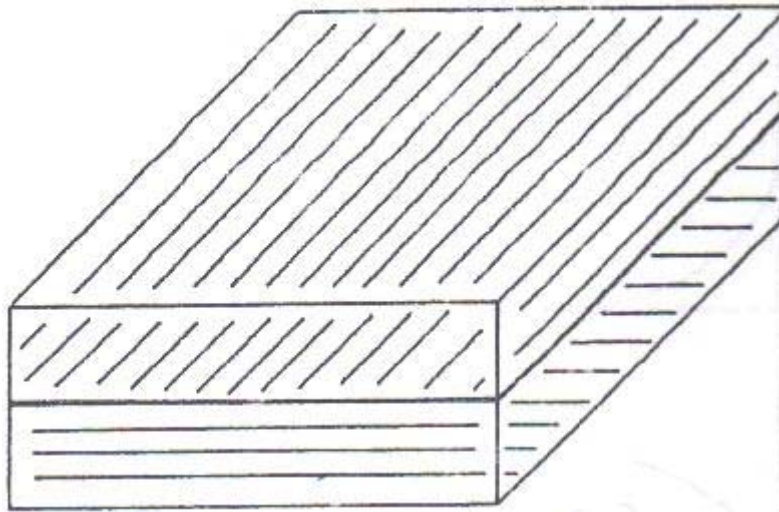
Fig 2.28: A schematic of 90° "cross-plying" fiber composite.

Cross-plying of composites illustrated schematically in fig 2.28, is often used in these cases and other more complex "laminate" are also found useful for multiaxial stress applications.(24,25,26)

2.7 Statistical failure of composites:

All fibers in the composite fail at the same stress, i.e., at $(T.S.)_f$. This is demonstrably not true for most of the nonmetallic fibers whose properties are listed in table 2.2. The tensile strength of these are affected markedly by the presence of defects within them or on their surface. The most common of these are small surface flaws or cracks that appreciably reduces their tensile strength. Even high strength metallic fibers display variations in tensile strength from fiber to fiber, although this variation is nowhere near as large as it is for nonmetallic fibers having comparable strengths.

The tensile strength listed in table 6.1 are average values obtained from a series of tests. A schematic illustration of the results from such a test series is given in fig 2.29, where the fraction of fibers of uniform length l that fail at a given stress level is plotted against the stress level.
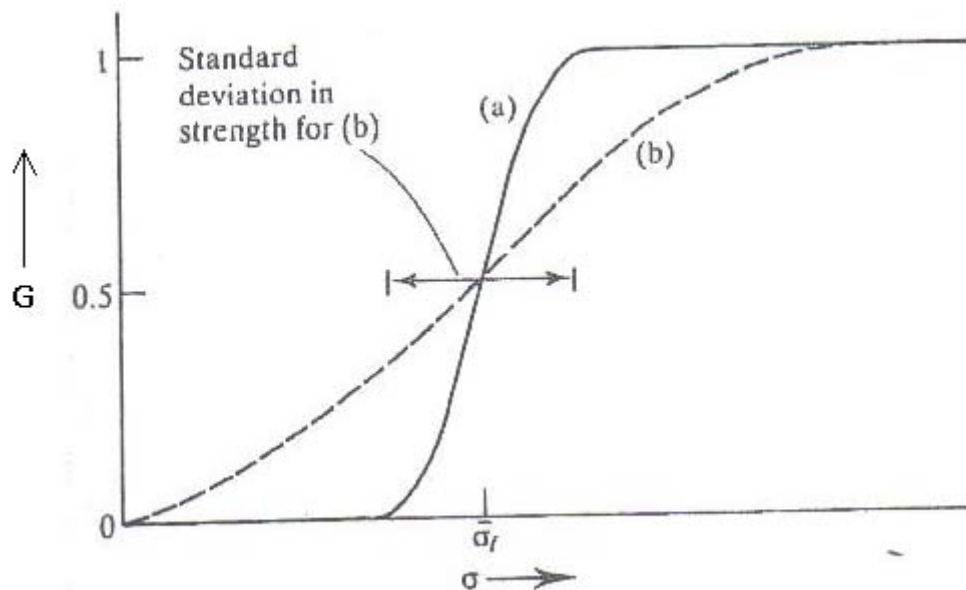
Fig2.29 : method of describing the fiber strength variation. (a) the fiber donot demonstrate a wide variability in strength. (b) the variation can be defined by the standard deviation in fiber strength.

The ordinate on the curve ia labeled $G(\sigma)$; that is , $G(\sigma)$ represents the fraction of fibers that fail at a stress level less than or equal to σ. An "expectation" value of the fiber strength ($<\sigma_f>$ can be

defined as that stress for which 50 percent of the fibers fracture; i.e., $G(<\sigma_f>)= [1 – G(<\sigma_f>)] = 0.50$.

Fibers may have the same value of $<\sigma_f>$ but exhibit significant differences in their strength variations. Thus, curve (a) in fig 2.29 is for a material that exhibits little variation in strength from fiber to fiber, whereas curve (b) is for a material manifesting intrinsically large strength variations. The strength variation is defined by the standard deviation in fiber strength a sin fig 2.29 an d this parameter is closely related to another term called the fiber co efficient of variation.

Closely related to $G(\sigma)$ is fraction of fibers that fail between the stress levels σ and $\sigma +d\sigma$. This function , $g(\sigma)d\sigma$, is thus defined by $G(\sigma +d\sigma) – G(\sigma) = dG (\sigma)$ or

$$dG(\sigma) = g(\sigma)d\sigma \qquad\qquad\qquad 2.25a$$

and

$$G(\sigma)=\int_0^\sigma g(\sigma)d\sigma \qquad\qquad\qquad 2.26b$$

These components can be illustrated further by considering the tensile behavior of a bundle of fibers of number N_o and length l for which the expected fiber strength and standard deviation are determined by the function $G(\sigma)$ for alternatively $g(\sigma)$. Such a bundle subjected to a varying tensile force F is illustrated in fig 2..30 and resembles a "composite" for which V_f is unity.
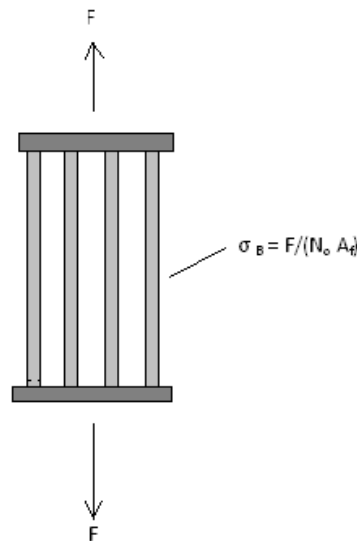
Fig 2.30: schematic of a tensile test on a bundle of fiber.

On initial loading , the tensile force is divided equally among the individual fibers so that the force on each is F/N_o and the stress (σ_f) on each is F/N_oA_f , where A_f is the transverse cross sectional area of the fiber. The nominal tensile stress carried by the bundle ,σ_B is defined by,

$$\sigma_B = F/N_oA_f = N_o\sigma_f/N_o \qquad\qquad 2.27$$

Equation 2.27 applies up to the stress at which fibers within the bundle commence fracturing. Beyond this stress level, the $N_o$term in the numerator of the right hand side of eq.2.27 must be replaced by N, the number of unbroken fibers. ($N_o$in the denominator remains unchanged because the bundle stress is still based on the original cross section area (N_oA_f)of the bundle) thus,

$$\sigma_B = N\sigma_f/ N_o \qquad\qquad .2.28$$

and since N/N_o is the fraction of unbroken fibers it is identically equal to [$1 - G(\sigma_f)$]. Hence,

$$\sigma_B = \sigma_f [1 - G(\sigma_f)] \qquad\qquad 2.29$$

Figure 2.31 schematically plots σ_f [$1 - G(\sigma_f)$] , and σ_B (the product of these terms)as a function of σ_f .
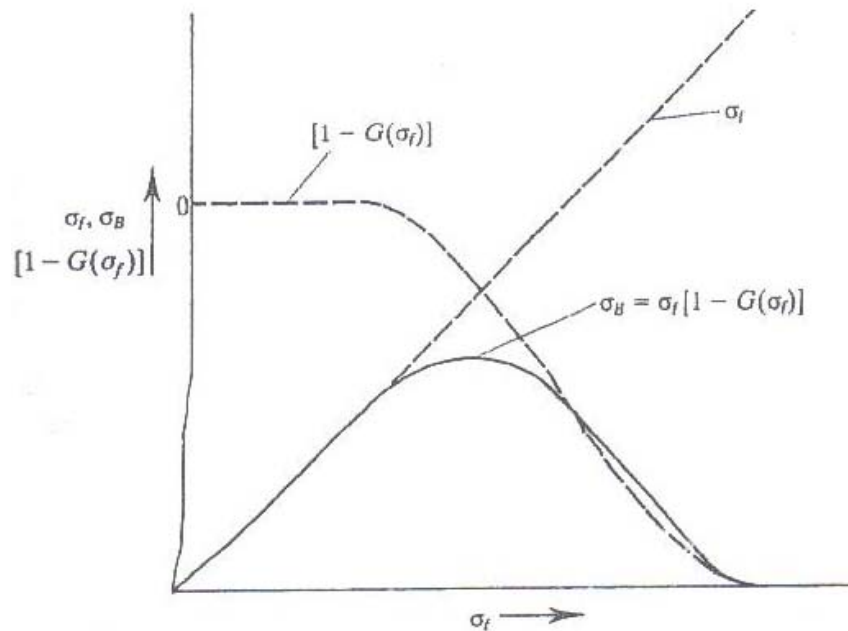
Fig :2.31 The bundle stress as a function of σ_f is obtained by multiplying σ_f by the fraction of unbroken fibers [$1 - G(\sigma_f)$]. The variation of σ_f [$1-G(\sigma_f)$], and their product , σ_B is shown here as a function of σ_f .Bundle tensile strength is obtained when the product σ_f [$1 - G(\sigma_f)$] is maximum .

It is evident that maximum strength is obtained at the stress, $\sigma_{f\,max}$,such that,

$$(d\ \sigma_B\ /d\ \sigma_f)\ \sigma_{f\ max}\ =\ [1 - G\ \sigma_{fmax}\ ] - \sigma_{fmax}\ g(\sigma_{fmax})\ = 0 \qquad 2.30$$

The value of the bundle tensile strength is given by,

$$<\sigma_B> = \sigma_{fmax}\ [\ 1 - G\ (\sigma_{fmax})] \qquad\qquad 2.31$$

Since the bundle contains fibers characterized by a distribution in strengths bundle strengths also exhibit such variations. However, if the number of fibers in the bundle is reasonably large, these variations will be much less than those exhibited by individual fiber strengths.

Bundles are utilized in a number of applications. The ones that come to mind most readily are standard steel wire and ropes and yarns. At first glance it is surprising that the fibers in these ,and other , bundles are of finite length and do not traverse the whole of the bundle length. However , the standing operation allows tensile stress to be transferred from one strand to another as a result of the friction force generated when the strands attempt to slide by one another. The stress transfer in a bundle is however, nowhere near as efficient a sit is in a fiber composite.

That is, the matrix within a fiber composite allows for effective stress transfer to fibers, ans as a result fiber reinforced materials utilize fiber strengths better than do bundles.

This is illustrated by application of bundle theory to fiber composite ,as illustrated infig 2.32
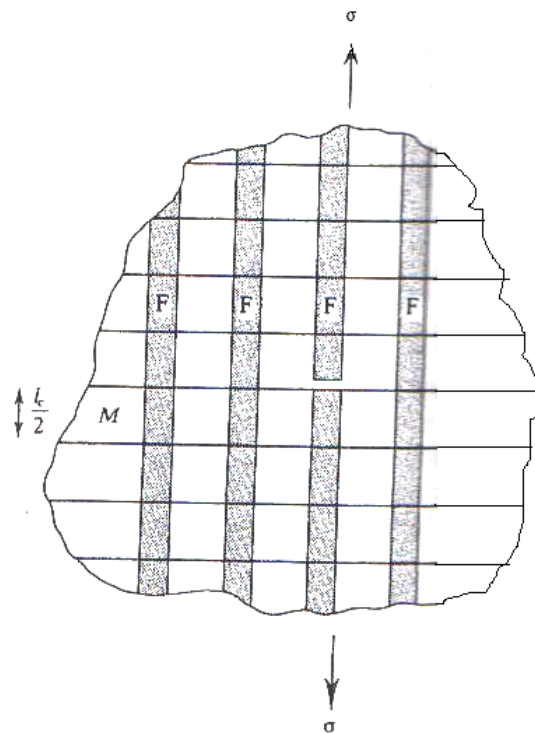
Fig 2.32: bundle theory can be applied to composite containing fiber.

So that we can neglect the complication required by the modification of the VFR for finite length fibers, fig 2.32 is applied to composite containing continuous fibers of length l , the same as the sample length. When a fiber in such a composite fails at some random location along the gage length, it is not, as it is in a bundle , precluded from carrying tensile load at other locations along its gage length. Instead, the matrix reloads thee fiber to its expected stress level at a distance $\pm$ $l_c/2$ from the original fiber fracture location. Subsequent to the first fracture, the unbroken fibers in the transverse cross – section where the first break occurred carry the load previously borne by the now fractured fiber. If the fibers all have the same strength level, the composite will fracture at the cross section where the first fiber break takes place. On the other hand, if the distribution in fiber strengths is large , the remaining fibers are able to withstand this stress concentration, and the next fiber fracture takes place at some other location along the gage length. For this situation,composite fracturetakes place by a statistical accumulation of fiber breaks along the gage length withfinalfracture (or tensile strength) corresponding to the failure of one additional fiber "link" such tahht the remaining unbroken fibers within a given trenssverse cross section are unable to absorb the incremental load transferred to them as a result of the "critical" fracture event. We see thaht ,, as distinct from bundle fracture, fibers may be broken at more than one location along their gage length during this "statistical" composite fracture.(24)

Composite tensile behavior in this scenario is described by considering each fiber as consisting of a series of links of length $l_c/2$. Composite tensile strength (neglecting the contribution from the matrix) will be given by an equation analogous to Eq.(2.31) with one important difference: that the function $G(\sigma)$ is replaced by one that described the variation instrenghts of fibers having length $l_c/2$ rather than l.

Calling this function $F(\sigma)$, the expected composite strength is given as

$$< \sigma_c > = \sigma_{fmax} \left[1 - F(\sigma_{fmax}) \right] \qquad\qquad 2.32$$

Where σ_{fmax} is the stress at which the product $\sigma_f \left[1 - F(\sigma_f) \right]$ is a maximum. Composite strengths will always exceed those of bundles for the following simple reason. A fiber in a bundle will fail at its weakest link , and thereafter is incaple of contributing to the strength of the buudle. Provided $l > l_c/2$, this is not so in a composite, and a broken fiber contribuuyes to composite stress carrying capability all along its length expect in the immediate vicinity of the break.

How much stronger a composite is than a bundle depends on the number of links withineach fiber , i.e., on the number of links within each fiber i.e., on the ratio l/l_c . If there are a great number of links(if l/l_c is alarge), composite strength can far excedd that of the corresponding bundle. Likewise, composite strnght canfra exceed that of the corresponding bundle.

Likewise, composite strength vis-à-vis bundle strength is ggreatest for for fibers with intrinsically large strength variations. In a bundle, the weak links fail at alow stress level and

partilly negate the higher strength capacities of the remaing fibers. This is not so if the fiber is imbedded in an efficient of stress tranfering matrix.

These concept are illustrated in fig 2.33, where the ratio of composite to biundle strength is plotted versus the fiber coefficient of variation for various values of l/l_c . high values of l/l_c enhance composite strength ,and this effect is most pronounced for fibers with intrinsically large strength variations.
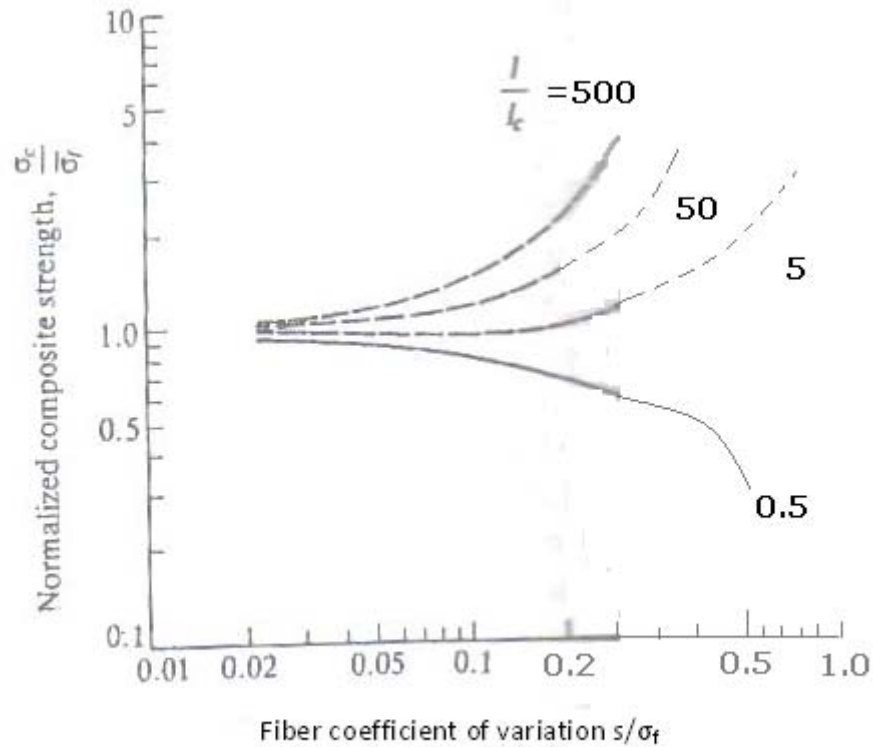
Fig 2.33 : curve between fiber coefficient of variation s/σ_f Vs Normalized composite strength σ_C/σ_f.

2.8 Strain rate effects:

Many composites are , or will be, utilized in the temperature regime where they are strain rate sensitive and thus subject to time dependent deformation. Strain rate sensitivity is also displayed even at room temperature by a few metals and some polymers. This sensitivity can be described by the empirical Eq.

$$\sigma_m = K_m (\varepsilon'_m)^m \qquad\qquad 2.33$$

where m is the matrix of strain rate ,constant K_m is measure of the intrinsic flow stress, and depends implicitly on strain provided that work hardening occurs during matrix deformation.

Potential high temperature composites include those that at the design operating temperatures and stresses are comprised of fibers displaying linear elastic behavior and matrix that is expected to creep under the same conditions. Thus, the fibers in these composites are expected to enhance not only the strength but also creep resistance.
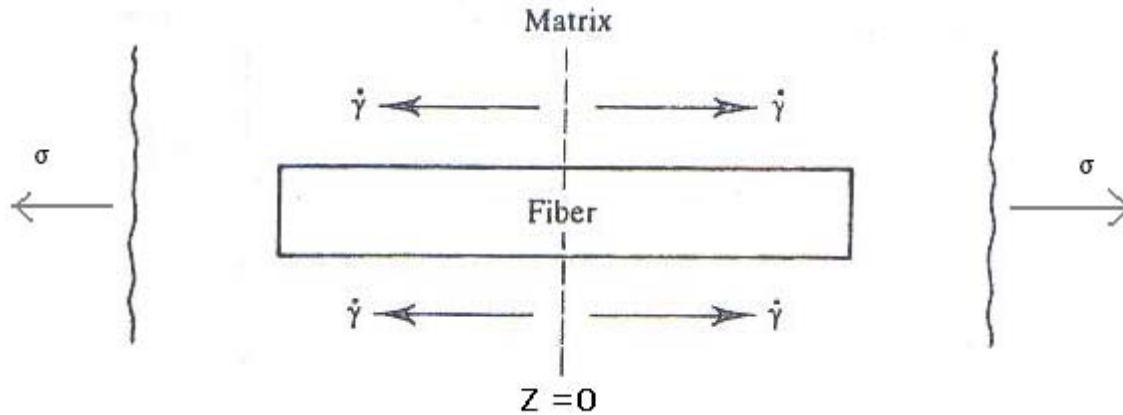
Fig: 2.34 an elastic fiber imbedded in a matrix deforming at the tensile strain rate ,ε'_m. the tensile strain rate results iin a relative shear strain rate displacement,γ', at the fiber matrix interface.

An elastic fiber imbedded in a matrix flowing past the fiber at a relative shear strain rate γ' . The magnitude of γ' varies along the length of the fiber; it is zero at the fiber mid point (z =0) and a maximum at the fiber end (z = 1/2). We assume that this variation is linear with position and also that it increases linearly with the matrix tensile strain rate, ε'_m , i.e.,

$$\gamma = \beta' z \varepsilon'_m \qquad\qquad\qquad .2.34$$

where β is proportionality constant β' has dimensions of (length)$^{-1}$.

For purpose of analysis following, we take $\beta' = \beta/d_f$ where d_f is the fiber diameter.

The shear stress –shear strain rat behavior of the matrix is described by the relation analogous to Eq. (2.33), i.e., $\tau = K_\tau (\gamma')^m$. Thus, the shear stress at the fiber matrix interface is given as ,

$$\tau = K_\tau (\beta' \varepsilon'_m)^m (z/d_f)^m \qquad\qquad\qquad 2.35$$

The variation of τ with position along the fiber length is illustrated in fig(2.35a & b). The former shows that the stress increases to higher values the greater the strain rate sensitivity of the matrix, and also shows that when m is low (i.e., when the material is not strain rate sensitive), the shear stress, as expected on previous discussions, is constant along the fiber length and equal to the

57

matrix shear yield strength. Figure 2.35b illustrated that the shear stress increases with increasing matrix strain rate.

(a)   (b)
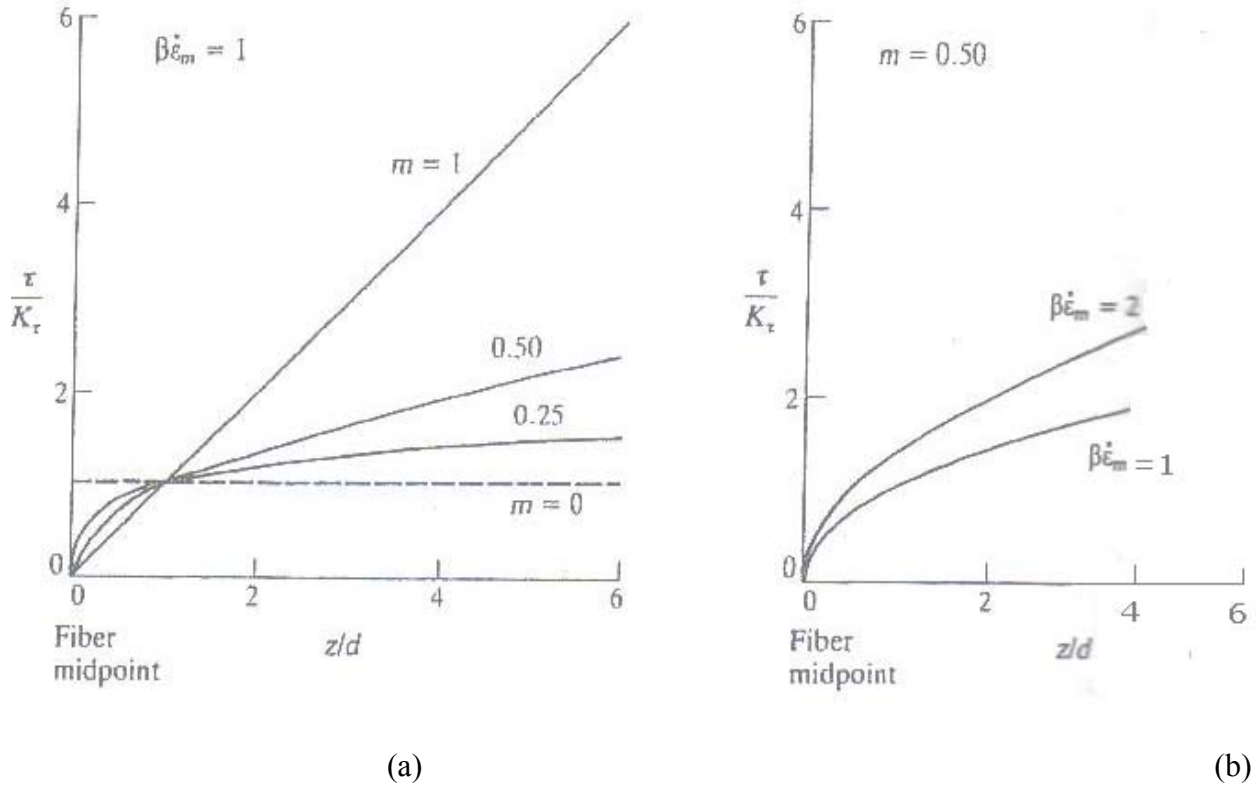
Fig 2.35 : The shear stress developed at the fiber matrix interface as a function of position along the fiber.(a) For fixed strain rate ,τ increases most rapidly for strain rate sensitive materials. (b) As the strain rate increases, τ does like wise.

The tensile stress carried by the fiber is obtained in a manner used previously, i.e., by integration of Eq. (2.22) subject to the boundary condition $\sigma_f = 0$ at $z = l/2$. The result is

$$\sigma_f(z) = (4K_\tau/m + 1)(\beta\varepsilon'_m)^m \left[(l/2d_f)^{m+1} - (z/d_f)^{m+1}\right] \qquad\qquad 2.36$$

The variation of the σ_f with z is shown in fig 2.36 a(with $\beta\varepsilon'_m = 1$ and $l/d_f = 100$) for various values of the strain rate sensitivity. As expected on the basis of the shear stress sensitivity to strain rate, tensile stress is built up most rapidly in strain rate sensitive matrices. Likewise (fig 2.36 b), the fiber is loaded to higher stress levels with increases in matrix strain rate.

(a)   (b)
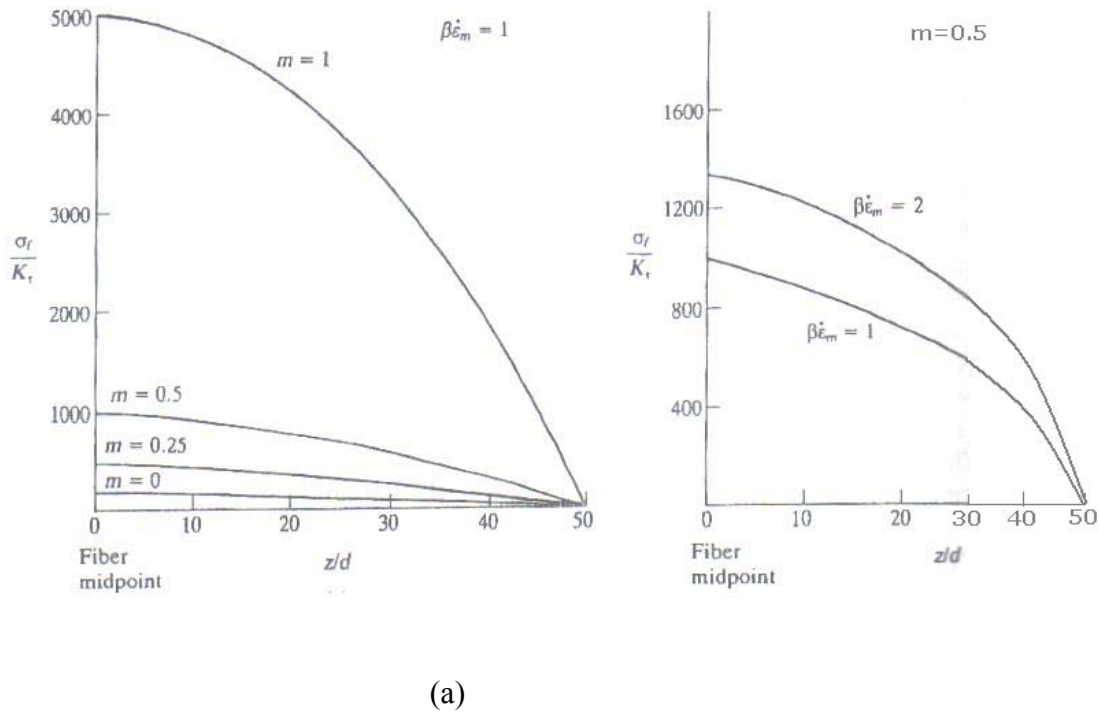
Fig 2.36: The fiber tensile stress, developed via the shear stress as in fig 6.22 as a function of position along the fiber . The variation in σ_f parallels that of τ ; i.e., σ_f increases as the strain rate sensitivity of the matrix increase (a) and is greater ,too when the matrix strain rate is increased(b).

Both Eqs.(2.35) and (2.36) apply only when the maximum fiber load is less than that obtaining for the equal strain condition ($\sigma_f = E_f \varepsilon_c = E_f \varepsilon'_m t$). Since these values of stress are the maximum that can be supported , the variation of σ_f and τ with position when these conditions are met are illustrated schematically in fig 2.37a and b. As shown , the maximum stress increases with time. This means that a low strain (or short times) a great fraction of the fiber is experiencing strain equal to that of the matrix. As time progresses, however , the continuing matrix strain makes it more difficult for this condition to hold. Thus, even though the stress on the fiber increases with matrix strain, it does not do so linearly. In fact, It reaches a constant value given by the suitable average of σ_f along the fiber length as obtained by integrating the σ_f vs. z curve of fig 2.37a. The variation of this average,$<\sigma_f>$ with time is shown schematically in fig 2.37c.
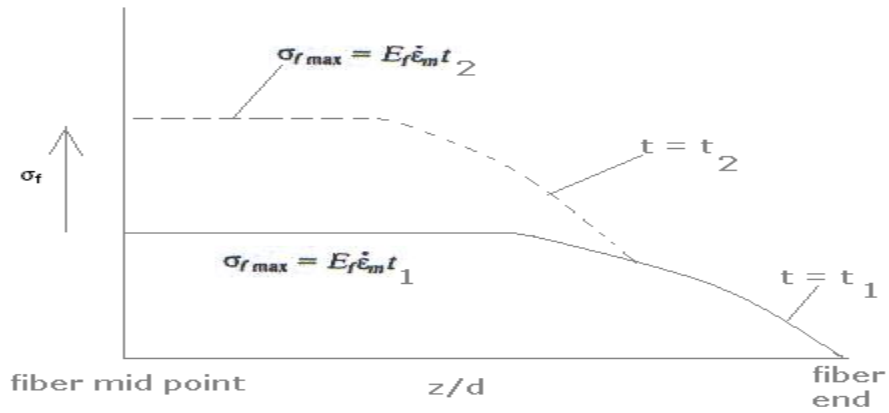
(a)
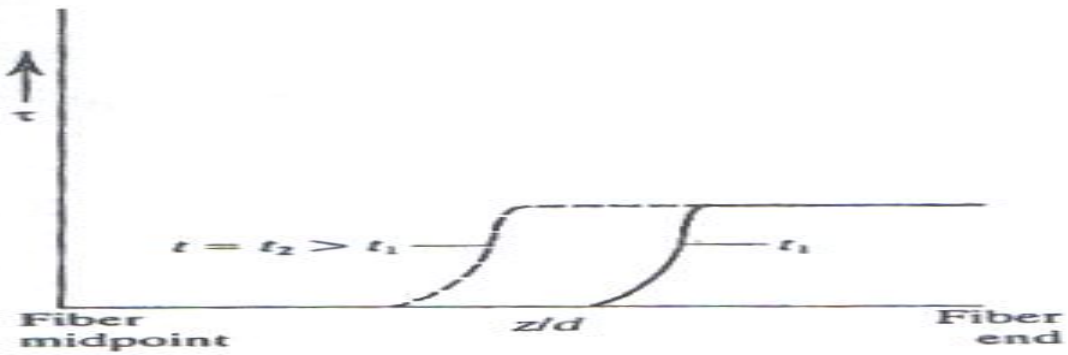
(b)
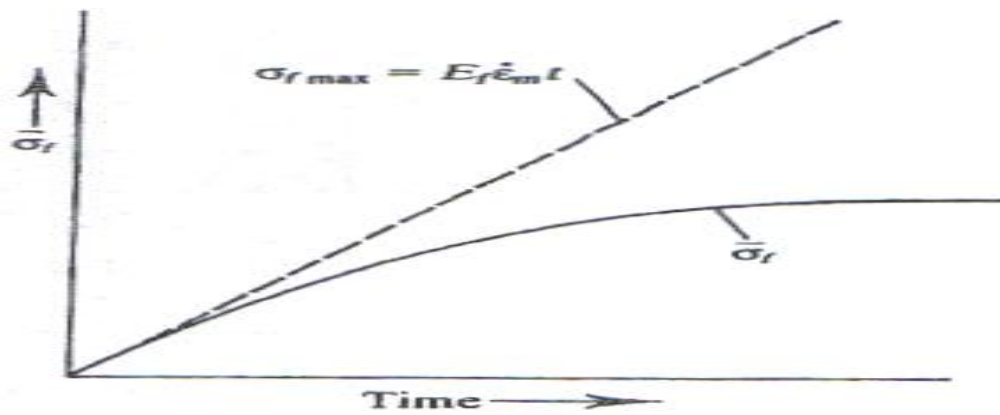
(c)

Fig 2.37 : The variation in τ and σ_f shown in figs(2.35 and 2.36) are appropriate only when the fiber mid point is stressed to a level below that of the equal strin condition and this applies only at long creep times.(a) at shorter times ,σ_f attains the maximum stress and (b) τ approaches zero at the fiber middle . (c) the average fiber stress increases with time but obtained limiting value characteristic of average stress.

60

The VFR for composites containing strain rate sensitive matrices van be expressed as

$$\sigma_c = V_f <\sigma_f>(t) + V_m K_m (\varepsilon'_c)^m \qquad\qquad 2.37$$

where $<\sigma_f> = E_f \varepsilon_c \, g(t)$, with the function g(t) decreasing with increasing time as a result of the effects described above. A stress strain curve for such a composite would , in comparison to that for one containing a nonstrain rate sensitive matrix, exhibit a smaller slope of the σ-ε curve, with such decreases becoming more pronounced with increasing strain.(26,27)

The creep behavior of a composite containing elastic fibers dispersed within a strain rate sensitive matrix can be discussed along similar lines. In a creep test, the composite is subjected to a fixed stress, and the resulting strain rate(ε'_c) and accumulated strain is measured. At the beginning of such a test, the elastic fibers support none of the applied stress since a finite matrix strain must be effected before a fiber matrix interface relative displacement is produced. As strain increases, more of the tensile force is supported by the fibers and the matrix (and composite)strain rate can be written as,

$$(\varepsilon'_c)^m = [(\sigma_c - V_f) <\sigma_f>(t)/V_m K_m] \qquad\qquad 2.38$$

After a certain period , $<\sigma_f>(t)$ attains its limiting value and creep rate becomes constant. The resulting composite strain rate and strain are shown schematically as a function of time and V_f in figs.2.38 a and b. it can be seen that strong fibers are useful in enhancing creep resistance because, in effect, they reduce the stress borne by the matrix. In the latter stages of composite creep , the two phase matrix can be viewed as an aggregate in which the fibers carry a certain fraction of the applied load, but do not deform further. Thus composite creep is caused by matrix flowing by the fibers that are loaded but rigid. (26)

(a)   (b)
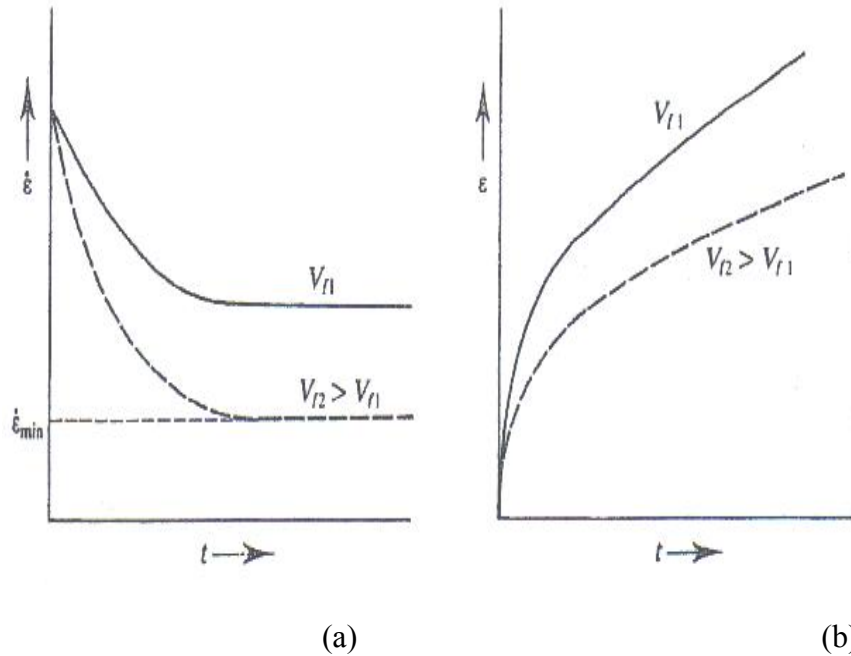
Fig 2.38: (a) Strain rate and (b) Strain for a creeping composite.

2.9 Microscopic effects:

To this point, discussion of composites has been couched in macroscopic terms. In effect, we have assumed that the presence of the fiber does not fundamentally alter the flow behavior of the matrix and vice versa. For this to be true for the matrix , for example, requires an interfiber spacing that is large in comparison to those of other flow obstacles in the matrix. If say, the matrix is metal strengthened by grain size, this requirement translates into the grain size being less than the interfiber spacing. If ,on then other hand , each metal matrix grain contains a large number of fibers, these will act as additional obstacle s to the matrix flow, and any constitutive equation describing composite mechanical response in terms of thee properties of the individual phase will have to take this microscopic feature into account
.

Most currently utilized processing of composite produces fiber dispersions on a scale large enough that microscopic interaction between the phase need not be considered in describing composite properties. However , some fabrication procedures produce in situ composites in which typical interphase spacing are small, on the order of micrometers or less. Examples of such materials are aligned two-phase composite produced by directional solidification of eutectics or directional eutectoid decomposition (fig 2.39).
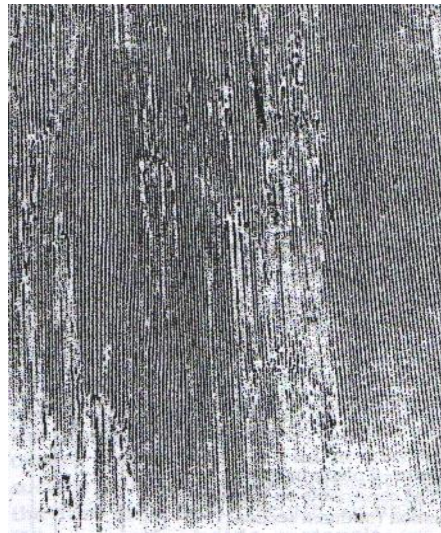
(a)
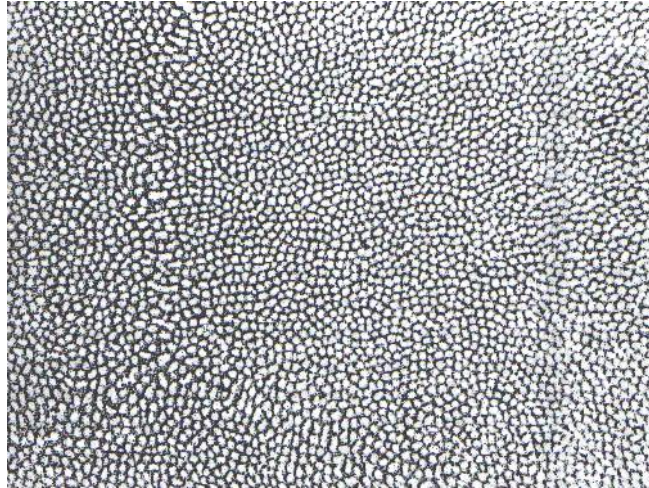
(b)

Fig 2.39: (a) transverse section of a Cr fiber –NiAl matrix composite obtained by eutectic directional solidification. The Cr fibers (ca.1micron meter diameter) extend in and out of the plane of the photograph, (b)longitudinal section of a Co-Co$_2$Si lamellar in situ composite produced by directional eutectoid decomposition. A transverse section of this platelike array would appear very similar. Typical spacings for directionally decomposed eutectoid are an order of magnitude finer than they are for eutectics.

That microscopic effects must be considered in describing the mechanical behavior of in situ composite is demonstrated in fig 6.27, which shows numerous σ – β phase lamellae contained within one grain of a eutectic(eutectoid). In a typical such composite, one of the phases (say σ phase) is stronger and more resistant to plastic flow than the other.(27,28)
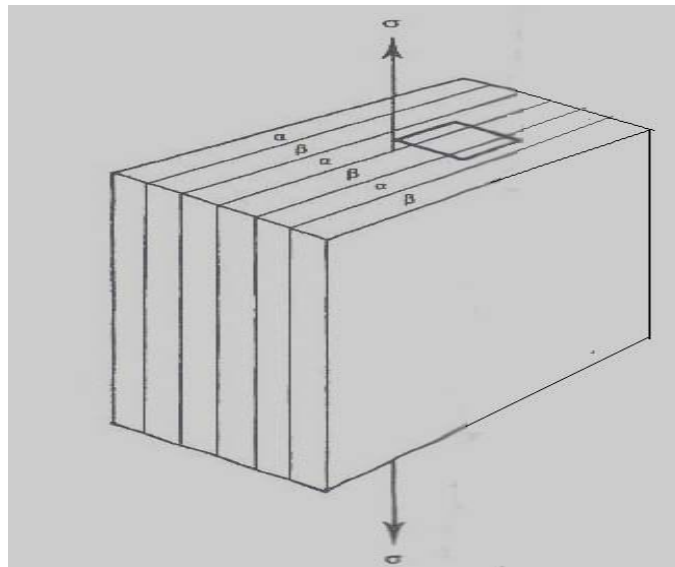
Fig 2.40: An σ- phase and β-phase lamellar array. The constraints on β-phase deformation (outlined section) are provided by the more rigid σ phase , which restricts – phase deformation in the vicinity of the interphase boundary. The deformation constraints becomes more pronounced with decreasing interlameller spacing.

Additionally, the interphase boundary in an in situ composite is frequently of the semi coherent type.

Plastic deformation of the β phase is restricted by the constraints imposed on it by the σ – phase and the interface, and these becomes more effective as the interrphase spacing reduced. Similar consideration apply to in situ fiber composites. Here, the fiber serves as an obstacle to plastic flow as well as load carrying member. A fiber shape , moreover is more effective in terms of increasing matrix flow stress than is a spherical shape , for cross-slip processes by which prismatic loops are left around the particle are more difficult to accomplish when the particle is fibrous in shape. In spite of these complexities, a "modified" VFR can be used to describe the stress- strain behavior of in situ composites. The important modification is the implicit incorporation in it of a matrix flow stress that takes into account the strengthening provided by the other phase.

In situ composites are potentially attractive high temperature materials, as they are chemically stable and quite resistant to coursing processes that, for example, degrade the high temperature properties of precipitation hardened alloys. However, thermal cycling of in situ composites produces an internally generated and likewise fluctuating stress field. This comes about as a result of the different thermal expansion co-efficient of the phase and, in extreme cases, can lead to dimensional instability of parts fabricated from in situ composites. (27,28)

2.10 Elastic deformation:

When a solid is subjected two external forces , it undergoes a change in shape. When load is reached , the shape may not return to what it was prior to the application of the force ; under these circumstances we say that the material has deformed permanently . forces less than cause permanently . forces less than those that cause permanent deformation deform the solid elastically; that is , when the force is subsequently removed , the body returns to the dimensions it had prior to its application.

(a)   (b)   (c)
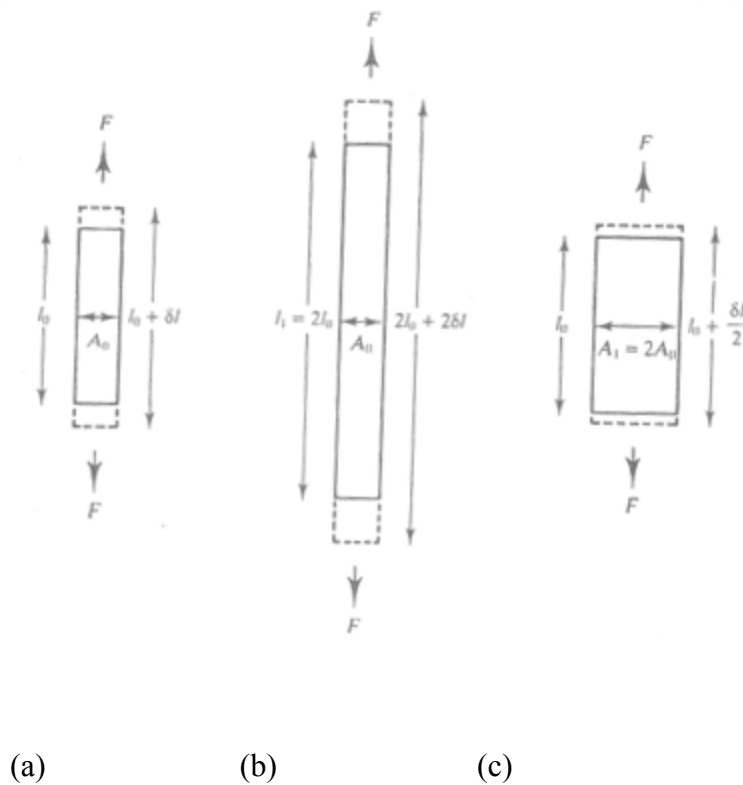
Fig : 2.41 (a) Applied force F with elongation l_0, (b) Applied force F is kept constant   but elongation is double (c) Applied force F is constant but cross sectional area is dougle.

The elastic behavior of many material can be a form of Hook's law. This is illustrated in Fig 2.41.,which indicates that the extension of a sample (=l- l , where l is the sample length prior to , and l is this length following , application of the extending force) is linearly related to the force F , i.e ,

$$(l - l_o) = \delta\, l_o = F \qquad\qquad\qquad 2.39$$

The extension also depends on sample dimensions. For example (fig 2.41b) , a doubling of the initial sample length leads to a doubling of extension, whereas if the sample cross-sectional area normal to the applied force(the transverse cross-sectional area) is doubled , the halved (fig2.41c). Other alteration in sample length or transverse cross – sectional area lead to equivalent results in the sense that extension is found to vary linearly with initial sample length and inversely with cross –sectional area. Thus,

$$(l - l_o) = \delta\, l_o = F l_o\, /\, A \qquad\qquad\qquad 2.40$$

Equation (2.40) is often written in normalized form . that is the "normalized" force is defined by F/A (with dimensions of Newton's per square meter or pound per square inch) ; this ratio is called stress and is given the symbol σ. The "normalized" extension , which is dimensionless, is defined as $\delta l\, /\, l_o$ and is called the strain and given the symbol ε. Thus , esq. (2.40) can be written as

$$\varepsilon = \sigma\, /\, E \qquad\qquad\qquad 2.41$$

 where the proportionality constant E is a property of material , called the young's or tensile modulus.

A material having a high value of the tensile modulus is considered stiff; i.e it is resistant to tensile deformation of the kind just described.

Linear elasticity of this kind is found in all classes of solid materials at all temperatures. It is also the dominant mode of elastic deformation in all solids at low temperatures, and in crystalline solids and inorganic glasses up to moderately high temperatures. The extent of linear elastisicty is , however , usually quite limiteds ; that is , most materials are capable of being linearly elastically extened only to strain on the order of several tenths of a percent.

As shown in figure 2.42 , a change in the shape of material can also be caused by the application o f shearing stresses. These cause the relative displacement of the upper and lower surfaces of the solid shown in this figure .
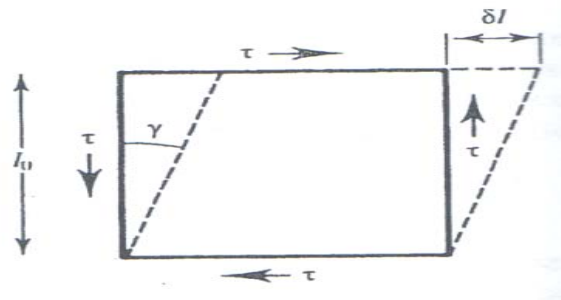
Fig 2.42: A shear stress (τ) distorts the body on which it acts

The shear stress is defined as the magnitude of the shear forces divided by the cross-sectional area over which it acts; it is designated τ. The shear strain ,γ defined in fig 2.42 , is given by the relationship $\tan \gamma = \delta l/l_o$ where δl is the relative displacement of the surfaces and l_o is their vertical separation. When the shear strain is linear elastic one , it is usually small so that $\tan \gamma = \gamma$, and γ and τ are related through

$$\gamma = \tau / G$$

where G is shear modulus , is also a material property . to a good approximation G is a measure of the resistance to bond distortion within a solid. This can be more readily visualized by considering the simple –cubic single crystal of fig 2.43 her the shear force acts on a (001) plane in the [010] direction , with the plane of the drawing representing atoms in a plane (100). The change in atomic position causes the bending of atomic bonds.
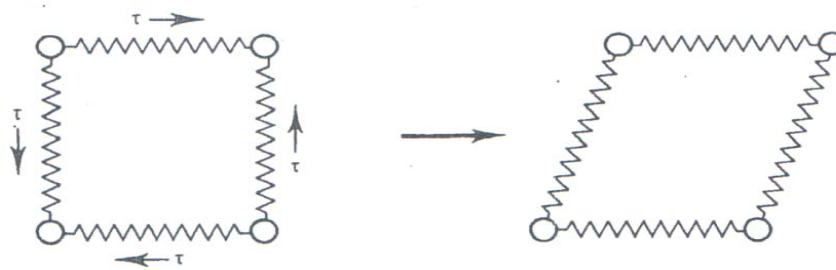
Fig 2.43 : A shear displacement at the atomic level results in bond distortion. Atoms are represented by circles and atomic bonding with springs.

A material 's tensile modulus can be ascertained by careful measurement of the linear stress-strain relation ship in a tension test, which is a test similar to that illustrated in fig 2.41. the shear modulus an be obtained indirectly from a tension test or directly by other testing procedures.

Almost all classes of solids also exhibit , at least over a certain temperature range , non linear and time-dependent elasticity. This viscoelasticity, as it is called , is most common to amorphous

67

polymers, but also occurs in crystalline solids and inorganic glasses, albeit to a more limited extent.
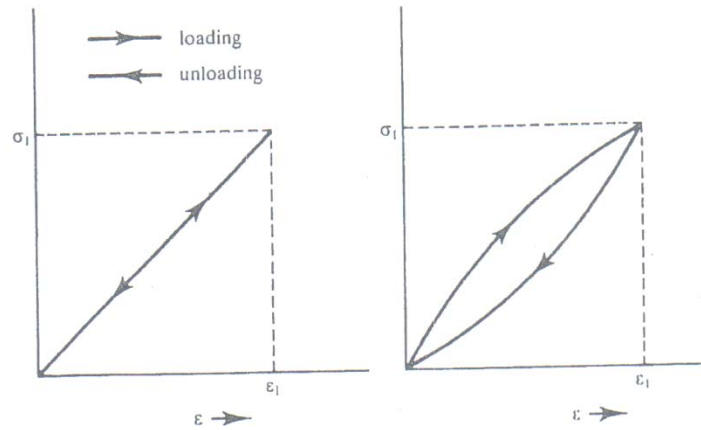
Fig 2.44: difference b/w linear elasticity and viscoelasticity.

One essential difference between this kind of non linear elasticity and linear elasticity is illustrated in fig 1.4. this illustration shows that the strain in a linear elastic solid is a single – valued function of the stress; that is the loading and un loading segments of the $\sigma - \varepsilon$ relationship are coincident (fig2.44A). in contrast, the stress-strain relationship in a viscoelastic material (fig2.44b) depends on the senses of loading. Moreover , the level of stress depends too, on the rate the viscoelastic material will stretched(the strain rate).(25,27)

Viscoelastic behavior is also manifested by a strain that varies with time under conditions of a constant applied stress. That is , upon initial application of the stress some instantaneous(linear elastic) strain is first experienced, after which the material continues to extend and the strain is instantaneously recovered and the viscoelastic strain sluggishly recovered. Non-linear elasticity , of which viscoelasticity is one example , need not be time –dependent. For example , non linear time in dependent elasticity is observed in certain fine , strong crystalline solids called whiskers.

Whiskers typically have diameters on the order of micrometers, and when they arte stretched in tension they deform in a linear elastic way up to strains the order of half a percent. Fro elastic strains in excess of this , and whiskers are capable of such strains, the $\sigma - \varepsilon$ relationship is non linear. An extreme example of non linear tine independent elasticity is found in elastomers. These are the special class of polymers that over a limited temperature range are capable of suffering extension elastic strains (up to the order of a thousand percent or so).

This rubber elasticity is clearly quite different from linear elasticity, which is as mentioned, ordinarily quite limited and , as might be expected, the causes of rubber elasticity differ fundamentally from those of linear elasticity .

2.11   Permanent deformation

A : The tension test.

The material response to uniaxial loading is assessed most often by means of a tension test(fig 2.45). in this test a materiola is ususlly stretched at a specific rate, and the force required to cause an extension δl is measured. Force is measured by means of a load cell that is often a calibrated , stiff spring, and the extension is measured often by means of a device called an extensometer.

Knowledge of F, δl , and sample geometry allows calculations of the stress and strain.
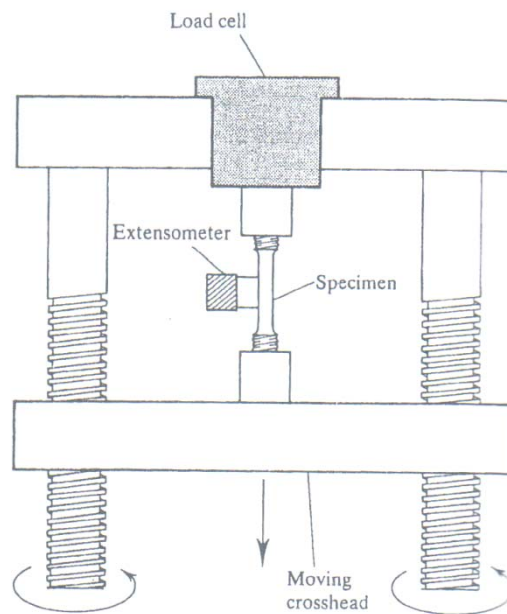
Fig2.45 : A schematic of torsion test

A material's elastic modulus can be measured by such a procedure, although to do so requires a particular accurate measurement of the extension ,since linear elastic strain are limited. Some materials brittle ones manifest only macroscopic elastic deformation up to the stress at which they fracture. Examples include inorganic glasses and many polycrystalline ceramics at room temperature , and some metals and their alloys at low temperatures. On the other hand , most metals at ordinary temperatures, and many ceramics at high temperatures, deform permanently before they fracture. A schematic tensile stress 0strain curve for such nonpolymeric solids that exhibits permanent deformation is given in fig2.46.

(a)   (b)
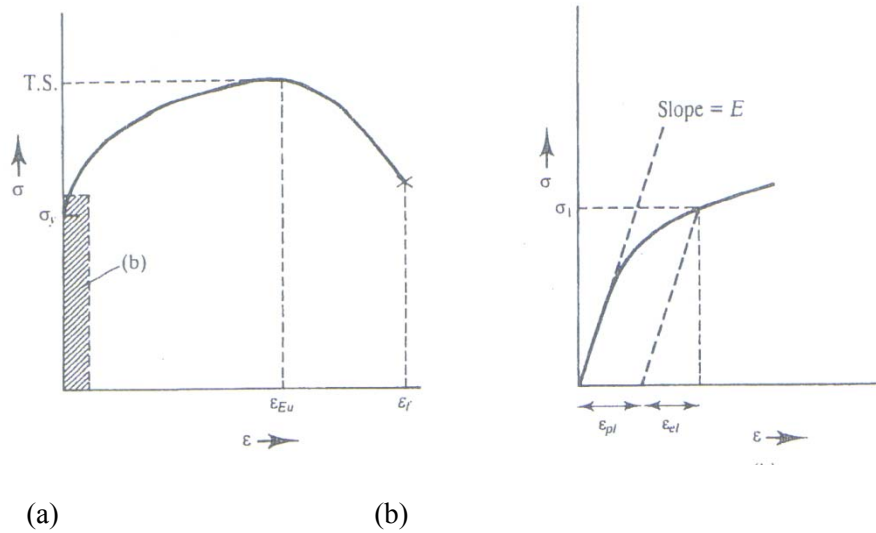
Fig 2.46 : (a) A schematic tensile stress – strain curve, which shows elastic and plastic responcse on stress (b) An expanded view of shaded protion in (a).

If the material is loaded to a stress σ_1 and then the load is removed , some permanent or plastic strain (ε_{pl}) remains (fig 2.46b). Prior to unloading, the strain at the stress σ_1 is $\varepsilon_{pl} + \varepsilon_{el}(\varepsilon_{el} = \sigma_1 /$ E). The transformation linear elastic to plastic behavior is gradual , and it is most difficult to assess accurately the lower limiting stress below which no plastic deformation at all is formed. Consequently , a different strtess , one neede to effect a small but readily measureable plastic strain asi used to characterize a material's resistance to plastic deformation.

This stress is called the yield strength (σ_y) and it can be measured in the manner shown in fig 2.46b. A line parallel to the initial (linear) modulus line is drawn from an offset point on the strain axis (typically ε_{pl} =0.002=0.2%)

The intersection of this line with the stress –strain curve defines the material's offset yield strength σ_y clearly σ_y depends on the specified offset strain , and so this must be stated when a yield strength is quoted. As mentioned, however , quite often the offset strain is 0.002, and this can be assumed in the absence of qualifying remarks.

That σ_y represents the stress required to produce the offset strain can be deduced by recalling that on unloading the material recovers elastic strain according to eq (2.41). thus , if the material were loaded to the stress σ_y and then unloaded , the resulting permanent strain would be equal to the offset strain. Hence while σ_y could be determined by a repetitive loading and unloading procedure, involving measuring the progressively inmcre4sing permanent strain at each unloading step, the offset procedure accomplishes the same end and with far less effort.

Following yielding , the stress required to continue plastic flow (the flow stress) increases with strain (fig 2.46). the positive slope of the stress-strain curve indicates that the material is made

more resistant to plastic deformation by virtue of the deformation itself; that is the material work hardens.

(a)   (b)
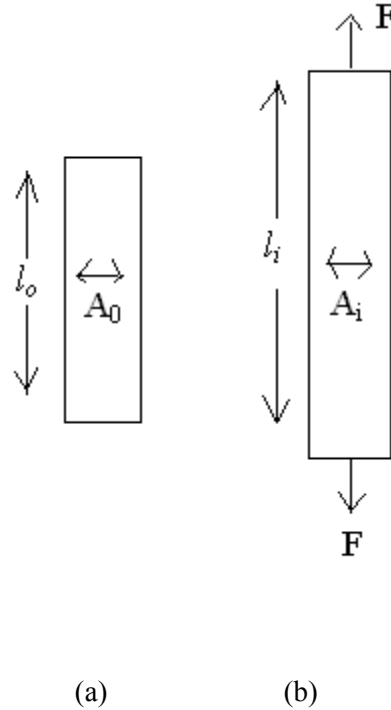
Figure 2.47 : sample dimension change during uniform tensile deformation.

During plastic deformation , the material volume remains constant and if the deformation is uniform along the sample length then the sample shape is changed as shown in fig 2.47b. we se that the original and strained dimensions are related through $A_o l_o = A_i l_i$ where A_o and l_o are the original transverse cross-sectional area and sample length, respectively , and A_i and l_i represents these quantities in the strained condition. As th e cross sectional area decrease with increases strain, the sam0ple experiences an effective stress greater than that suggested via calculation of stress based on the initial cross-sectional area. We can define a true stress (σ_T) as the ratio of force to the instantaneous area; i.e.

$$\sigma_T \quad = F / A_i \qquad\qquad\qquad 2.42$$

hence forth the subscript T will used to designate true stress (or strain) and the subscript E to denote engineering stress(or strain).

 It is also worthwhile to reconsider our definition of strain when plastic deformation is appreciable. On the basis of the comparative gage length remaining the same and equal to the

initial one, each increment of plastic extension δl produce an equivalent strain. However ,as the sample length increases , one should consider then instantaneous gage length as a basis for strain calculation. If this is done , it is apparent that strain is overestimated by the initial definition. True strain is based on instantaneous sample length. It can be approximated by considering the total strain to result from a series of small, incremental extension (δl) with the gage length at each increment being the instantaneous sample length. Thus,

$$E_T = \frac{\delta l}{L_o} + \frac{\delta l}{l_1} + \frac{\delta l}{l_2} + \ldots = \sum_i \frac{\delta l}{l_i} \qquad \text{2.43}$$

Where $l_1 = l_o + \delta l$, $l_2 = l_1 + \delta l$,etc. when expressed in differential form , eq (2.43) becomes exact ; i.e.

$$d\,\varepsilon_T = dl\,/\,l \qquad \text{2.44}$$

on integrating eq 2.44 from $l = l_o$ to $l = l_i$ we have

$$\varepsilon_T = \ln \frac{l_i}{l_o} \qquad \text{2.45}$$

the constant –volume condition of plastic deformation allow relationships to be developed among the various stresses and strains, provided deformation along the gage length is uniform. Equation (2.42) can be rearranged as

$$\sigma_T = \frac{F}{A_i} = \frac{F}{A_o} \frac{A}{A_i} = \sigma_E \left(\frac{A_o}{A_i} \right) \qquad \text{2.46}$$

Since $\left(\dfrac{A_o}{A_i} \right) = \left(\dfrac{l_i}{l_o} \right)$

$L_i = l_o + \delta l$

We have $\left(\dfrac{A_o}{A_i} \right) = \left[1 + \dfrac{\delta l}{l_o} \right]$

So that ,

$$\sigma_T = \sigma_E \, (1 + \sigma_E) \qquad \text{2.47}$$

$\sigma_T > \sigma_E$ for tensile test , a result intuitively deduced previously. In contrast, if the material were compressed so that the cross-sectional area increased during permanent deformation (and $\varepsilon_E < 0$) ,we would find $\sigma_E < \sigma_T$.

For uniform gage length deformation ε_T and ε_E are related through

$$\varepsilon_T = \ln (1 + \varepsilon_E) \qquad\qquad 2.48$$

equation 2.48 shows that $\varepsilon_T < \varepsilon_E$ in a tension test

(i.e., $\ln (1 + x) < x$).

Thus , a point define the equivalent $\sigma_E - \varepsilon_E$ in a stress –strain diagram is disp0laced upwards and to the left to define the equivalent $\sigma_T - \varepsilon_T$ point.

The difference between the true and engineering stresses and strains increases with the extent of plastic deformation . Thus at low strains, $\sigma_T \approx \sigma_E$ and $\varepsilon_T \approx \varepsilon_E$, so that , for example , in our discussion of elastic deformation, there is no need to differentiate between engineering and true stress strain.

As shown in figure 2.46a, engineering stress attains a maximum value at the strain ε_{Eu} . This stress maximum is called the material' tensile strength(T.S., also sometimes called the ultimate tensile strength, U.T.S.). Continued straining beyond ε_{Eu} ,and has begun to work soften for strains greater than this. However materials do not behave so capriciously. Instead, the tensile point is associated with a geometrical instability , and not with a fundamental alteration in material behavior.(15,17)

The geometrical stability associate with the tensile strength can be discussed with reference to fig 2.48 .
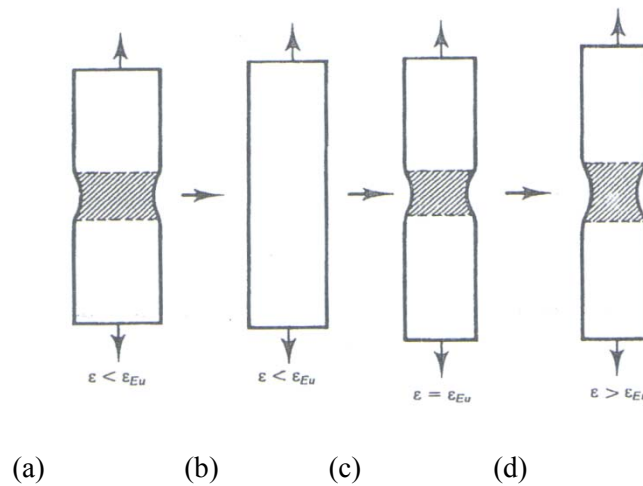
Fig 2.48: Geometrical stability under tensile deformation

Each and every tensile bar has in homogeneities along its length either within it (e.g., small inclusion or porosity) or on its surface (e.g., machining marks or a gradual taper along the bar surface). Strain is localized in the regions of the defects, and this leads to a locally greater reduction in area there (fig 2.48a) . for strains less than ε_{Eu} , the increases in flow stress accompanying the greater strains less enough to lead to removal of the incipient instability(fig 2.48b). this process occurs regularly and repeatedly during tensile loading , and could be monitored if sufficiently accurate instrumentation were available. The rate of work hardening decreases as deformation continue ; that is the increase in flow stress per unit strain becomes less with increasing strain. Thus, it becomes progressively more difficult to work harden an incipient instability sufficient to remove it. At the tensile point the work -hardening capacity has been diminished enough that an instability once formed continues to develop. As shown in fig 2.48c, in a cylindrical bar the instability takes the form of a neck.(12,13)

Clearly ,the criterion for necking is related to the

material 's work hardening tendencies vis-à-vis those that initiate instability .

the criterion can be expressed in a quantitative way by realized that at T.S. the engineering stress or equivalent, the force reaches a maximum , i.e., d F = 0 . using the definition of true stress (eq 1.5) we have,

$$d F = 0 = \sigma_T \, d \, A_i + A_i \, d \, \sigma_T \qquad\qquad 2.49a$$

or

$$\frac{d \, \sigma_T}{\sigma_T} = \frac{- d \, A_i}{A_i} \qquad\qquad 2.49b$$

as the necking criterion.

In other words, the onset of necking is characterized by having the fractional change in flow stress(as defined by d σ_T / σ_T) exactly balanced by the fractional decreases in load –bearing area (as measured by

d A_i / A_i). Prior to necking, $\left| d \, \sigma_T / \sigma_T \right| > \left| d \, A_i / A_i \right|$ and incipient instabilities are removed. Following necking, the instability that eventuates in fracture continues to develop(fig 2.48d).

After the neck has developed, further plastic deformation is constrained to its vicinity. Indeed , the remainder of the sample actually undergoes some elastic strain relaxation as a result of the decreases in tensile force concomitant with neck formation. Because of these considerations the engineering stress strain curve is of little fundamental value when

$\varepsilon > \varepsilon_{Eu}$. Nevertheless, other properties are often quoted from the result of a tensile test. One of these is the fracture strain (ε_f ,fig 2.46a), often called percent elongation when ε_f is expressed in term of a percentage (percent elongation = [($l_f - l_o$)/ l_o] x 100, where l_f is the sample length at fracture). Percent elongation is often taken as a rough measure of a material's ductility. However , since deformation following necking is restricted to the necked region , percent elongation depends on initial sample parameter to have meaning. Although not quoted as often as percent elongation, ε_{Eu} represents the resistance of a material to neck development ; that is, it is a measure of the material 's work – hardening capability. In this capacity the uniform strain can be used to assess a material to manifest a strong resistance to necking. Finally , the uniform strain has one other significance ; it is the strain at fracture that would be found in a sample of " infinite" gage length ; in this respect, it is clearly more of a material property than ε_f .(12- 17)

another measure of material ductility is reduction in area at fracture, usually expressed as percent R.A.(% R.A.= [(A_0 - A_f)/ A_o] x 100, where A_o and A_f represent the initial and final sample cross sectional area is measured as the area of the neck following fracture. Since % R.A. is independent of sample gage length, it is more of a material property than percent elongation. Nonetheless, initial sample cross-sectional areas are usually specified when % R.A. s are quoted.

As a result of the non unifrom deformation following commencement of necking, true stress and strain cannot be calculated from engienrring stress and strain via Eqs.(2.47) and (2.48). however true stress can still be defined as the force divided by the instantaneous area, provided the latter is taken as the minimum(i.e., the neck) cross-sectional area. Some care must be taken when doing this , particularly at the later stages of neck development and at strain close to the fracture strain.

A well-developed neck alters the stress state in the neck region from that of a simple tension , and the effect is that σ_T = (F/ A_{neck}) becomes only an approximation. Additionally , internal voids, which are precursors to final fracture, form in the last stages of a tensile test, and this leads to an underestimate σ_T when it is calculated by the above expression.

By considering the necking as the deforming volume , true strain can be also be redefined following necking.

Before necking , ε_T = ln (A_o / A_i). following necking , it is defined only on a area basis, that is by the latter expression with A_i taken as the neck area. Because confusion often arise as to the condition under which Eqa.(2.47) and (2.48) are appropriate , as well as they are not , table 2.3 synopsizes engineering and true definition of stress and strain , and expression for them apropos to tensile flow before and after necking are also listed there.

Table 2.3

Definition of and relationships between true and engineering stress and strain

Parameters	Fundamental Definition	Prior to necking	Following necking
Engineering stress	$\sigma_E = \dfrac{F}{A_o}$	$\sigma_E = \dfrac{F}{A_o}$	$\sigma_E = \dfrac{F}{A_o}$
True stress	$\sigma_t = \dfrac{F}{A_i}$	$\sigma_t = \dfrac{F}{A_i} = \sigma_E(1 + \varepsilon_E)$	$\sigma_t = \dfrac{F}{A_{neck}}$
Engineering strain	$\varepsilon_E = \dfrac{\delta l}{l_o}$	$\varepsilon_E = \dfrac{\delta l}{l_o}$	$\varepsilon_E = \dfrac{\delta l}{l_o}$
True strain	$E_t = \ln \dfrac{A_o}{A_{min}}$	$E_t = \ln \dfrac{l_o}{l_{min}}$	$E_t = \ln \dfrac{A_o}{A_{min}}$

A graph of type stress –true strain does not demonstrate anything unusual at the tensile strength (fig2.49).
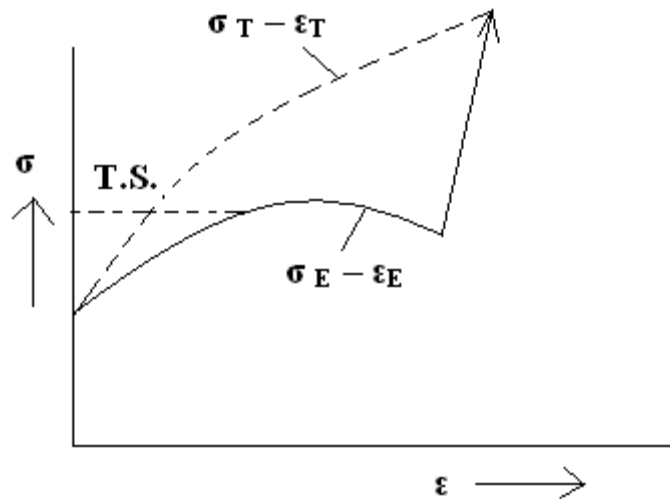
Fig 2.49 A schema showing the relationship between tensile true stress- true strain (dotted line) and enginerring stress-strain (solid line). For enginerring strains less than ε_{Eu}, $\sigma_T > \sigma_E$ and $\varepsilon_t < \varepsilon_E$. the necking point ($\sigma_E$ = T.S.) has no particular significance in the true stress – true strain curve. At some strain greater than ε_{Eu}, ε_t (when calculated on the basis of neck area) becomes greater than ε_E, although σ_T remains greater than σ_E.

This is additional evidence that the necking phenomena is geometric in origin an does reflect changes in material properties. One final point is in order. We have mentioned

that , prior to necking , $\varepsilon_T < \varepsilon_E$. at some strain greater than ε_{Eu}, this is no longer so (fig 2.49). in effect, localized deformation leads to ε_E values that are no indication of the much greater strain effected in the neck region; true strain , as calculated by $\ln(A_o / A_{neck})$, is not subject to such a shortcoming. Equation 2.41 (i.e.,$\varepsilon = \sigma / E$) is a constitutive equation relation strain and stress during the linear elastic portion of tensile loading. This is fundamental basis relating to chemical bond strength that defines the form of this equation similar efforts have been made to develop such ab initio constitutive equations relating stress and plastic deformation , and the degree to which these vary among materials and material classes, has limited the usefulness of such fundamentally based description . As result, for the most part , empirical equation have been bused to describe the plastic –flow behavior of solids. A number of these have been put forth and have been found to describe plastic flow behavior satisfactory. One of the most common relates true stress and true strain by

$$\sigma_T = K (\varepsilon_T)^n \qquad\qquad\qquad 2.50$$

  where n , the strain –hardening coefficient , is a measure of the material's work hardening behavior and K is yielded the strength coefficient . there is no physical significance, per se, to the later parameter ; instead KL can be thought of simply as the true stress required to causes a true strain of unity. On the other hand , and as expected, n can be correlated with a material's resistance to necking . for metals at ordinary temperatures, n is in the range from ca. 0.02 to about 0.50. The stress - strain curve of fig 2.46a accurately schematizes the behavior of many engineering solids, including many metals at temperatures at which they exhibit time-independent plastic flow. However, the initiation of plastic flow in certain solids(including some metals , polymers, and ceramics and depending on temperature, strain rate and structural consideration)does not follow the scenario of fig .2.46. instead these materials exhibit yield point. The room temperature engineering stress-strain curve of a mild steel is characterized by a yield point , as shown fig2.50. (15,16,18)
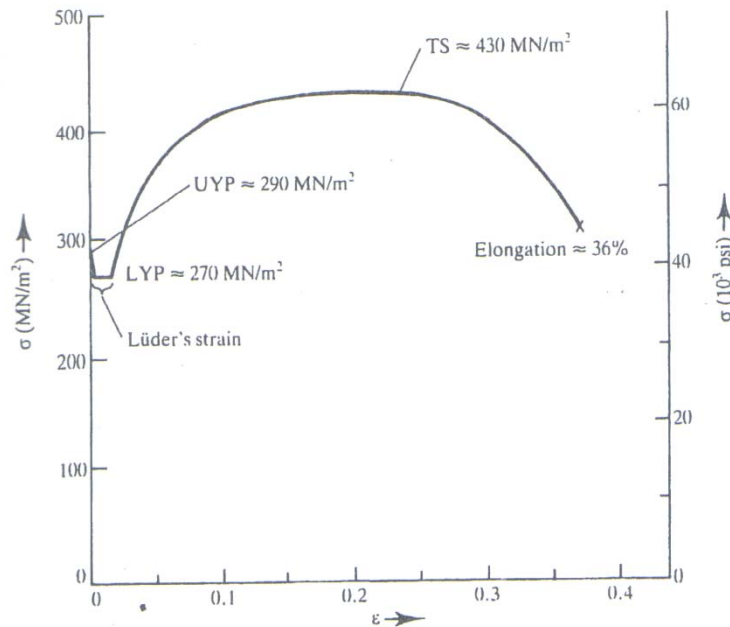
Fig : 2.50 Engineering stress –strain diagram for a mild steel (1018 hot – rolled), which exhibit a yield point. Plastic flow is initiated at the upper yield point (UYP). It is continue at the lower one (LYP). At LYP ,permanent deformation is heterogeneously distributed along the sample length. A deformation bond ,formed at the UYP, propagates along the age length at the LYP. The band occupies the whole of the gage length at the lüders strain. Beyond this point ,work hardening commences((*from K. M. Ralls , T. H. Courtney, and J. Wulff, an introduction to material science and engineering , Wiley, New York 1976))*

A small permanently deformed volume first forms at the UYP and spread along the gage length at the stress LYP until the sample is characterized by a uniform permanent strain . beyond this stage the stress –strain behavior is similar ti that of material that do not exhibit yield point behavior.

For mild steel , the macroscopic strain experienced during this initial nonuniform plastic strain is limited. This is not so for many polymers, which at ordinary temperature often display yield-point behavior. For these materials, the nonuniform strain may be on the order of a hundred percent or more. Ceramics, particularly in single –crystal form , can also manifest yield points under certain strain rate and temperature combinations. For ceramics , the strain immediately following yielding is not always heterogeneously distributed. In these circumstances, the yield point phenomena is evidence of a true "work softening" effect.

The present discussion has described plastic flow when it is time independent. This is generally appropriate for metal and ceramics at ordinary , but not at elevated temperatures. It is almost invariably not so for polymeric solids at temperature at which they exhibits extensive permanent deformation.

78

B : Strain rate sensitivity

As increase in strain rate generally increases the flow stress of a material, although the degree to which it dose so is a strong function of the temperature and is specific to the material. There are a number of reason for the strain –rate sensitivity of flow stress, and they are all related to the atomistic and /or microscopic mechanics of permanent deformation. The strain rate sensitivity of the flow stress is often represented by the empirical equation

$$\sigma_T = K'(\dot{\varepsilon}_T)^m \qquad\qquad 2.51$$

where $\dot{\varepsilon}_T$ is the true strain rate , m is the strain rate sensitivity , and K' a constant that signifies that it is the material flow stress at a true strain rate of unity. The stain rate sensitivity varies between zero (in which case the material is not strain rate-sensitive) and unity (in which instance the stress increase linearly with stain rate and the material is called a viscous solid). High values of m indicate resistance to neck development in tension, just as do high values of the strain –hardening coefficient in eq.(1.13). Thus, in a sense, materials are capable of "strain rate" hardening. This can be illustrated by considering the behavior of a glass rod when it is stretched in tension at high temperature, or by the slow extension of silly putty at room temperature. In both cases , m is unity or close to it the glass at high temperature, and the silly putty at room temperature, draw down to a point(%R.A.= 100)before they mechanically fail , and any "neck" that develops is diffuse one. This behavior is a direct result of thee material's high strain - rate sensitive.

Metals and alloys at ordinary temperatures are not particularly strain rate sensitive; e.g. for most of these material m = 0.00-0.10 at room temperature. Their strain rate sensitive increases with temperature and for certain metallic alloys "m" can be as ca. 0.8 over a limited range of temperature and stress. The associated resistance to neck development renders them "super plastic" at the appropriate stress –temperature combinations, and allows them to be extensively deformation – processed.

The flow stresses of amorphous polymers at temperature at which they can be permanently deformed are generally more strain rate –sensitive than metals' flow stresses. As with metals , m increase with temperature for polymers, but for this classes of materials the strain rate 0-sensitivity approaches unity as the equilibrium melting temperature is reached. Equation 2.51describes strain rate hardening in the absence of strain hardening , whereas eq. (2.50) describes strain hardening in the absence of strain –rate sensitivity. When both kinds of hardening are important , these equations can be combined to incorporate both effect ; that is , we can write

$$\sigma_T = K''(\varepsilon_T)^n \ (\dot{\varepsilon}_T)^m \qquad\qquad 2.52$$

we see that when the material does not strain harden (n=0), eq. (2.52) reduces to eq. (2.51) and K'' = K' .

Conversely, when m =0 , it becomes Eq. (2.50) with K''=K' .

The form of equation (2.52) indicates clearly that hardening is caused by increases in both strain and strain rate, and that high values of n and m are associated with this effect.

2.12   Hardness test:

Hardness test is a some what imprecise term . It is essential a measure of a material's resistance to surface penetration by an indenter with a force applied to it since the indentation process takes place by plastics deformation in metals and alloys. Hardness is inherently related to these material's plastic flow resistance. However brittle solids ,such as glass and polycrystalline ceramics at room temperature, can be

indentation –hardness tested. That they can be indicates that the materials are capable of plastic s flow , at least at the microscopic level.

However indentation hardness testing of brittle solids is frequently accompanied buy micro crack formation, and this makes the relationship between hardness and flow strength less direct than it is for metals.

As mentioned , indentation is accomplished by applying a load to a suitable indenter positioned on the material ' surface . to achieve the purpose of the test, the indenter material must be considerably harder than the material to be indented. Typical indenters are hardened steel and diamond and depending on the material tested and the type of test, various combination of load and indenter are used I hardness testing.

2.13 Fracture:

2.13.1 Tensile fracture:

Tensile fracture refers to mechanical failure taking place under conditions of a positive mean pressure. The microscopic processes accompanying crack nucleation and crack propagation during tensile loading.

Ductility fracture is characterized by a finite %R.A. in tensile tested by the formation of a neck prior to fracture. Ductility fracture is observed in most polycrystalline metals at ordinary temperatures, in metallic and many nonmetallic single crystals at even lower temperatures, and occurs in certain polycrystalline nonmetallic at somewhat higher temperatures.

Fracture is frequently promoted y microscopically heterogeneous plastics deformation. This can be caused by inherently heterogeneous plastic flow or by that associated with internal boundaries(e.g., grain boundaries or in many case interphase boundaries between precipitates or inclusion and the matrix). The plastic strain gradient accompanying this kind microscopic flow results in internal stress concentration that serve first to nucleate cracks or voids(e.g., by inclusion fracture or decohesion) and then to promote their subsequent growth. Void growth takes places by plastic deformation processes and, when the intervoids spacing becomes small enough , the voids link up by a mechanical shearing process. In a tensile test this produces an internal penny-shaped crack, with final tensile separation happening by shearing of the "tube" surrounding the crack. High values of % R.A. are promoted ,therefore by,

(1) prevention of crack nucleation.
(2) Having a small density of potential void nucleation sites
(3) Having the voids grow to a large extent before the link up.

In this sense , %R.A. is a measure of a material's fracture resistance as well as of its malleability. When a brittle material is tested I tension , its R.A. is zero or is limited to a few percent , and necking does not occur . thus , a brittle solid manifests no .or only very little, capacity for macroscopic permanent deformation. In some brittle solids, microscopic plastic deformation is also not associated with crack propagation ; glass at room temperature is an example. For these materials, preexisting surface or interior cracks serve as the crack nuclei. Stress is concentrated at the tips of such flaws and when the resulting stress magnification attains a crack , the less the applied nominal stress has to be to cause fracture; that is the stress concentration is increased larger flaws.(24,26,27)

In some "brittle" solids (e.g., some polycrystalline metals at low temperatures and some polycrystalline nonmetals at low and intermediate temperatures) microscopic plastic deformation precedes crack nucleation , and may also accompany crack propagation. Thus even though macroscopic plastic deformation is quite limited, such deformation takes place on a microscopic level , and the materials are , therefore ,"tougher" than inherently brittle material such as glass.

As mentioned ,the fracture criterion for many solids is associated with the mean pressure ($p_m = I_1$ / 3) reaching a critical value . In a tensile test this is equivalent to the applied stress attaining a value directly related to the critical mean pressure.

Materials, especially inherently brittle ones , can also fail under compressive loading. This is unexpected on the basis of pervious discussion , and especially surprising is that rather than by the continuing to grow individually. The later criterion is clearly analogous to the one controlling void link up during low temperature fracture.

The creep fracture strain is composed of two parts : due to the creep strain itself and that resulting from void growth following void nucleation. The later strain can be appreciable if voids are distributed homogenously throughout the material volume and their link up occurs with I the grains, leading to transgranular creep fracture. However the frequently the voids whose growth leads to eventually fracture are situated on the grain boundaries. Intergranular creep fracture(ICF) happen s these circumstances, and the strain due to the void growth in these cases is limited.

Indeed, %R.A., for ICF is closed to zero , and the macroscopic ICF surface appearance bears a distinct resemblance to a low – temperature brittle fracture, even though considerable permanent deformation may precede ICF.

Stress state influences creep fracture ,just as it does other kinds of fracture. One particularly important factor differentiates low – and high- temperature tensile fracture. Without an applied external tensile force, voids spontaneously shrink at high temperature and they eventually disappear, this sintering does not happen at low temperature because atomic motion is responsible for it cannot take place the extent necessary to effect void shrinkage. Void shrinkage is accelerated further by compressive stresses. Thus, void growth leading to creep fracture does not occur under this kind of loading and, infect , a tensile stress exceeding the inherent "void shrinkage stress"(called the sintering limit) must be applied for void growth to occur.

even some ductile materials can fracture under this kind of loading. However , heterogeneous plastic deformation can serve to concentrate stress and cause crack nucleation under compressive , as tensile ,forces. Some of these cracks will be oriented at angles to the loading axis conducive to their propagation, and this is what leads to compressive fracture of ductile solids. However both the crack nucleation an crack propagation stress are higher in compressive than in tension.

The preexisting cracks in a brittle solid can also lead to compressive fracture in them, even though the compressive fracture stress is typically much greater than the tensile one. As with the ductile solids described above , some cracks are oriented with respect to applied stress in a way faroverable their growth. Current ideas on this type of fracture, which is prone to large experimental variations in measured fracture strengths, involve statistical analysis of crack size ,shape , and orientation with respect to the loading axis.

Fracture caused by void nucleation and growth also occurs at high as well as at low temperatures.

2.13.2 Creep fracture:

Material at high temperature can flow plastically and eventually fracture under condition of a constant external stress. The continuing permanent deformation with time at a fixed stress is called creep, and the resulting failure is called creep fracture. Creep deformation and fracture are both related to thermally assisted deformation processes that provide for and /or assist creep strain , the void nucleation events, and the subsequent growth of voids until they link up , resulting in material failure.

Some material at high temperature neck down to a point before separating into two parts. Thus %R.A. = 100 for these viscous solids, as they are called .more limited high – temperature R.A.s., however ,are far more common. Void nucleation in these solids is thermally assisted ,and takes place at regions of microscopic heterogeneous deformation such a grain boundaries and /or particle – matrix interfaces.

It should be noted ,though ,that thermally assisted deformation to some extent relaxes strain gradient associated with heterogeneous deformation; this kind of stress relaxation dose no t happen at o5rdinary temperatures. Thus strains at which voids are nucleated at high temperature are often greater than they are at low temperature.

Nucleation voids often grow by the same deformation processes responsible of creep strain. Creep fracture take place when voided volume fracture attain some critical value or when the intervoid spacing becomes small enough that the void link up by the permanent deformation

2.13.3 Fatigue fracture:

Fatigue refer to material failure under a time – varying stress that would not result in fracture under an equivalent static applied stress. For example if a material were loaded at low temperature to a stress below its tensile strength and the stress were held constant thereafter , the material could with stand this load indefinitely without fracture. However ,if it were loaded initially to this same stress and then the stress reduced somewhat, followed by an increase to the initial stress, and the process were repeat as shown in fig 2.51the material might eventually fracture.
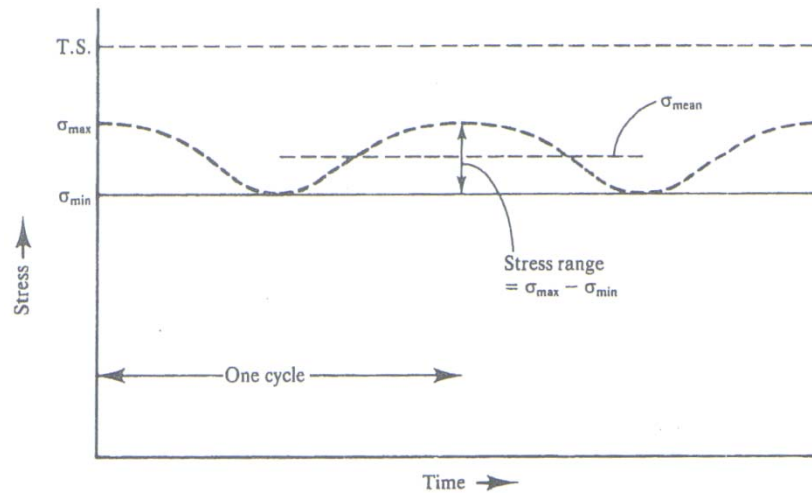
Fig : 2.51 A time varying tensile stress that could eventuate in fatigue fracture. The maximum stress is less than the material tensile strength (the stress needed to cause static tensile failure). The number of stress cycle required to cause fatigue rapture depends on the material and the stress range (σ_{max} - σ_{mim}) and the mean stress(½)(σ_{max} + σ_{mim}). The higher stress range and higher the mean stress, the fewer the number of cycles of failure.

In many cases the stress range are large enough that the material deformed plastically at a macroscopic level. when this happen fatigue lives correlates better with the plastic strain range than they do with the stress range or men stress. During high – cycle fatigue the material deforms only elastically in a macroscopic sense. Fatigue lives then correlates equally well with elastic strain range($\Delta\varepsilon_{el}$) and the stress range ,since the two are related through $\Delta\varepsilon_{el} = \Delta\sigma / E$, where E is the material 's modulus.

Plastic deformation takes place even during high – cycle fatigue, albeit on a microscopic , rather than macroscopic ,scale. Local stress concentration or microstructural inhomogeneities promote this kind of flow , and the repetition nature of the loading eventuates in nucleation of a crack in region deforming in this way. After a certain time the crack continues too grow slowly and in a direction normal to the stress axis (for uniaxial loading). The arte of crack advance per cycle (the crack growth arte) is many cases found to correlate well with the stress range , the mean stress having a decidedly secondary effect on the slow crack growth rate. After the neck has grown to some critical length , it advances rapidly and fracture ensues. The latter is caused either by having the cross – sectional area reduced to extent that the material cannot withstand

the maximum applied stress or by the crack ti having grown to a sufficient depth that the maximum stress- crack depth combination exceeds the material ' critical stress intensity factor.

Fatigue fracture surfaces often mirror the processes described above. For example , visual inspection of a fatigue fracture surface is often sufficient to delineate clearly the respective areas of fast and slow crack growth. The latter are often smooth and burnished as a result of the abrasive of the separated mating surfaces during the slow crack growth period. Moreover ,if the material is exposed to a corrosive environment , corrosion products (e.g., rust, if the material is a steel) are often developed on the slow crack growth surfaces.

At the microscopic level , particularly when high cycle fatigue is occurring, the slow crack growth surfaces are often characterized by fatigue striae. These are ridge or undulation on the fracture surfaces, with spacing between these features being the distance of slow crack advance per stress/ strain cycle. The presence of striae is often used to identify a failure as being due to cyclic loading. However , it is important to note that they can be obscured by environmental and other factors associated either failure, and therefore lack of a clear – cut identification of striae does not necessarily mean the failure was not due to fatigue. The other side of the coin is that attritions are found in other cases of intermittent crack growth (e.g., as happened in some environmental assisted fracture.

The response of a material to cyclic loading Is different from that to monoatomic loading. The tensile flow curve serves as an example of monoatomic loading and, at least at low temperatures , work hardening is a ubiquitous characteristics of such a curve. In contrast, metals may either work harden or work soften during cyclic deformation . if the stress required to maintain a specified maintain range decreases with the number of cycles, the material is considered to cyclically soften , whereas soften alloys of the same material cyclically work harden. In some cases the "steady state" cyclical flow stress is independent of the same material may eventually require the same cyclical stress range to produce the same cyclical strain, even through the cold work alloys initially required a much greater stress rang than the annealed one. When this occurs, an equivalent steady state deformation microstructure which can be observed electron – microscopic level ,characterize the alloy. One knowledge of the cyclical deformation behavior of the materials has increased rapidly in the past decade or so. This will eventually add immeasurably to our basic knowledge of fatigue mechanism.

Brittle solids, such as glass and many polycrystalline ceramics at room temperature, are not considered subject to fatigue. This is because, if fatigue crack do form in them, they grow to a size sufficient to induce brittle fracture after only a few cycles. Polymers are subject to fatigue, and in a phenomenon logical sense their cyclical response comparable to that of metals.

But the microscopic manifestation of fatigue in the two classes of materials are often quite different. As one example, the viscoelastic character of many polymer leads to hysteretic heating,

and an increase in temperature of the material during cyclical loading. As a result, polymer fatigue lives are sensitive to the frequency of cyclical stressing / straining, whereas this is seldom the case for metals. Certain micrsocpic features of polymer deformation , particularly at temperature near their glass transition temperature, also make their response to cyclical loading differ from that of metal.

CHAPTER # 3

Materials and Experimental Setup
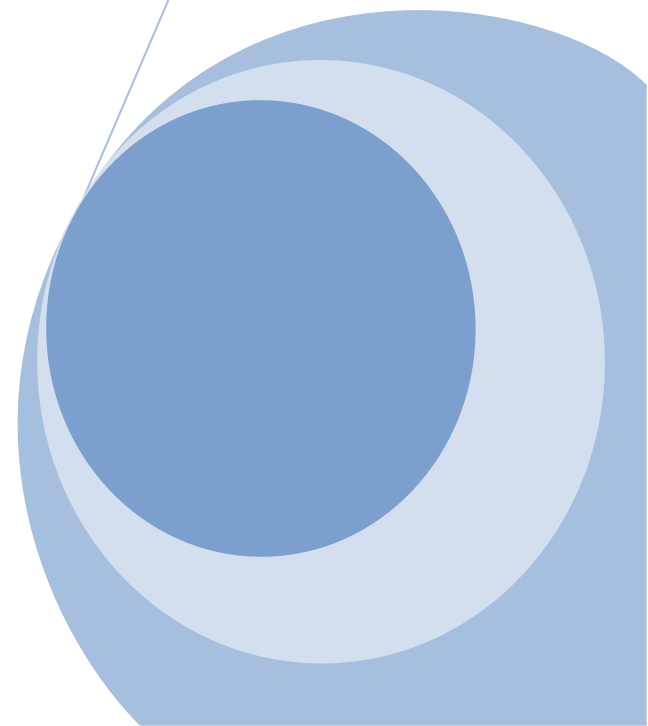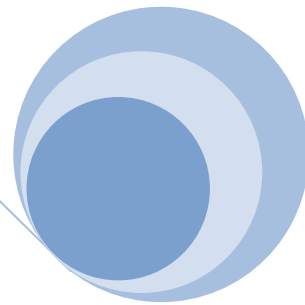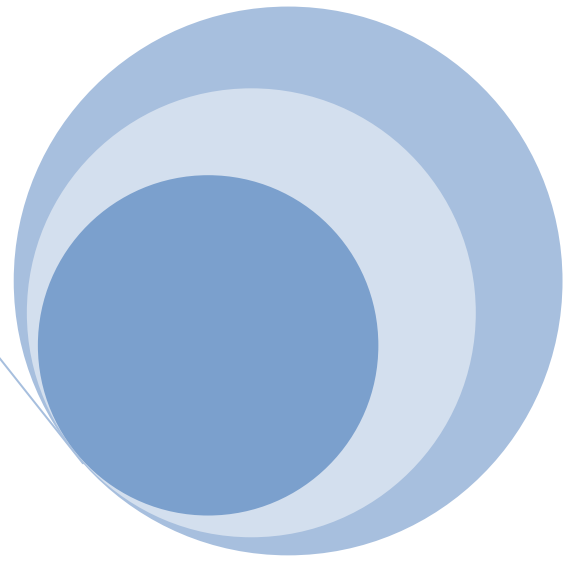
3.1 <u>**Aim of research work**</u>

The purpose of this research work is the investigation of passive and active composite armor with the best of the following properties:
1) Tensile strength
2) Impact strength
3) Fracture toughness
4) Fracture analysis

3.2 <u>**Materials and their properties**</u>

3.2.1 Ethylene-Propylene-Diene-Terpolymer

It belongs to a family of synthetic rubbers that is prepared by polymerization of ethylene, propylene and optically, a non conjugated diene. Unlike the majority of synthetic elastomers, these polymers contain a saturated backbone.

Degradation of synthetic elastomers often occurs by reactions involving backbone double bonds (attack by ozone, oxygen, ultraviolet, etc.) , which results in bond cleavage and loss of physical properties. The saturated backbone found in EPDM is fairly resistant to chemical attacks. this gives EPDM excellent weatherability and heat resistance. In use
EPDM will not develop cracks due to reactions with ozone, oxygen, and light as readily as other elastomers. Due to the nonpolar hydrocarbon nature of polymer, EPDM has excellent water resistance but poor oil resistance.(10)

$$-CH_2-CH_2-CH_2-CH_2-CH-CH-CH_2-CH_2-CH_2-CH-$$
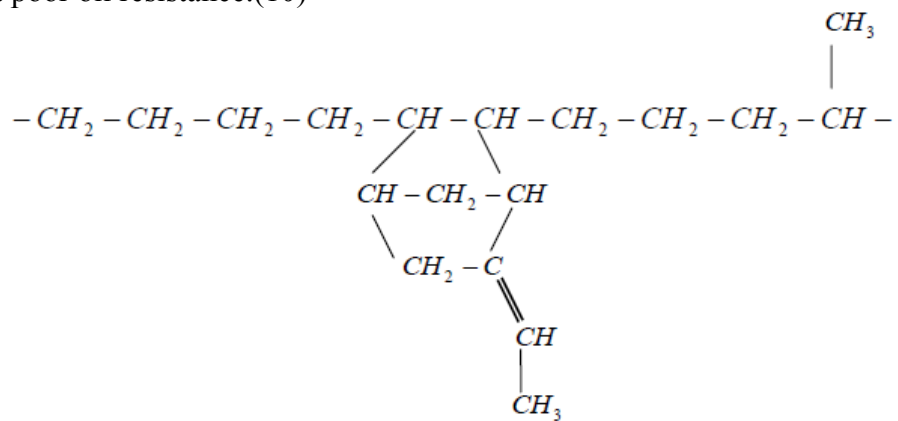
Formula of EPDM

3.2.2 Characteristics of EPDM

Table 3.1   Characteristics of EPDM

Advantages	Limitations
• Good mechanical properties flexing and resilience characteristics. • Outstanding resistance to ozone and weathering. • Wide range of operating temperatures: continuous 125o C (specials 175o C) intermittent exposure to 200o C, low temperature flexibilityis good at -70o C; retains 60% of tensile strength at 100o C. • Resistant to superheated steam and hot water. • Good resistance to acids and bases. • Accepts paints. • Wide range of formulations with compounds exhibiting high and low hysteresis for energy absorption and resilience respectively. • Some formulation suitable for injection molding. • Excellent abrasion resistance.	• Moderate adhesion to fabrics and metals. • Must be reinforced with Carbon black or special white fillers. • Very poor oil and hydrocarbon resistance. • Tear resistance not as good as NR but similar to SBR. • Relatively new elastomer class.

3.2.3 Carbon black

Carbon black is composed of ultrafine particles of 10-400 nm diameter that aggregates: this aggregate is the so-called "structure." Carbon black is 90-99% carbon, 0.1-10% oxygen, 0.2-1.0% hydrogen , and a small amount of sulphur and ash.

Carbon black has oxygen-containing groups, such as carboxyl, phenolic hydroxyl, and quinonic oxygen groups on the surface. It is well known that these functional groups undergo normal organic reactions, such as methylation, esterification, neutralization, and nucleophilic substitution.

3.2.3.1   Properties

Carbon black is heat resistant, chemical proof, weather proof, lightweight, electroconductive, a deep black pigment, and a low thermal expansion. It is widely used industrially as a filler of polymer-composite. Carbon blacks are also excellent reinforcing agents for rubbers.

By surface grafting polymers onto carbon black, the dispersibility in solvents and compatibility in polymer matrices are markedly improved. IN addition, grafting onto carbon black enables us to give various functions to carbon black such as photosensitivity, bioactivity, cross-linking ability, and an amphiphilic property. Therefore, the surface grafting of various polymers onto carbon black has been widely investigated.(13)

3.2.3.2   Applications

It can be used in electrical shielding, heating, and the prevention of static electricity accumulation. Because polymer grafted carbon blacks disperse uniformly in organic solvents and polymer matrices, it is possible to make conductive materials with uniform conductivity over the entire surface. In addition, polymer-grafted carbon black-polymer composition, which was cross linked with a variety of cross-linking agents, shows a large positive temperature coefficient (i.e., at near the glass-transition transition temperature or melting point of the matrix polymer). This is considered to be a result of widening the gap between carbon black particles and/or decreasing the carbon content by thermal expansion of the polymer matrix.

Only about 10% of carbon black products are used in non-rubber applications, these consist of: plastics (36%), printing inks (30%), coating (9%), paper (4%), and miscellaneous applications. The blacks for these applications are produced primarily by processes other than the furnace method.

In plastics, carbon black can have several functions: electrical conductance, UV shielding, opacity, pigment, and mechanical performance improvement. These properties have been used in wire and cable manufacture for electromagnetic interference and electrostatic shielding, in plastics protection of UV degradation or to provide color. Each application needs special carbon black properties.

With the development of xerography carbon black continues to be the most important pigment in printing or duplicating toner applications. The black loading in toner particle formulation is 5-10%. High blackness, good dispersion, and electric properties are necessary in this case. Uses of carbon black in inks, paints, and coatings have similar requirements as in the xerographic toners, but with specific rheological property in liquid media.

3.2.4 Silica

Chemically, the most simple silicate material is silicon dioxide, or silica (SiO_2). Structurally it is a three dimensional network that is generated when every corner oxygen atom in each tetrahedron is shared by adjacent tetrahedral. Thus the material is electrically neutral and has stable electronic structures. Under these circumstances, the ratio of Si to O atoms is 1:2. If these tetrahedral are arrayed in a regular and ordered manner, a crystalline structure is formed. There are three primary polymorphic crystalline forms of silica: quartz, cristobalite and tridymite. Their structures are relatively complicated, and comparatively open; that is the atoms are not closely packed together. As a consequence, these crystalline silica have relatively low densities; for example, at room temperature quartz has a density of only 2.65 g/cm^3. The strength of the Si-O interatomic bonds is reflected in a relatively high melting temperature 1710 ^{O}C. It improves dimensional stability, thermal conductivity, electrical insulation, moisture resistance and also increases gas transition temperature, modulus and compressive strength. It reduces swelling in solvents.

3.2.5   Other ingredients used

Some other ingredients are also used for manufacturing of different EPDM based composites. Zinc oxide is used as a filler and curing agent. Stearic acid and wax as processing aids. N-tert-butyl-alpha-phenyl-nitrone (PBN) as a stabilizer and as an 30 Oxidant. Mercaptobenzothiasole (MBTS), diphenylguanidine (DPG) as curing agents as well as accelerators and sulphur as a curing agent.

3.3 **Common Raw Materials & Their Properties**

There are three factors which mainly constitute a composite:
  1. Matrix Material
  2. Reinforcement
  3. Interface/Interphase

3.3.1 Matrix Material

The matrix serves two very important functions:
It holds the reinforcement phase in place, and under an applied force it deforms and distributes the stress to the reinforcement constituents. Sometimes the matrix itself is a key strengthening element. In other cases, a matrix may have to stand up to heat or cold. It may conduct or resist electricity, keep out moisture, or protect against corrosion. It may be chosen for, weight, ease of handling, or any other properties.

Polymers are particularly attractive as matrix materials because of their relatively easy process-ability, low density, and good mechanical and dielectric properties. High-temperature resins used in composites are of particular interest to the high-speed aircraft, rocket, space, and electronic fields. The temperature capability of matrix resin is determined by its softening temperature, its oxidation resistance, or its intrinsic thermal breakdown.

Polymers are structurally much more complex than ceramics. They are cheap and easily possible. On the other hand, polymers have lower strength and modulus and lower temperature use limits. Prolonged, exposure to ultraviolet light and some solvents can cause the degradations of polymer properties. Because of predominantly covalent bonding, polymers are generally poor conductors of heat and electricity.(16,30)

Polymers, however, are generally more resistant to chemicals than are metals. Structurally, polymers are giant chainlike molecules (hence the name macromolecules are also used) with covalently bonded carbon atoms forming the backbone of the chain.The process of forming large molecules from small once is called polymerization; that is, polymerization is the process of joining many monomers, the basic building blocks together to form of polymers. There are two important classes o polymerization.

a. Condensation Polymerization
In this process there occurs a stepwise reaction of molecules and in each step a molecule of a simple compound, generally water, forms as a by-product.

b. Addition Polymerization
In this process monomers join to for a polymer without producing any by-product. Addition polymerization is generally carried out in the presence of catalysts. The linear addition

of ethylene molecules (CH_2) results in polyethylene (a chain of ethylene molecules), with the final mass of polymer being the sum of monomer masses.

Two major classes of polymers produced by either condensation or addition polymerization, based on their behavior, are thermoplastic polymer. Their different behavior, however, stems from their molecular structure and shape, molecular size or mass, and the amount and type of bond (covalent or Vander Waals). We first describe the basic molecular structure in terms of the configurations of chain molecules.

(i) Linear Polymers

As the name suggests, this type of polymer consists of a long, chain of atoms with attached side groups. Examples include polyethylene polyvinyl chloride, and polymethyl methacrylate.

(ii) Branched Polymers

Polymer branching can occur with linear, cross linked, or any other type of polymer.

(iii) Cross Linked Polymers

In this case, molecules of one chain are bonded with those of another cross linking of molecular chains results in

(iv) Three Dimensional Network

Cross-linking makes sliding of molecules past one another difficult, thus making the polymers strong and rigid.

(v) Ladder Polymers

If we have two linear polymers linked in a regular manor we get a ladder polymer. Not unexpectedly, ladder polymers are more rigid than linear polymers.

There are three ***principal types*** of polymers:
    a. Thermoplastics
    b. Thermosets
    c. Copolymers

a. Thermoplastics

The thermoplastics are largely one- or two –dimensional in molecular structure. At high temperature they soften and show a discrete melting point. The process of softening at temperature and regaining rigidity upon cooling is a reversible one. These molding compounds are processed by us of conventional techniques of compression, transfer, or injection molding or extrusion. Polyethylene, polystyrene, polypropylenes, polyamides, and nylon are examples of thermoplastics.

Thermoplastic-reinforced resin systems are the most rapidly growing class composites. In this class the focus is on improving the base properties of the resin to allow these materials to perform functionally in new application or in those previously requiring metals, such as die casting. Thermoplastics may be crystalline or amorphous. For crystalline thermoplastics may be

significantly influenced by the reinforcement,which can act as a nucleation catalyst. In both types there is range of temperature over which creep of the resins increases to the point where it limits usage. The reinforcement in these systems can increase failure load as well as creep resistance. Some shrinkage also occurs during processing, plus a tendency of shape to remember its original form. The reinforcement can modify this response as well. Thermoplastic systems have advantages over thermosets in that there is no chemical reactions involved that cause release of gas products or exothermal heat. Processing is limited only by the time needed to heat, shape, and cool the structure, and the material can be salvaged or otherwise reworked. However, solvent resistance, heat resistance, and absolute performance are not likely to be as good as those of thermosets.

Generally, thermoplastics resins are marked in the form of molding compounds. Usually, these compounds are reinforced by short glass fibers.

Graphite and other fiber materials may also be used, in most cases; the fibers are dispersed randomly, making the reinforcement nearly isotropic. Molding processes, however, may cause the fibers to lie directionally.

Fillers can be added to raise the heat resistance of thermoplastic, but all thermoplastic composites tend to lose strength dramatically at high temperature. At normal temperature however, thermoplastic composites offer toughness rigidity, and resistance to creep.

b. Thermosets

Thermosets, on the other hand, develop a well-bonded three dimensional molecular structure upon curing. Once cross-linked or hardened, these polymers will decompose rather than melt. The condition necessary to effect cure and the characteristics of the uncured resin can be varied by changing the formulation. Moreover, some thermosets can be varied held in a partially cured condition (B-stage) for prolonged periods of time. This inherent flexibility makes the thermosets ideally suited for use as matrix materials for the newer continuous fiber composites. Most often, however, the Thermosets are used in chopped fiber composite in which the starting material is a premix or molding compound containing fibers of a desired quantity and aspect ratio. Epoxy, polyester, phenolic and polyamide resins are examples of Thermosets. A list of all the composites products with thermosets matrices would fill a book.

Some of the most important uses involve fiber composites designed for structural use. Many aircraft, space, military, and automotive parts fall under this heading. The electrical industry uses epoxy-matrix materials in such parts as printed circuit boards.

Thermosets resins are generally produced either by condensation polymerization-directly or by additional polymerization followed by a condensation rearrangement reaction to form the heterocyclic entities. That is, H_2O is a reaction product in either case and creates inherent difficulties in producing void-free composites. Voids have a deleterious effect on shear strength, flexural strength, and dielectric properties, among others. As stated earlier, there are several types, thermosets resins. Two of the most prominent are epoxies and polyesters.

Epoxy resins play a major role in filament-wound composites and are well suited for use in molding compounds and prepregs. They also have good chemical stability and flow properties, and exhibit excellent adherence and water resistance slow shrinkage during cure and (about 3%), and freedom from gas evolution. However, the epoxies are relatively expensive and

are generally limited to service temperature below 150 ^{0}C. This restricts many aerospace applications, where higher use temperatures are required. There is another very important type of thermoset resin called Phenolics. Most of the high temperature and electric insulate applications of composites area made of phenolic resins. At high temperature phenolic based composites show a sacrificial behavior called Ablation thus protecting the structure or other important equipment.

Polyester resins are cheep and versatile resins and are widely used. Liquid polyester can be stored at room temperature for months or even years, and can be brought to cure in a matter of minutes simply by adding a catalyst. Reinforced polyesters are used in boat hulls and building panels, and in structure parts in aircraft, automobile, and applications. (9)

C. Copolymers:

There is another type of classification of polymers based on the type of repeating unit. When we have one type of repeating unit forming the polymer chain; we call it a homopolymer. Copolymers, on the other hand, are polymer chains having two, different monomers. If the two different monomers are distributed randomly along the chain, then we have a regular or random copolymer .if, however, a long sequence of one monomer is followed y a long sequence of another monomer, we have a block copolymer. If we have a chain of one type of monomer and branches of anther type, then we have a graft copolymer.

3.4 **Common Polymeric Matrix Materials**

Among the common polymer matrices used with continuous fiber are polyester and epoxy resins. The advantages of the former include their adequate resistance to water and a variety of chemicals, weathering aging, and, last but not least, their very low cost. They can withstand temperatures up to about 80 ^{0}C and they combine easily with glass fibers. Polymers shrink between 4 and 8% on curing.

A majority of common glass fiber reinforced composites has polyester as the matrix. A condensation reaction between a glycol (ethylene, propylene, diethylene glycol) and an unsaturated dibasic acid (malefic or fumaric) results in a linear polyester containing double bonds between certain carbon atoms. Cross linking is provided by means of an addition reaction with styrene. Hardening and curing agents and ultraviolet absorbents are usually added.

Thermosetting epoxy resins are more expensive than polyesters'. But they have better moisture resistance, lower shrinkage on. Curing (about 3%), a higher maximum use temperature, and good adhesion with glass fibers. A large number of proprietary formulations of epoxies are available and a very large fraction of high-performance polymer matrix composites has thermosetting epoxies as matrices.

Polyamides are thermosetting polymers that have a relatively high service temperature range, 250-300 ^{0}C. But, like other thermosetting resins, they are brittle. A major problem with polyamides is the elimination of water of condensation and solvents during the processing.

Bismaleimides (BMI) thermosetting polymers can have service temperatures drops between 180 and 200 ^{0}C. They have good resistance to hydrothermal effects. Being pera-

94

thermosets, they are quite brittle and must be cured at higher temperature than conventional epoxies.

Thermoplastic resins are easier to fabricate than thermosetting resins;
Besides, they can be recycled. Heat and pressure are applied to form and shape them. More often than not, short fibers are used with thermoplastic resins but in the late 1970s continuous fiber reinforced thermoplastics began to be produced. The disadvantages of thermoplastics include their rather large expansion and contraction characteristics.

An important problem with polymer matrices is that associated with environmental effects. Polymers can degrade at moderately high temperatures and through Small moisture absorption. Absorption of moisture from the environment causes swelling in the polymer as well as a reduction in its strength. In the presence of fibers bonded to the matrix, this hydrothermal effect can lead to sever internal stresses in the composite. The presence of thermal stresses resulting from thermal mismatch between matrix and fiber is of course a general problem in all kinds of composite materials. It is much more so in polymer matrix composites because polymers have high a thermal expansivity.

Carbon/graphite matrix materials used in aerospace industry i.e. carbon/graphite. There is another very important type of matrix used particularly carbon and graphite are superior high-temperature materials with strength and stiffness properties maintainable at temperature up to 2500 K. (4,8)

The combination of carbon or graphite fibers in a carbon or graphite matrix results in a most advanced material with unusual property characteristics. This material is referred to as a carbon/carbon composite. Briefly, carbon/carbon composites are fabricated by the multiple impregnations of porous "all-carbon" frames or configurations. These frames of fibers are impregnated with a liquid carbonizable precursor (for example, pitch), which is subsequently. Pyrolized. Carbon/carbon composite can be produced through a process of chemical vapor deposition of pyrolytic carbon. The gas-impregnation method is difficult to perform because of the tendency for pore closure instead of pore filling in the fiber skeleton. The resultant composites are not particularly impressive at ambient temperature. In fact, many conventional structural materials are stronger. The main feature of carbon/carbon composites, however, is their retention of useable properties at temperature from room temperature to 2760 ^{0}C. These composites also remain dimensionally stable over a comparable temperature range.

Over the past 20 years, carbon/ carbon composites have used for various aeronautical, biomedical, defense, industrial, and space applications. Originally, these materials were produced for application where hardware was exposed to extreme temperature, requiring high performance standards, such as solid rocket motors. Today, carbon/carbon composites are used in commercial as well as military applications. The combination of high-temperature resistance, light weight, and stiffness makes them ideal candidates for use in missiles space vehicles.

3.5 <u>**Reinforcements**</u>

Reinforcement materials supply the basic strength of the composite. They can however contribute much more than strength, they can conduct heat or resist chemical corrosion; they can resist or conduct electricity; and they may be chosen for their stiffness (modulus of elasticity) or for many other properties.

If reinforcement is to improve the strength of given matrix, it must be both stronger and stiffer than the matrix, and it must significantly modify the failure mechanism in an advantageous way. The requirement of high strength and high stiffness implies little or no ductility and, thus, relatively brittle behavior. Fibers are probably the most important class of reinforcement due to their ability to transfer strength to matrix materials and greatly influence their properties. Other typed of reinforcement include fillers.Sometimes known as particles, and flakes.

Composites materials are reinforced with both organic fibers and inorganic fibers. Organic fibers made from polypropylene, nylon, and graphite can be characterized in general as lightweight, flexible, elastic and heat-sensitive.

3.5.1 Fiber-Reinforced Composites:

Glass-fiber reinforced resins were among the earliest fiber reinforced composites. These initial composites were fabricated from solid glass fibers of circular cross section and flexible plastic matrices. As work with composites continued, it was discovered that other materials besides glass fiber and plastic could be combined to from useful materials. Hollow fiber and fiber of noncircular cross section were combined with stiffer and more heat-resistant matrices. Today, fiber-reinforced composites are produced from a wide range of constituents. Of all the composites, fiber-reinforces composites have evoked the most interest among engineers concerned with structural application.

The orientation, length, shape, and composition pf the fibers the mechanical properties of the matrix, and the integrity of the bond between fiber and matrix determine the engineering performance of a fiber composite. Fiber orientation (how the individual strands are positioned) determines the mechanical strength of the composite and the direction in which that strength will be the greatest. There are several ways of thinking about fiber orientation and how orientation affects the strength of a composite. First, however, it must be realized that unidirectionally oriented fibers (or longitudinal fiber) provide maximum composite strength and modulus when loads are applied in the direction of the fibers. In contrast, when loads are applied at even very small angles form the fiber direction, composite strength is drastically lowered. Since very few structures are loaded unidirectionally, it is necessary in most cases to mix orientations in a given part or structure.

Both continuous and discontinuous fiber can be unidirectionally oriented in thin layers (monolayer tapes). These tapes can be stacked and consolidated into plies containing many layers pf filaments oriented in the same direction. Plies can also be made by direct means by many different methods. Plies, however, are planer structure. Layers of tapes or plies with longitudinally oriented fibers ca be stacked together so that the fibers in each layer area at different orientations. Thus, plies ca be stacked so that the fibers are oriented at right angles to each other (cross plied), or so that the fiber are oriented at other angles to each other (angle plied), plies can be stacked in very complicated ways, and computer frequently are used to determine the orientations needed to achieve desired properties. Thus, strength in planar composites (sheets) can be varied for, those of unidirectionally oriented fiber composites to produce composites with almost isotropic properties (quasi-isotropic composites).

As an example of possible orientations, the quasi –isotropic material has plies with fibers at $0^0/90^0/+45^0/-45^0/-45^0/+45^0/90^0/0^0$ .Rule-of thumb strengths and moduli for the latter type of composite are about one-quarter and one-third, respectively, of those of longitudinally oriented composites. For angle-plied composites other than quasi-isotropic ones, properties can very with the number of plies ant their respective orientations. These ratios assume that the composite variables are constant and that the matrices (e.g., plastic) are very weak relative to the fiber. To go to a three-dimensional orientation of continuous fiber, it is usually necessary to weave fiber in 3D and infiltrate materials into their interstices later. Assuming that fiber volume percentages would be equal in all three axes of such composites, the strength in any axis about one-third that of unidirectional fiber composites

It is possible to orient short-length fiber differently than by the methods noted above. For example, short fibers can be given random orientations by sprinkling or shaking them onto a given plane (to achieve random orientation in two dimensions). The matrix could be added either before or after deposition of the fiber using liquid or solid-state methods, Three-dimensional random orientation can be achieved by mixing solids or liquids with the short fiber by several methods. Randomizing fiber orientations in 2D would yield a composite with a strength about one-third that of a composites with unidirectional fiber stressed in the direction of the fiber, while randomizing the fibers in 3D would yield a composite with a comparable ratio of somewhat less than one-fifth as shown schematically in figure-3.1
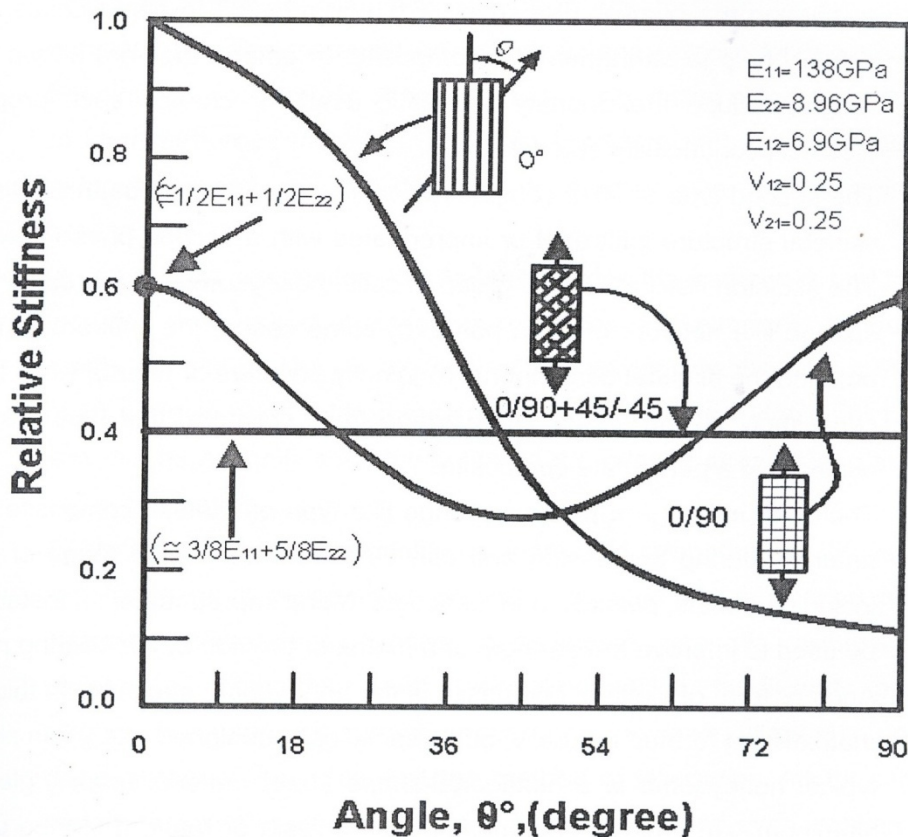

Figure-3.1   An Isotropic Behavior Of Composites

The length of a fiber impacts not only the mechanical properties of a composite, but also its process-ability. In genera, continuous fibers are easier to handle than short fibers. Continuous filaments can be incorporated by the filament winding process, which wraps a continuous fiber (impregnated with a matrix material) around a mandrel having the fiber in the finished article. Filament winding is limited chiefly to the fabrication of bodies of revolution, but flat and irregular shapes can also be made. Short fiber composites, on the other hand, can be made by the numerous open and closed-mold processes. These output and lower cost than filament winding.

3.5.2 Glass Fibers

Glass fibers composite well over 90% of the fibers used in reinforced plastics because they are inexpensive to produce and possess high strength, high stiffness (relative to plastics), low specific gravity, chemical-resistance and good insulating characteristics. One problem with glass, however, is that when subjected to tensile loads for prolonged periods of time, glass breaks at stress levels much below those measured in short-time (2 to 5 minutes) laboratory tests. This behavior, known as static fatigue (actually it is more like a tress- rupture phenomenon), effectively reduces the useful strength of glass if it is intended to sustain such loads for months or years in service. The reduction can be as much as 70% to 80% depending on the load duration, temperature, moisture conditions, and other factors, and if fracture occur, to gives little or no prior warning since glass is brittle material. Conservation design practices and periodic inspections are recommended preventive measures in such applications where failure could have critical consequences.

Because they are available in so many different forms, glass fibers lend themselves to are variety of fabrication processes e.g., filament winding, matched-die molding, lay0rp, etc. glass fibers come in the forms of cloths, mats, tapes, continuous or chopped filaments, roving ,and yarns. Common applications for glass-reinforced plastics are automobile bodies and steel poles because of their lightweight and flexibility.

Several chemicals may be added to silica sand in preparation for glassmaking. Different combinations give rise to different types of glass. At present there are four major types of glass used to make glass fiber(1,2)

a) A-glass is a high-alkali glass. the important alkalis in A-glass are soda, (sodium oxide) and lime (calcium oxide). Together they make up about 25% of A-glass by weight. A-glass offers very good resistance to chemicals. However, its high alkali content lowers its electrical properties.

b) C-glass (chemical glass) is a special mixture with extremely high resistance to chemical. It sis intended for use in situations where even the chemical resistance of A-glass would not be good enough.

c) E-glass is named for its electrical properties. With low alkali content, it offers much better electrical insulation than A-glass. As a fiber, it has good all–around strength, and it strongly resists attack by water. This is important in many glass fiber/resin composites that require high performance under moist conditions. At present, E-glass accounts for more than half of the glass-fiber reinforcements made.

d) S-glass is a high-strength material. For example its tensile strength better at high temperature and resists fatigue well. It has found wide use in such high performance materials as rocket-motor casings and aircraft parts.

e) A fifth type, D- glass, has also been developed. It has even better electrical properties than E-glass.(the 'D' stands for low dielectric constant.) although its mechanical properties are not as good as those of E-glass or S-glass

3.5.3   **Kevlar (aramid) fiber reinforced polymers**

Kevlar is the trade name (registered by DuPont Co.) of aramid (poly-para-phenylene terephthalamide) fibers. Kevlar fibers were originally developed as a replacement of steel in automotive tires. Distinctive features of Kevlar are high impact resistance and low density. Kevlar fiber*s* possess the following properties:
- High tensile strength (five times stronger per weight unite than steel);
- High modulus of elasticity;
- Very low elongation up to breaking point;
- Low weight;
- High chemical inertness;
- Very low coefficient of thermal expansion;
- High Fracture Toughness (impact resistance);
- High cut resistance;
- Textile processibility;
- Flame resistance.

The disadvantages of Kevlar are: ability to absorb moisture, difficulties in cutting, low compressive strength. There are several modifications of Kevlar, developed for various applications:
a) Kevlar 29 – high strength (520000 psi/3600 MPa), low density (90 lb/ft³/1440 kg/m³) fibers used for manufacturing bullet-proof vests, composite armor reinforcement, helmets, ropes, cables, asbestos replacing parts.
b) Kevlar 49 – high modulus (19000 ksi/131 GPa), high strength (550000 psi/3800 MPa), low density (90 lb/ft³/1440 kg/m³) fibers used in aerospace, automotive and marine applications.
c) Kevlar 149 – ultra high modulus (27000 ksi/186 GPa), high strength (490000 psi/3400 MPa), low density (92 lb/ft³/1470 kg/m³) highly crystalline fibers used as reinforcing dispersed phase for composite aircraft components.

Kevlar filaments are produced by extrusion of the precursor through a spinnert. Extrusion imparts anisotropy (increased strength in the lengthwise direction) to the filaments. Kevlar may protect carbon fibers and improve their properties: hybrid fabric (Kevlar + Carbon fibers) combines very high tensile strength with high impact and abrasion resistance. The most popular matrix materials for manufacturing Kevlar (aramid) Fiber Reinforced Polymers are Thermosets such as Epoxies (EP), Vinylester and Phenolics (PF). Kevlar Fiber Reinforced Polymers are manufactured by open mold processes, closed mold processes and Pultrusion method. (4,8)

3.6 **Particle-Filled Composites**

Fillers can constitute either a major or a minor part of the composition of a composite. The structure of filler particles can range from irregular masses to precise geometrical forms such as spheres, polyhedrons, or short fibers. Filler are used for non-decorative purposes, although they may incidentally impart color or opacity to a composition. Filler are used extensively in reinforced plastics. Typical fibers include clay, sand or silica, calcium carbonate, alumina, calcium silicate carbon black, and titanium dioxide, as inert additives, fillers area capable of modifying nearly any basic resin property in the direction desired, thereby

overcoming many of the limitations f the basic resins, particle size, size distribution, shape, surface treatment, and blends of particle types all affect the final composite properties.

When a plastic is combined with filler, the two act as two separate constituents. The materials do not alloy, and, except for the necessary bonding, do not combine chemically to any significant extent as in the case of fiber-reinforced materials. t is also important that the constituents be compatible and do not degrade or destroy one another 's inherent properties.

In some filled composites, the matrix provides the framework and the filler provides the desired engineering properties. For example, although the matrix usually makes up the bulk of the composite, the filler materials is often used to such a large extent that it becomes the dominant material and makes a significant contribution to the over-all strength and structure of the composite. Fillers offer a variety of benefits i.e. increased strength and stiffness, heat resistance, heat conductivity, stability, wet strength, fabrication mobility, viscosity, abrasion resistance, and impact strength reduced cost. Shrinkage, exothermic heat, thermal-expansion coefficient, porosity, crazing, and improved surface appearance. However, filler also possess disadvantages; they may limit the methods of fabrication, inhibit curing of certain resins, shorten the pot life of some resins, and even weaken some composites.(8,10)

3.7   **Syntheses of Composites**

Basically, there are two steps involves in the syntheses process of ablative composite samples i.e.
a) Mixing
b) Molding

a) Mixing:

Mixing plays key and basic role in the manufacturing of elastomeric ablative composites. All the characteristics of mechanical properties depend on the proper and accurate mixing. We mixed our materials for 18 to 20 minutes on 2 roll mixing mill. Mixing is carried out due to friction ration (ratio of bigger roll dia to small roll dia). Proper water channels are provided to the rollers so the mixing temperature may not exceed 100 ^{o}C

Figure 3.2   : Sample in Mixing Process Using Twin Rollers in Longman Mills Lahore

b) Molding:

This is the most common type of molding used in the rubber industry. Essentially, it consists of pacing a pre-cut or shaped slug or a composite item into a two piece mould which is closed. The pressure applied by the press forces the materials to fit the shape of the mould and the excess flows out of the rim of the mould or through special vents. This excess in known as mould lash. Source of investigation.(5)

Figure 3.3   : Sample during Molding

3.8   <u>Experimental Techniques and Setup</u>

The source to measure impact strength, tensile strength, fracture toughness and fracture analysis , are as following:
1) impact tester
2) universal testing machine
3) fracture toughness

3.8.1 Charpy Impact Testing Machine

Charpy impact testing machine for evaluating the toughness in both materials and composites. Before looking at impact testing let us first define what is meant by 'toughness' since the impact test is only one method by which this material property is measured.

Toughness is, broadly, a measure of the amount of energy required to cause an item - a test piece or a bridge or a pressure vessel - to fracture and fail. The more energy that is required then the tougher the material.

There are two main forms of impact test, the *Izod* and the *Charpy* test. Both involve striking a standard specimen with a controlled weight pendulum traveling at a set speed. The amount of energy absorbed in fracturing the test piece is measured and this gives an indication of the notch toughness of the test material.

These tests show that metals can be classified as being either 'brittle' or 'ductile'. A brittle metal will absorb a small amount of energy when impact tested, a tough ductile metal a large amount of energy.

It should be emphasized that these tests are *qualitative*, the results can only be compared with each other or with a requirement in a specification - they *cannot* be used to calculate the fracture toughness of a weld or parent metal. Tests that can be used in this way will be covered in future *Job Knowledge* articles. The Izod test is rarely used these days for weld testing having been replaced by the Charpy test and will not be discussed further in this article.

The Charpy specimen may be used with one of three different types of notch, a 'keyhole', a 'U' and a 'V'. The keyhole and U-notch are used for the testing of brittle materials such as cast iron and for the testing of plastics. The V-notch specimen is the specimen of choice for weld testing and is the one discussed here.

The standard Charpy-V specimen, illustrated in *Fig.1*. is 55mm long, 10mm square and has a 2mm deep notch with a tip radius of 0.25mm machined on one face.
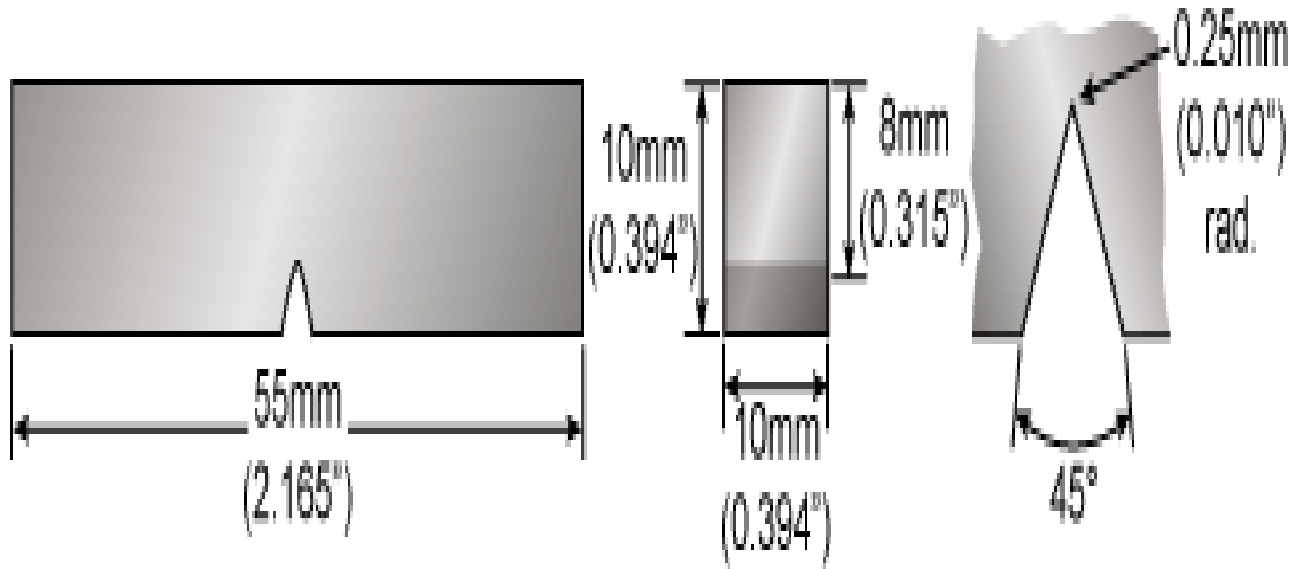
Figure 3.4   Standard Charpy-V notch specimen

To carry out the test the standard specimen is supported at its two ends on an anvil and struck on the opposite face to the notch by a pendulum as shown in *Fig.3.5*. The specimen is fractured and the pendulum swings through, the height of the swing being a measure of the amount of energy absorbed in fracturing the specimen. Conventionally three specimens are tested at any one temperature, and the results averaged.(8,11)
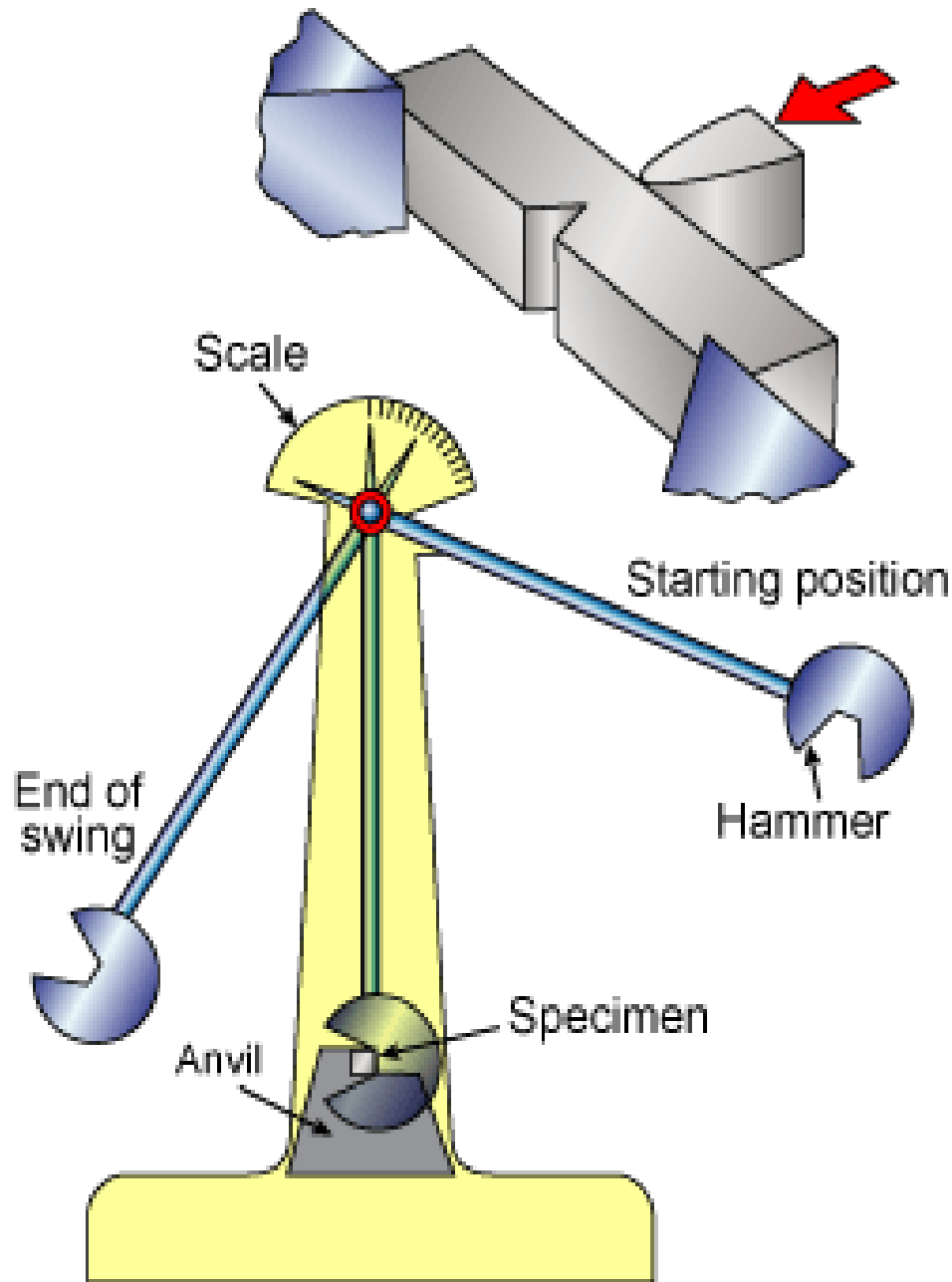
Figure 3.5.   Charpy testing machine

3.8.1.2   What is the Charpy Impact Test and why is it used?

Materials are used to build load-bearing structures. An engineer needs to know if the material will survive the conditions that the structure will see in service. Important factors that adversely affect the toughness of a structure include low-test temperatures, extra loading and high strain rates due to over pressurization or impacts and the effect of stress concentrations such as notches and cracks. These all tend to encourage fracture. To some extent, the complex

interaction of these factors can be included in the design process by using fracture mechanics theory. Tests for the impact toughness, such as the Charpy Impact Test , were developed before fracture mechanics theory was available. The impact test is a method for evaluating the relative toughness of engineering materials. The Charpy impact test continues to be used nowadays as an economical quality control method to assess the notch sensitivity and impact toughness of engineering materials. It is usually used to test the toughness of metals. Similar tests can be used for polymers, ceramics and composites. The charpy impact test measures the energy absorbed by the high strain rate fracture of a standard notched specimen.

In the Charpy Impact Test, the specimen is supported as a simple beam with a notch in the center. The specimen is supported so that the notch is on the vertical face away from the point of impact. Figure 3 and 4 show the dimensions of the Charpy Impact Test specimen and the positions of the striking edge of the pendulum and the specimen in the anvil. The specimen is broken by the impact of a heavy pendulum hammer, falling through a fixed distance (*constant potential energy*) to strike the specimen at a fixed velocity (*constant kinetic energy*). **Tough** materials absorb a lot of energy when fractured and **brittle** materials absorb very little energy.

Charpy impact tests are instrumented: for each experiment the force vs. deflection curve is recorded by PC controlled test execution and four channel recording system. Strain gauges applied to the striker allow measurement of the force curves. The impact energy is determined by integration of the force vs. deflection curves.

A mechanical drag indicator attached to the pendulum allows controlling of electronically acquired results. The recorded force vs. deflection curve enables identification of phases of crack initiation (rising of the curve), stable crack propagation (slow drop-off after the maximum) and instable crack propagation (steep fall). Additionally classification of fracture types is possible.(8,9)

3.8.2   <u>Determination of yield force</u>

One more important parameter deduced from the instrumented Charpy impact tests is the yield force F_{gy}. It characterizes the transition from pure elastic to elastic-plastic behavior of the material, i.e. the onset of the yield. The dynamic yield stress is then estimated from the yield force. Details of the estimation are found in the literature.
The determination of the yield force from the force vs. deflection curve is defined in SEP 1315. First a straight line is put through the middle development of the first three oscillations. Then an average-value curve is drawn through the subsequent data. The yield force is determined as the value of the average-value curve at the intercept point of the straight line with a tangent of the average-value curve.

The oscillation free force vs. deflection curves obtained by means of the perturbation compensation software package enable reproducible determination of the yield force by means of the mentioned method of tangents.

3.8.3 Technical data:

Striker radius 2 mm
Distance between supports 22 mm
Impact velocity 3.85 m/s
Strain gauge in the striker
Sampling rate 1 MHz
Gain Bandwidth 1MHz (-3dB)
A/D converter resolution 1.2 mV
Automated specimen transporting mechanism
Transport time max. 2 s
PC controlled test execution
Test temperature range -180° to +600°C
The facility can be equipped with other strikers, e.g. for 15 J impact energy.
Lifting of the striker up to angles between 40 and 160° is carried out automatically.
Any impact velocity up to 3.85 m/s is available this way.
The magazine offers place for up to 15 specimens for test series.
The facilities are fully automated enabling remote data access via the computer network.

3.8.4 Specimen Geometry

The geometry of the Charpy specimens
according to DIN 50115:
Height 4mm, Width 3 mm, Length 27 mm,
Notch depth 1mm, Notch angle 60°, Notch radius 0.1 mm.
Miniaturized materials are used in the case of materials shortness or when materials are subjected to expensive treatment, such as irradiation. One more advantage of the miniaturized specimens is the easily achievable temperature homogeneity during the tempering and experiment. The influence of the size effects on the results is thoroughly

3.9 . Universal Testing Machine (UTM):

Universal testing machine(UTM) for the mechanical testing of both metal and composite sample.

3.9.1 Machine Equipped With Straining Unit

This consists of a hydraulic cylinder and power pack motor with chain and sprocket drive and a table coupled with the ram of the hydraulic cylinder, mounted on to a robust base. The cylinder and the ram are individually lapped to eliminate friction. The upper crosshead is connected to two screwed columns, which are driven by a motor. Axial loading of the ram is ensured by the Provision of the ball seating. An elongation scale with a minimum graduation is provided to measure the deformation of the specimen. Tension test is conducted by gripping the test specimen between the upper and lower crossheads, The lower crosshead can be raised or lowered rapidly by operating the screwed columns thus facilitating ease of fixing of the test specimen. Compression, transverse, bending, shear and hardness tests are conducted between the lower cross head and the table.

- **Power Pack:**

The power pack generates the maximum pressure of 200 kgf/cm2 the hydraulic pump provides continuously non-pulsating oil flow. Hence the load Application is very smooth.

- **Control Panel:**

The control Panel consists of a power pack complete with drive motor and an oil tank, control valves a pendulum dynamometer a load indicator system and an autographic recorder.

- **Hydraulic Controls:**

Hand operates wheels are used to control the flow to and from the hydraulic cylinder. The regulation of oil flow is infinitely variable incorporated in the hydraulic system is a regulating valve which maintains a practically constant rate of piston movement. Control by this valve allows extensometer readings to betaken.

- **Accuracy & Calibration:**

All Test well Universal Testing Machines are closely controlled for sensitivity, accuracy and calibration during every stage of manufacture. Every machine is then calibrated over each of its measuring ranges in accordance with the procedure .

Test well Universal Testing Machines comply with Grade "A" of BS: 1610: Part 1:1992 and class 1 of IS 1828: (Part 1): 1991 and accuracy of + 1.0% is guaranteed from 20% of the load range selected to full load. Below 20% of the selected range, the maximum permissible error is 0.2% of the full load reading.

- **Application:**

Test well Universal Testing Machine is designed for testing metals and other materials under

tension, compression bending, transverse and shear loads. Hardness test on metals can also be conducted.

3.9.2 Principle of operation:

Operation of the machines is by hydraulic transmission of load from the test specimen to a separately housed load indicator. The hydraulic system is ideal since it replaces transmission of load through levers and knife-edges, which are prone to wear and damage due to shock on rupture of test pieces.Load is applied by a hydrostatically lubricated ram. Main cylinder pressure is transmitted to the cylinder of the pendulum dynamometer system housed in the control panel. The cylinder of the dynamometer is also of self-lubricating design. The load transmitted to the cylinder of the dynamometer is transferred through a lever system to a pendulum. Displacement of the pendulum actuates the rack and pinion mechanism, which operates the load indicator pointer and the autographic recorder. The deflection of the pendulum represents the absolute load applied on the test specimen.Return movement of the pendulum is effectively damped to absorb energy in the event of sudden breakage of a specimen.

Figure 3.6   Universal testing machine

3.10 <u>Fracture Toughness</u>

Fracture toughness is an indication of the amount of stress required to propagate a preexisting flaw. It is a very important material property since the occurrence of flaws is not completely avoidable in the processing, fabrication, or service of a material/component. Flaws may appear as cracks, voids, metallurgical inclusions, weld defects, design discontinuities, or some combination thereof.
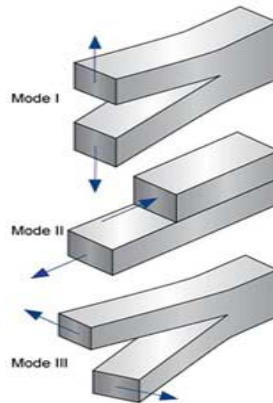
Figure 3.7   Different modes of fracture

Since engineers can never be totally sure that a material is flaw free, it is common practice to assume that a flaw of some chosen size will be present in some number of components and use the linear elastic fracture mechanics (LEFM) approach to design critical components. This approach uses the flaw size and features, component geometry, loading conditions and the material property called fracture toughness to evaluate the ability of a component containing a flaw to resist fracture.

A parameter called the stress-intensity factor (K) is used to determine the fracture toughness of most materials. A Roman numeral subscript indicates the mode of fracture and the three modes of fracture are illustrated in the image to the right. Mode I fracture is the condition in which the crack plane is normal to the direction of largest tensile loading. This is the most commonly encountered mode and, therefore, for the remainder of the material we will consider K_I

The stress intensity factor is a function of loading, crack size, and structural geometry. The stress intensity factor may be represented by the following equation:

$$K_I = \sigma \sqrt{\pi a \beta}$$

Where: K_I is the fracture toughness in $MPa\sqrt{m}$ ($psi\sqrt{in}$)

      s is the applied stress in MPa or psi

      a is the crack length in meters or inches

      B is a crack length and component geometry factor that is different for each specimen and is dimensionless.

3.10.1   Role of Material Thickness

Specimens having standard proportions but different absolute size produce different values for K_I. This results because the stress states adjacent to the flaw changes with the specimen thickness (B) until the thickness exceeds some critical dimension. Once the thickness exceeds the critical dimension, the value of K_I becomes relatively constant and this value, K_{IC} , is a true material property which is called the plane-strain fracture toughness. The relationship between stress intensity, K_I, and fracture toughness, K_{IC}, is similar to the relationship between stress and tensile stress. The stress intensity, K_I, represents the level of "stress" at the tip of the crack and the fracture toughness, K_{IC}, is the highest value of stress intensity that a material under very specific (plane-strain) conditions that a material can withstand without fracture. As the stress intensity factor reaches the K_{IC} value, unstable fracture occurs. As with a material's other mechanical properties, K_{IC} is commonly reported in reference books and other sources.
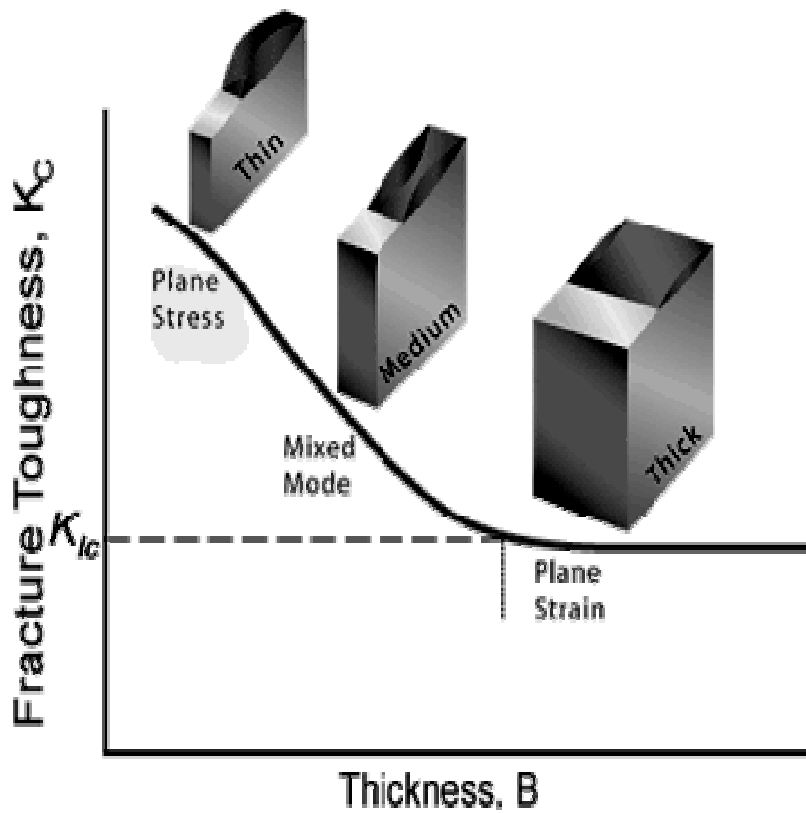
Figure 3.9   Sample thicknesses versus fracture toughness profile

3.10.2   Plane-Strain and Plane-Stress

When a material with a crack is loaded in tension, the materials develop plastic strains as the yield stress is exceeded in the region near the crack tip. Material within the crack tip stress field, situated close to a free surface, can deform laterally (in the z-direction of the image) because there can be no stresses normal to the free surface. The state of stress tends to biaxial and the material fractures in a characteristic ductile manner, with a 45° shear lip being formed at each free surface. This condition is called "plane-stress" and it occurs in relatively thin bodies where the stress through the thickness cannot vary appreciably due to the thin section.
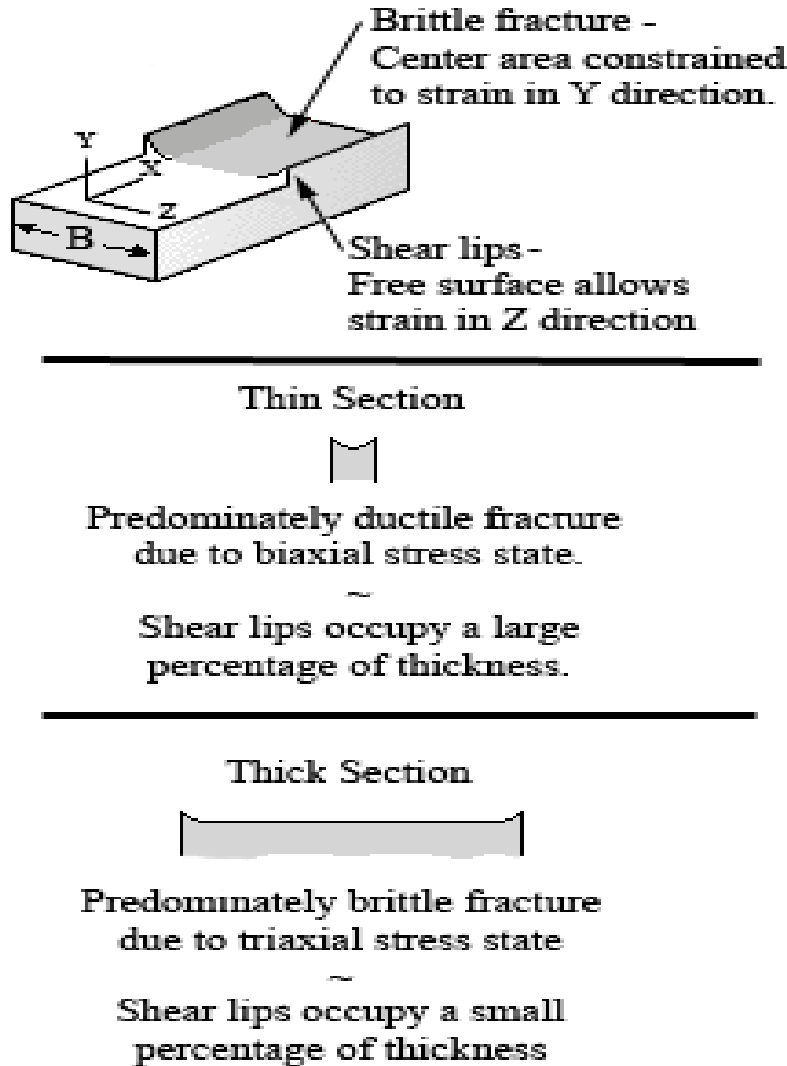
Figure 3.10   Uniaxial, biaxial and triaxial Strain profile

However, material away from the free surfaces of a relatively thick component is not free to deform laterally as it is constrained by the surrounding material. The stress state under these conditions tends to triaxial and there is zero strain perpendicular to both the stress axis and the

113

direction of crack propagation when a material is loaded in tension. This condition is called "plane-strain" and is found in thick plates. Under plane-strain conditions, materials behave essentially elastic until the fracture stress is reached and then rapid fracture occurs. Since little or no plastic deformation is noted, this mode fracture is termed brittle fracture.(12,13)

3.11 <u>Plane-Strain Fracture Toughness Testing</u>

When performing a fracture toughness test, the most common test specimen configurations are the single edge notch bend (SENB or three-point bend), and the compact tension (CT) specimens. From the above discussion, it is clear that an accurate determination of the plane-strain fracture toughness requires a specimen whose thickness exceeds some critical thickness (B). Testing has shown that plane-strain conditions generally prevail when:

$$B \geq 2.5 \left(\frac{K_{IC}}{\sigma_y} \right)^2$$

Where: B   is the minimum thickness that produces a condition where plastic strain energy at the crack tip in minimal

K_{IC} is the fracture toughness of the material

s_y is the yield stress of material

When a material of unknown fracture toughness is tested, a specimen of full material section thickness is tested or the specimen is sized based on a prediction of the fracture toughness. If the fracture toughness value resulting from the test does not satisfy the requirement of the above equation, the test must be repeated using a thicker specimen. In addition to this thickness calculation, test specifications have several other requirements that must be met (such as the size of the shear lips) before a test can be said to have resulted in a K_{IC} value. (23,24)
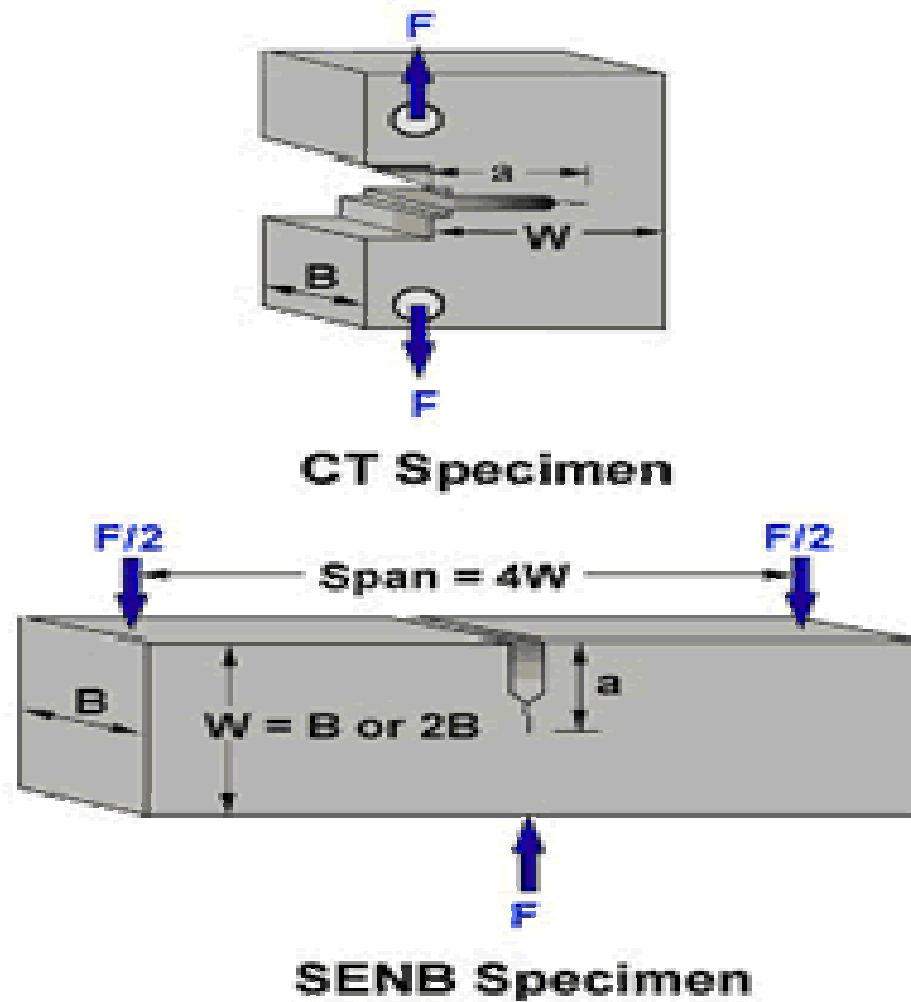
Figure 3.11 Types of testing samples

When a test fails to meet the thickness and other test requirement that are in place to insure plane-strain condition, the fracture toughness values produced is given the designation K_C. Sometimes it is not possible to produce a specimen that meets the thickness requirement. For example when a relatively thin plate product with high toughness is being tested, it might not be possible to produce a thicker specimen with plain-strain conditions at the crack tip. (30)

3.12 **Plane-Stress and Transitional-Stress States**

For cases where the plastic energy at the crack tip is not negligible, other fracture mechanics parameters, such as the J integral or R-curve, can be used to characterize a material. The toughness data produced by these other tests will be dependant on the thickness of the product tested and will not be a true material property. However, plane-strain conditions do not exist in all structural configurations and using K_{IC} values in the design of relatively thin areas may result in excess conservatism and a weight or cost penalty. In cases where the actual stress state is plane-stress or, more generally, some intermediate- or transitional-stress state, it is more appropriate to use J integral or R-curve data, which account for slow, stable fracture (ductile tearing) rather than rapid (brittle) fracture.

3.10.1` Uses of Plane-Strain Fracture Toughness
K_{IC} values are used to determine the critical crack length when a given stress is applied to a component.

$$\sigma_c \leq \frac{K_{IC}}{Y\sqrt{\pi a}}$$

Where: s_c is the critical applied stress that will cause failure

     K_{IC} is the plane-strain fracture toughness

     Y   is a constant related to the sample's geometry

     a   is the crack length for edge cracks or one half crack length for internal crack

K_{IC} values are used also used to calculate the critical stress value when a crack of a given length is found in a component.

$$a_c = \frac{1}{\pi}\left(\frac{K_{IC}}{\sigma Y}\right)^2$$

Where: a   is the crack length for edge cracks or one half crack length for internal crack

CHAPTER # 4
Result & Discussions
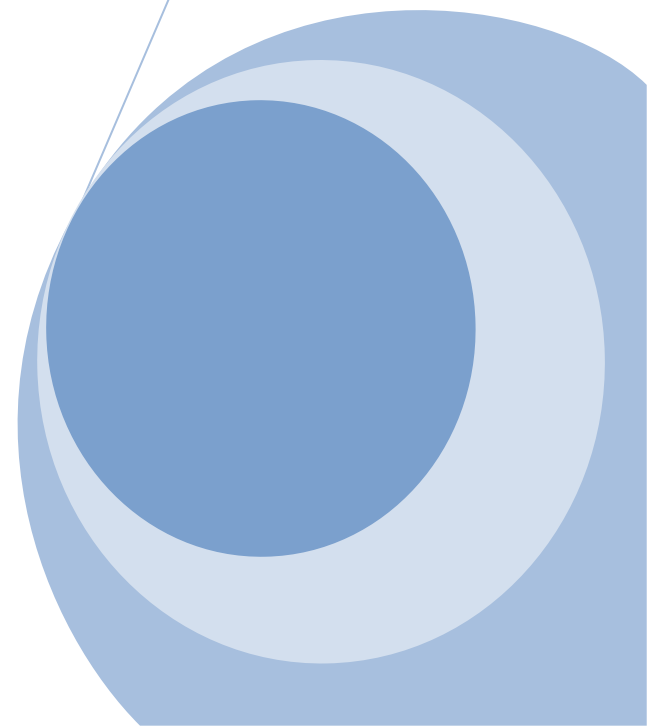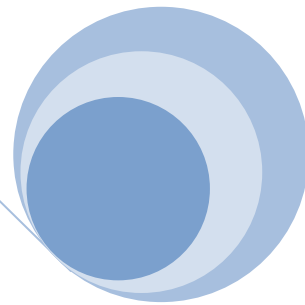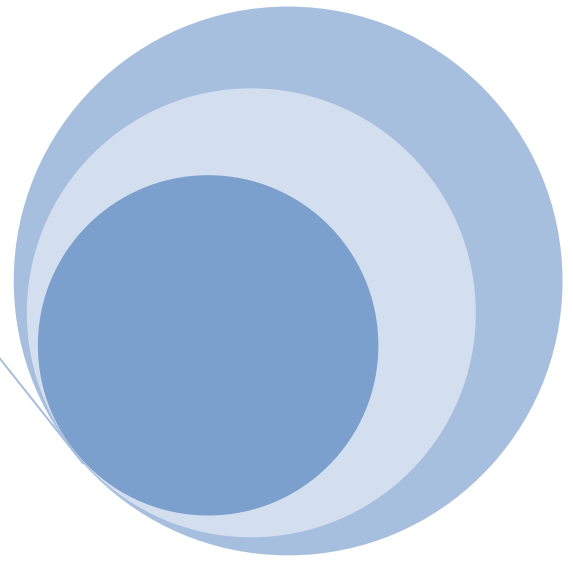
Chapter # 4

4.1 Chemistry of Samples:

Sample #1:

EPDM + Volcasil C + Zinc Oxide + Stearic Acid + Oil + Sulphur+ MBT+ DPG+ Wax.

Sample #2:

EPDM + Volcasil C + Zinc Oxide + Stearic Acid + Oil + Sulphur + MBT+ DPG+ Wax + MDH + Alumina.

Sample #3:

EPDM + Volcasil C + Zinc Oxide + Stearic Acid + Oil + Sulphur+ MBT+ DPG+ Wax + ATH.

Sample #4:

EPDM + Volcasil C + Zinc + Stearic Acid + Oil + Sulphur+ MBT+ DPG+ Wax+ chopped Kevlar fiber.

Sample #5:

EPDM + Volcasil C + Zinc Oxide + Stearic Acid + Oil + Sulphur+ MBT+ DPG+ Wax+ single layer of Nomax fiber.

Sample #6:

EPDM + Volcasil C + Zinc Oxide + Stearic Acid + Oil + Sulphur+ MBT+ DPG+ Wax + single layer of Kevlar fiber.

Sample #7:

EPDM + Volcasil C + Zinc Oxide + Stearic Acid + Oil + Sulphur+ MBT+ DPG+ Wax+ MDH + Alumina + single layer of Kevlar.

Sample #8:

EPDM + Volcasil C + Zinc Oxide + Stearic Acid + Oil + Sulphur+ MBT+ DPG+ Wax+ATH + Single layer of Kevlar fiber.

Sample #9:

EPDM + Volcasil C + Zinc Oxide + Stearic Acid + Oil + Sulphur+ MBT+ DPG+ Wax+ Three alternative layer of Kevlar Fiber with Ceramic coating.

Sample #10:

EPDM + Volcasil C + Zinc Oxide + Stearic Acid + Oil + Sulphur+ MBT+ DPG+ Wax + Four alternative layers of Kevlar fiber with ceramic coating.

4.1.2 COMPOSITIONS OF COMPOSITES

SR. NO	EPDM phr	Silica phr	ZnO phr	St.Acid phr	A. Oil phr	Sulpher phr	MBT phr	DPG phr	WAX phr	MDH phr	Alumina phr	ATH phr	Chopped Kevlar fiber phr	Continuous Nomex Fiber phr	Continuous Kevlar Fiber phr	Continuous SiC coated Kevlar Fiber phr
SNI	55.2	27.6	2.8	1.4	8.2	1.4	1.4	0.6	1.4							
SN2	39.5	19.7	2	1	6	1	1	0.4	1	14.2	14.2					
SN3	42.5	21.2	2.1	1.1	6.4	1.1	1.1	0.4	1.1	..__	__	23				
SN4	53.5	26.8	2.7	1.3	8	1.4	1.4	0.5	1.3	__	__	__	3.1			
SN5	53.6	26.8	2.7	1.3	8.1	1.3	1.4	0.5	1.3	__	__	__	__	3		
SN6	53.6	26.8	2.7	1.3	8.1	1.3	1.4	0.5	1.3	__	__	__	__	__	3	
SN7	36.8	18.4	1.9	0.9	5.5	1	0.9	0.4	0.9	13.3	13.3	__	__	__	6.7	
SN8	39.4	19.7	2	1	6	1	1	.4	1	__	__	21.4	__	__	7.1	
SN9	42.5	21.2	2.1	1.1	6.3	1.1	1.1	0.4	1.1	__	__	__	__	__	__	23.1
SN10	39.4	19.5	2	1	6	1	1	0.4	1	__	__	__	__	__	__	28.6

Function of other ingredients with EPDM in composites

1) Volcasil C (SILICA)

Silica-, nanoclay-, and carbon black (CB)-filled ethylene-propylene-diene terpolymer (EPDM) mixtures were prepared and subsequently vulcanized. Rheological property measurements indicated the storage modulus, loss modulus, and complex dynamic viscosity of silica-filled EPDM mixtures were much higher than those of CB-filled EPDM mixtures while tan δ values were lower. The optimum cure time of silica- and nanoclay-filled EPDM mixtures increased with filler loading, whereas the values for CB-filled mixtures slightly decreased with loading. The hardness, modulus, elongation at break, and tensile strength of all the vulcanizates increased with increasing filler loading. The elongation at break of CB-filled EPDM vulcanizates increased insignificantly with CB loading. Remarkably, for 30 phr silica-filled EPDM vulcanizates, a tensile strength and elongation at break of 23.5 MPa and 1045% , respectively was achieved.

2) Zinc Oxide:

Zinc oxide, the inorganic chemical is characterized with a variety of properties such as heat resistance and mechanical strength that are imparted to composites in the plastics field. It also imparts higher tensile strength and water resistance when it is added to EPDM . Fire-resistant is another property that, the chemical imparts to KEVLAR fibers and moldings. Zinc Oxide serves as the accelerator with some types of elastomer and the cross linking, which it induces, takes several forms. With some systems, Zinc Oxide is an effective co-accelerator in the vulcanization process.

3) Stearic Acid:

Stearic acid is one of most commonly used lubricants during injection moulding and for pressing of ceramic powder. Stearic acid is used with zinc oxide as zinc stereate as fanning powder for cards to deliver smooth fanning motion. Stearic acid

gives significant improvement in creep properties is obtained and resilience is also improved.

4) Oil :

Petroleum oils were regarded as inferior plasticizers, largely due to the variability of materials offered at the time. Oils aid processing of the polymer during milling, mixing and extruding by providing lubrication of the rubber molecules. It improves the physical properties of natural and synthesis rubber such as elasticity, flex life, and low temperature performance, and also aids in improvements in tensile strength and abrasion resistance.

5) Sulphur:

The first step is the investigation of the influence of the type and degree of cross-linking. EPDM can be vulcanized in different ways resulting in different cross-links:

a)   -S-   b)   -S-S-   c)   S-S-S-S

a) mono-sulfidic cross-link   *b) di- sulfidic cross-link*   *c) poly-sulfidic cross-link*

1. Conventional vulcanization   high sulfur/accelerator ratio, resulting in mainly polysulfidic cross-links
2. Semi-efficient vulcanization   medium sulfur/accelerator ratio, resulting in a cross-link of medium length (mainly di-sulfidic)
3. Efficient vulcanization low sulfur/accelerator ratio, resulting in short cross-links (mainly mono-sulfidic)

 6) MBT(Meracaptobenzothiazole):

 MBT(Meracaptobenzothiazole) is used as a primary accelerator, has an important role in achieving almost any required processing safety, cure time and modulus. It gives fast curing, high activity (Cross linking efficiency) , soluble in rubber (good dispersion) delayed action, Good storage stability, Effective over wide range of temperatures, compatible over a wide range of temperature, no safety or handling problem

7) DPG (1,3 – diphenylguanidine):

1,3-diphenylguanidine (DPG) is used as a secondary accelerator, has an important function in silica-filled EPDM rubber. In the present study, the focus is on the effect of DPG on the silane chemistry during processing.

8) MDH (magnesium hydroxide) & ATH (Aluminum trihydride)

One of the fastest growing classes of halogen free flame retardants is based on minerals such as aluminum trihydrate (ATH) and magnesium hydroxide (MDH). These are widely used as flame retardants in wire & cable and building & construction applications.

Although mineral flame retardants offer a relatively low cost solution for many Low Smoke Zero Halogen (LSZH) applications, they have some major drawbacks. The most prevalent one is the loss of physical properties which comes from the high loadings of ATH and MDH needed to obtain the flame retardancy ratings. As a consequence the mechanical properties of the polymer compounds deteriorate and processing can become very slow and difficult.

MDH can also be used in other polymer systems, such as EPDM, polypropylene and silicone elastomers, where it will benefit mechanical properties, low temperature
properties and water resistance.

9) Aluminum Oxide, Al_2O_3

Alumina is the most cost effective and widely used material in the family of engineering ceramics. The raw materials from which this high performance technical grade ceramic is made are readily available and reasonably priced, resulting in good value for the cost in fabricated alumina shapes. With an excellent combination of properties and an attractive price, it is no surprise that fine grain technical grade alumina has a very wide range of applications. Some characteristics features are;

Hard, wear-resistant

Excellent dielectric properties from DC to GHz frequencies

Resists strong acid and alkali attack at elevated temperatures
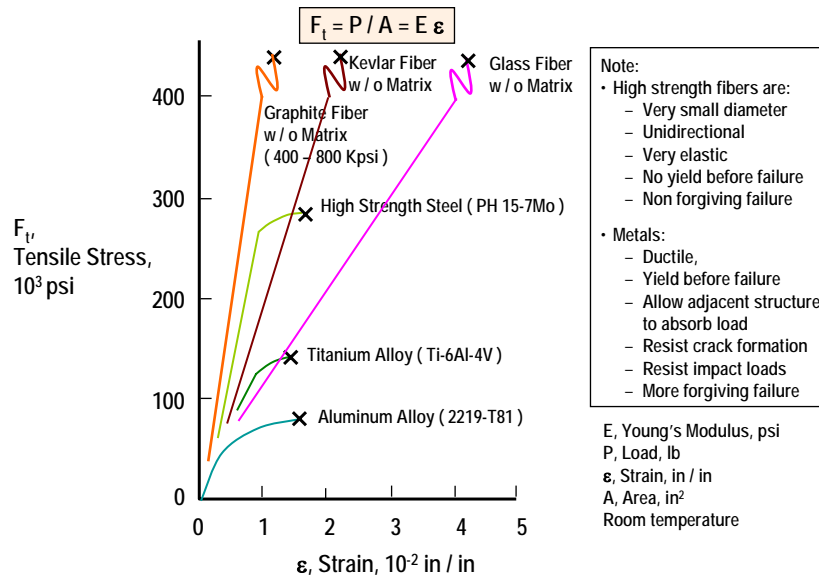
Excellent size and shape capability

High strength and stiffness

4.1.3 Ultimate tensile strength & Breakage behavior of Metallic and Non-metallic fibers.

   Important points are listed inside the below figure.

Polymeric fiber like Kevlar fiber shows ultra high strength which are comparable to graphite fiber and give high strength through molecular orientation during stretching of fiber. This contribute to the absorption of energy at the tip of projectile as the fiber pullout to elongate at high stress.

### Ultimate tensile strength & Breakage behavior of Metallic and Non-metallic fibers

$$F_t = P / A = E\,\varepsilon$$

Kevlar Fiber w / o Matrix

Glass Fiber w / o Matrix

Graphite Fiber w / o Matrix (400 – 800 Kpsi)

High Strength Steel (PH 15-7Mo)

Titanium Alloy (Ti-6Al-4V)

Aluminum Alloy (2219-T81)

F_t, Tensile Stress, 10^3 psi

ε, Strain, 10^{-2} in / in

Note:
- High strength fibers are:
  - Very small diameter
  - Unidirectional
  - Very elastic
  - No yield before failure
  - Non forgiving failure
- Metals:
  - Ductile,
  - Yield before failure
  - Allow adjacent structure to absorb load
  - Resist crack formation
  - Resist impact loads
  - More forgiving failure

E, Young's Modulus, psi
P, Load, lb
ε, Strain, in / in
A, Area, in²
Room temperature

4.2 Result & discussions

4.2.1: Table of Charpy Values of Tested Samples

Sr #	Sample Number	Charpy Value(J)	Average Charpy Value(J)	Velocity(m/S)	Energy(J)
1	SN 1A	3.336	3.336	5.09	272.1
	SN 1B	3.334		5.17	281.0
	SN 1C	3.337		5.06	283.4
2	SN 2A	3.336	3.336	5.09	272.6
	SN 2B	3.335		5.11	274.8
	SN 2C	3.337		5.06	263.4
3	SN 3A	4.408	4.408	5.33	298.3
	SN 3B	4.408		5.08	271.4
	SN 3C	4.407		5.24	263.5
4	SN 4A	2.628	2.628	5.07	270.0
	SN 4B	2.680		5.04	267.4
	SN 4C	2.548		5.08	265.6
5	SN 5A	3.336	3.335	5.05	268.1
	SN 5B	3.332		5.02	264.6
	SN 5C	3.338		5.03	265.6
6	SN 6A	6.289	6.232	5.07	270.3
	SN 6B	6.216		5.05	268.2
	SN 6C	6.192		5.04	269.4

7	SN 7A	3.336	3.336	5.08	271.4
	SN 7B	3.335		5.07	270.0
	SN 7C	3.338		5.09	273.4
8	SN 8A	4.048	4.046	5.08	271.0
	SN 8B	4.045		5.05	268.4
	SN 8C	4.046		5.06	269.4
9	SN 9A	17.70	17.967	5.08	268.0
	SN 9B	18.50		5.05	269.4
	SN 9C	17.70		5.04	265.5
10	SN 10A	19.05	19.05	5.04	267.4
	SN 10B	19.06		5.05	268.5
	SN 10C	19.04		5.06	269.6

Chart of Average Charpy Values
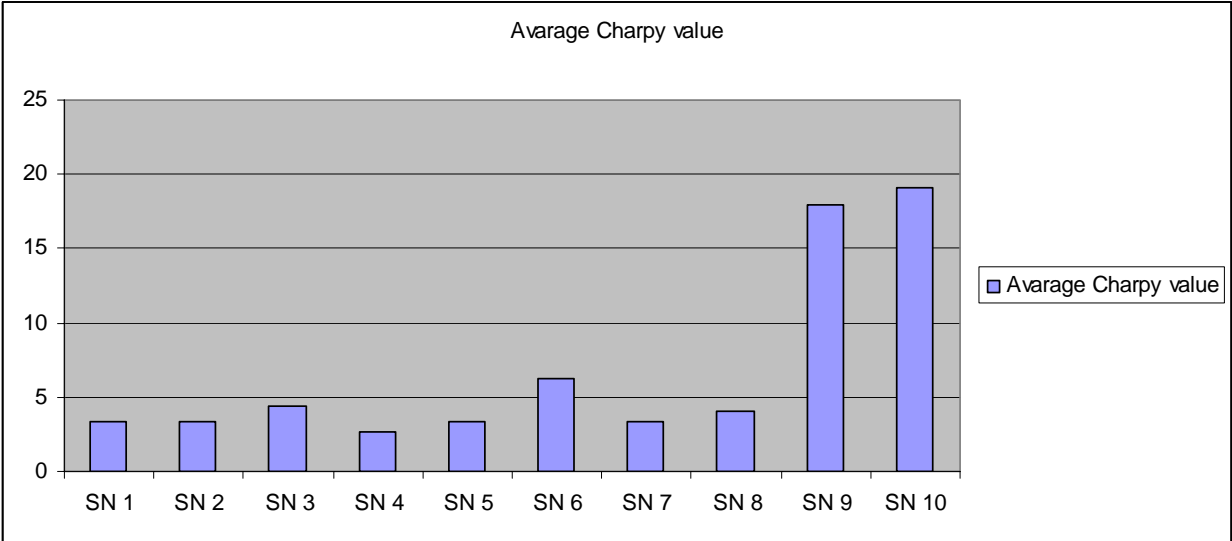
4.2.2 Sample SN1

Components	EPDM	SILICA	ZnO	Stearic acid	Oil	Sulphur	MBT	DPG	Wax
PPHR	55.2	27.6	2.8	1.4	8.2	1.4	1.4	0.6	1.4
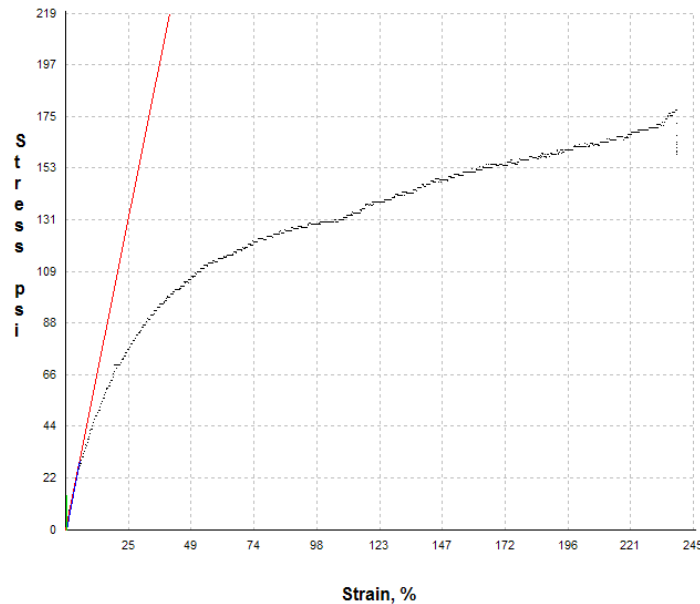
Figure 4.1   stress strain curve of SN1 sample

In this sample EPDM with best reinforcement agent silica particles of nanosized give the best strength because polymeric chains are of nanosized and maximum strain which shows maximum elongation with low stress. Its tensile strength with 177.9psi and its charpy 3.336J with impact energy of 281.0J to fracture. Its fracture is ductile.

K_{1c} =   16.00J

4.2.3 Sample SN 2

Components	EPDM	SILICA	ZnO	Stearic acid	Oil	Sulphur	MBT	DPG	Wax	MDH	Alumina
PPHR	39.5	19.7	2	1	6	1	1	0.4	1	14.2	14.2
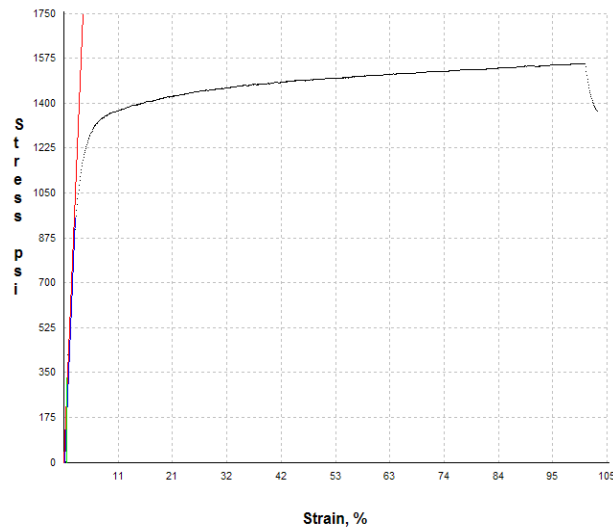
Figure 4.2   stress strain curve of SN2 sample

In this sample EPDM by adding Alumina As filler which increase its strength but decrease its strain because hardness is increased and elongation is decreased. Its tensile strength is increased.

These filler particles interact chemically with each other during diffusion and also MDH as curing agent to blend of filler particle, size of filler particle, filler particle increase its stiffness and strength. But overall mechnical properties suffer due to low strain. Its charpy 3.336J and 274.8J is impact energy. Fracture is ductile.

K_{1c} =   573.02 J

4.2.4 **Sample SN3**

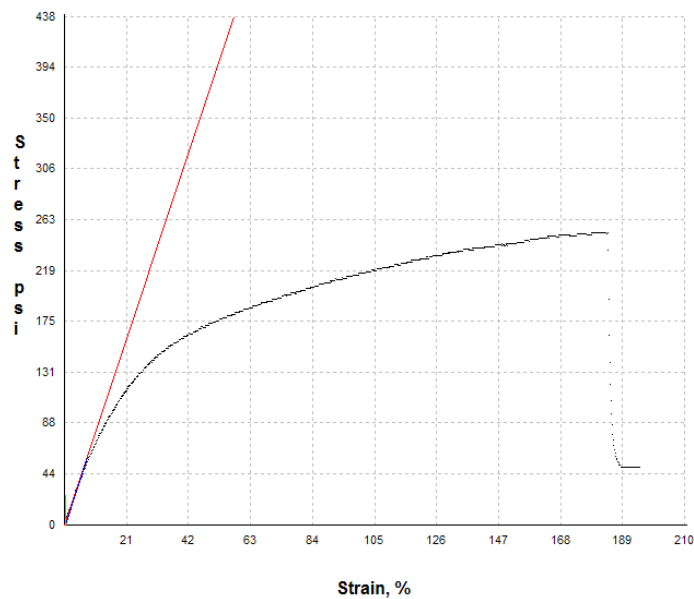| Components	EPDM	SILICA	ZnO	Stearic acid	Oil	Sulphur	MBT	DPG	Wax	ATH
PPHR	42.5	21.2	2.1	1.1	6.4	1.1	1.1	0.4	1.1	23

Figure 4.3   stress strain behaviour of SN3

Filler ATH doped in EPDM composite show elastic behavior and then deform plastically before fracture, its hardness is high , also give good strength with best mechanical properties. Its strain is very high. Its offset yield strength is 35.7psi , itscharpy is 4.408J and its impact energy is 298.5J with ductile fracture.

K_{1c} =   21.64 J

4.2.5 **Sample SN4**

Components	EPDM	SILICA	ZnO	Stearic acid	Oil	Sulphur	MBT	DPG	Wax	Chopped Kevlar Fiber
PPHR	53.5	26.8	2.7	1.3	8	1.4	1.4	0.5	1.3	3.1
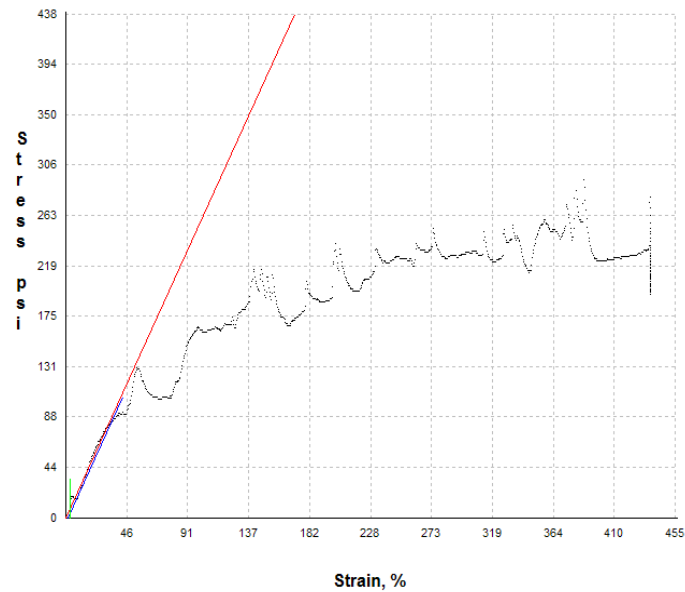
Figure 4.   stress strain behaviour of SN4

In this composite chopped Kevlar fiber is added in EPDM matrix which show very complex behavior. Chopped fiber is not completely diffuse in to matrix still remains in to the matrix like particle . that form increased hardness of composite and also improve its mechanical properties with very large elongation. Its strength is also very good but at low stress it give very large strain, this is not only with fiber but also strength of matrix is reason for it. Its charpy is 2.638J with 270.0J energy required to fracture the sample. Its fracture is ducitile.

K_{1c} = 43.50 J

4.2.6 **Sample SN5**

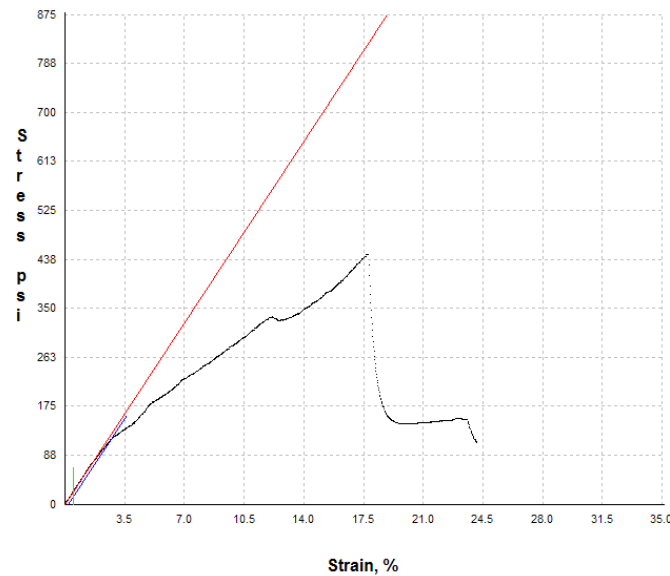| Components	EPDM	SILICA	ZnO	St.Acid	Oil	Sulphur	MBT	DPG	Wax	Con-Nomax Fiber
PPHR	53.6	26.8	2.7	1.3	8.1	1.3	1.4	0.5	1.3	3

Figure 4.5   stress strain behaviour of SN5

This composite is laminate of EPDM as matrix with single layer of weaved Nomax fiber. EPDM matrix contains nanosized silica particles which makes matrix very strengthen, and fiber has very good impact resistance.

Initially composite show very small with high stress value and also fiber and matrix deform elastically then with increase the stress matrix deform plastically but fiber behave elastic with increase   stress,and then fiber break into the matrix and show brittle behavior. As fiber break but matrix remains in break. Sudden decrease in stress take place and no more load is applied on it,sample stop to elongate due to internal fracture of fiber. Its charpy is 3.336J and impact energy is 264.6J with offset yield strength of 115.7psi

K_{1c}= 60.75 J

4.2.7 **Sample SN6**

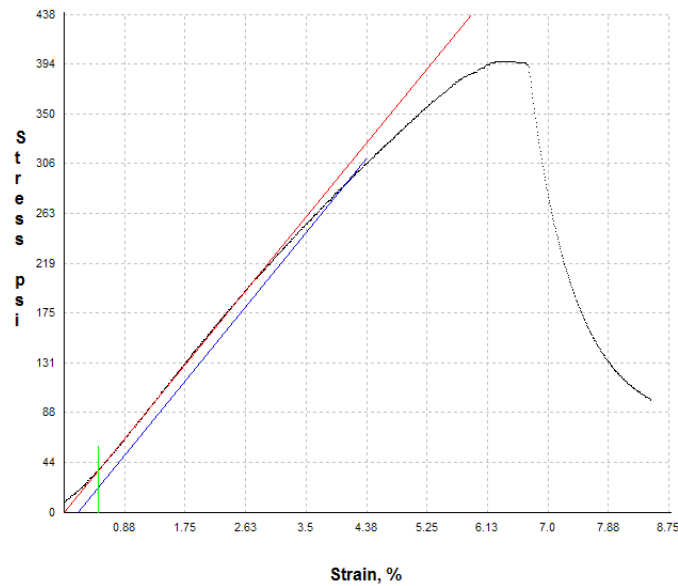| Components	EPDM	SILICA	ZnO	St.Acid	Oil	Sulphur	MBT	DPG	Wax	Con-Kevlar Fiber
PPHR	53.6	26.8	2.7	1.3	8.1	1.3	1.4	0.5	1.3	3

Figure 4.6   stress strain behaviour of SN6

This laminate is also EPDM based matrix with single layer weaved Kevlar fiber. Nanosized particle bassed matrix and fiber give high strength and low strain. Firstly Matrix composite behave elastically at high stress value up to 396psi. Then sudden break of fiber decrease its strength. Fiber increased its strength but decrease its strain. Its offset yield strength is 289psi. Its charpy is 8.84j and fracture energy is 272.6j.

K_{1c} = 175.22 J

4.2.8 Sample SN7

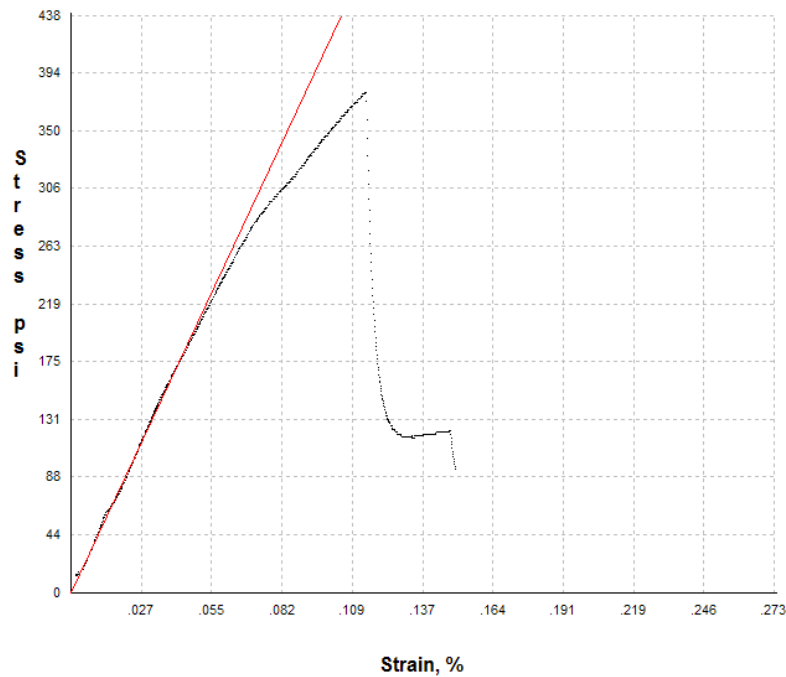| Components	EPDM	SILICA	ZnO	St.Acid	Oil	S	MBT	DPG	Wax	MDH	Al_2O_3	Con-Kevlar Fiber
PPHR	36.8	18.4	1.9	0.9	5.5	1	0.9	0.4	0.9	13.3	13.3	6.7

Figure 4.7   stress strain behaviour of SN7

This composite show very good strength with very low strain. This laminate contains alumina doped EPDM matrix with single layer Kevlar fiber. As stress is applied on the sample it show elastic behavior. High strength Kevlar fiber do not exhibit permanent deformation prior to fracture. So with increase stress fiber fracture within matrix and then sample would not be able to bear more load and sudden decrease take place, overall mechanical properties suffer. Its offset yield strength is ,its charpy is 4.766J, with absorbed energy of 65.8J.

K_{1c} =   20J

4.2.2   Sample SN8

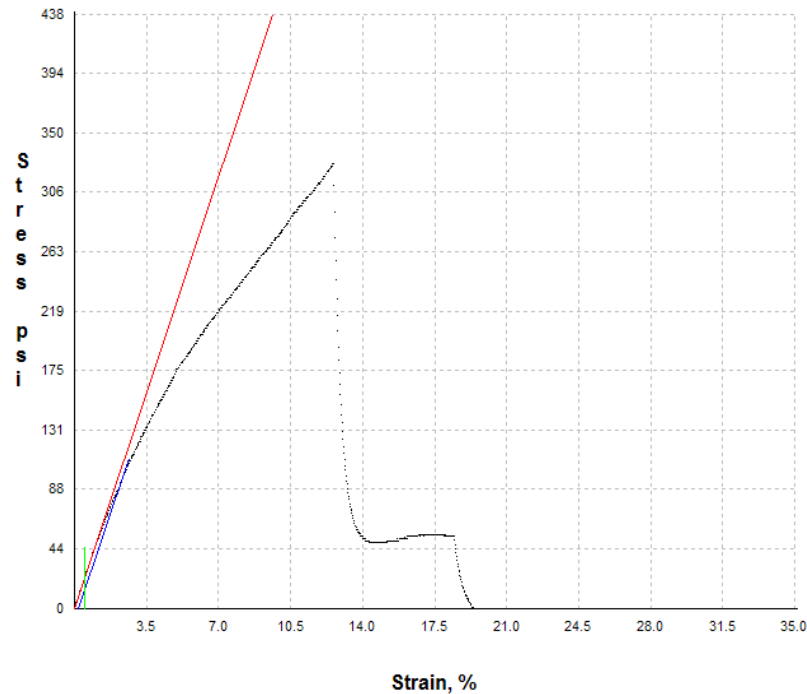| Compon ents	EPD M	SILICA	Zn O	St.Acid	Oil	Sulphur	MBT	DPG	Wax	ATH	Con- Kevlar Fiber
PPHR	39.4	19.7	2	1	6	1	1	0.4	1	21.4	7.1

Figure 4.8   stress strain behaviour of SN8

ATH filler doped EPDM matrix composite with single layer weaved Kevlar fiber. Typically fiber reinforced composite, the matrix begins to deform permanently at a strain at which fiber remains elastic. Both behave elastically at least up to and near the composite tensile strength.

Due to filler matrix strength increase but mechanical properties decreased and give low strain up to 25.2 with maximum stress 327psi. its charpy 3.336J and 274.6J, its absorb energy and fracture is ductile.

K_{1c}= 38.00 J

4.2.3   **Sample SN9**

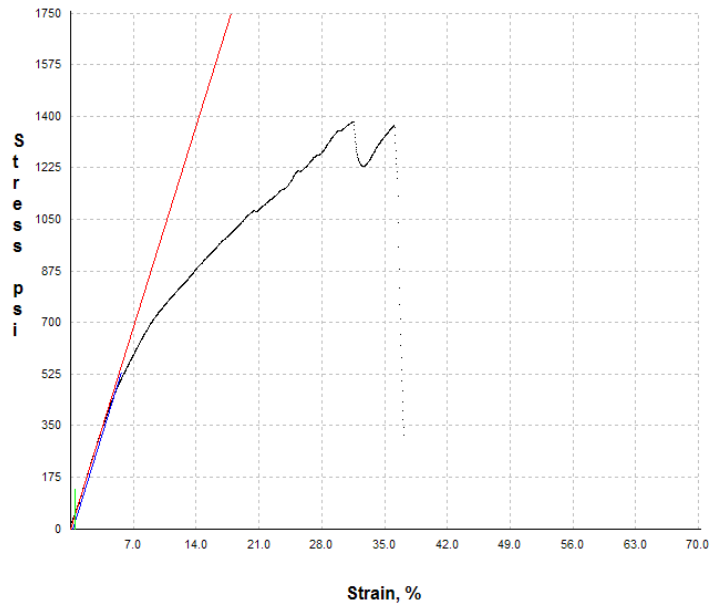| Components	EPDM	SILICA	ZnO	St.Acid	Oil	Sulphur	MBT	DPG	Wax	Coated SiC+ Con-Kevlar Fiber
PPHR	42.5	21.2	2.1	1.1	6.3	1.1	1.1	0.4	1.1	23.1

Figure 4.9   stress strain behaviour of SN9

        EPDM matrix with three layer of Kevlar fiber with ceramic coating. Matrix contain fine noanosized silica particle which give good reinforcement with EPDM and give high strength and good strain due to ceramics coating.

Also laminate of Kevlar fiber give very good strength with matrix deform elastically, but in second region matrix elastically , and slope of curve reduced plastically. As fiber failure occur matrix strength decrease. Its charpy 17.70J with 268.0J.

K_{1c} =233.66 J

4.2.11 **Sample SN10**

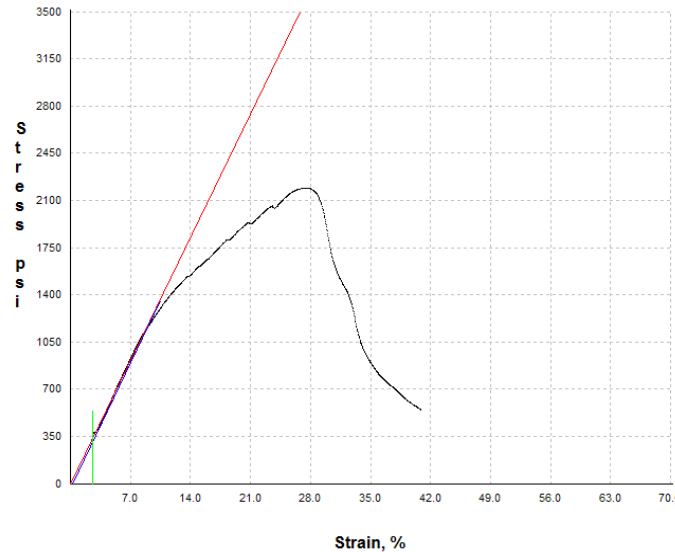| Compone nts	EPDM	SILICA	ZnO	St.Acid	Oil	Sulphur	MBT	DPG	Wax	C-SiC+ Con- Kevlar Fiber
PPHR	39.4	19.5	2	1	6	1	1	0.4	1	28.6

Figure 4.10   stress strain behaviour of SN10

This composite contains EPDM nanosized based silica particle matrix in which four layer laminate of weaved Kevlar with ceramic coating. With increase number of layers of Kevlar fiber with ceramic coating increase strength up to 2190psi with strain 59.6 .

According to the graph region I show elastic behavior as stress applied more fiber fail at its weakest point. Thereafter is in capable of contributing to strength. But broken fiber contribute to composite stress carry capability all along its length expect that point or vicinity of break. This is accordingly to bundle theory and caused for increases strength with good mechanical properties. Its charpy 19.05J with impact energy 269.5J.

$K_{1c} = $ 714.25 J

CHAPTER # 5
Conclusion & Future Work

Conclusion:

It is clear according to discussion that no distinctive appearance to fracture expect for a considerable reduction in cross sectional area and some tearing of the notch. Very ductile polymer may simply bend with some tearing at te notch but no complete fracture will occurs.

- SN 1 shows maximum strain at low stress because of the presence of Silica particle which of nanosized which enhanced the polymeric strength
- SN 2 contains filler which increase its strength but decrease its elongation because of increase in hardness in sample
- SN 3 gives best mechanical properties and show elastic behavior.
- SN 4 has chopped Kevlar fiber which increase its hardness but decrease its strength because its is not completely diffuse in polymer.
- SN 5 and SN 6 gives high strength and low strain ,both matrix and fiber behave elastically in elastic region but in plastic region fiber behave elastic and cause of decrease its strength.
- SN 7 and SN 8 shows high strength with low strain because of Alumina filler of nanosized. But with increase stress fiber fracture and hardness of sample shows that overall mechanical properties will suffer.
- SN 9 sample with three layers of(Kevlar fiber with ceramic coating) and Silica particle of nanosized give good reinforcement with EPDM and increased its strength its Charpy is 17.70 J with absorbance energy is 268.0 J.

- SN 10 sample with Four layers of (Kevlar fiber with ceramic coating) with same EPDM matrix of sample number SN 9 gives charpy is 19.05 J and absorbed energy is 269.50 J.

- Sample SN 9 AND SN 10 shows that coated silicon carbide continuous Kevlar fiber and the matrix such that EPDM is very strong. The binder that was used at the interface of Kevlar and EPDM is rubber solution that homogenized coated silicon carbide continuous Kevlar fiber with the matrix ,it also promoted the adhesion among the fiber and matrix. By doing so the hardness increased as compare to the other samples that is why its stress is very high but its strain is not very good.

- Charpy value of these two samples were observed higher due to the fact that silica reinforced EPDM is a good absorber of impact energy and also Kevlar fiber is very high energy strength material that have high tensile strength and impact strength. So reinforcement of Kevlar fiber in EPDM enhances energy absorption and also tensile strength.

Future Work:

We have successfully synthesized an armor composite that gives best performance both according to impact testing and tensile testing with the maximum strength is 2190 J .

But we are trying to synthesize such an composite armor that gives much better performance for both impact and tensile. In future ,we will synthesized more armor composite and also investigate the following properties of our armor composite specimens i.e.,

- ➢ Thermal conductivity

- ➢ Thermal diffusivity

- ➢ Specific heat

- ➢ DMTA

- ➢ SEM of all sample

- ➢ Comparison of properties between continuous and laminate structures of armor composite.

REFERENCES
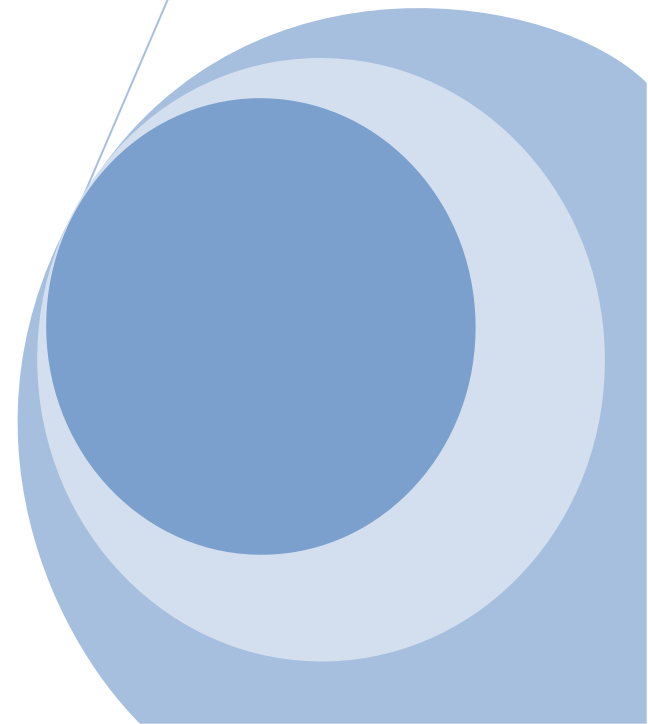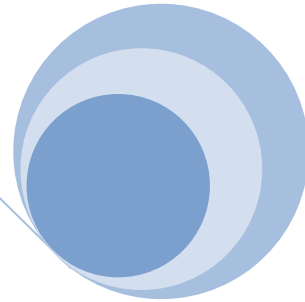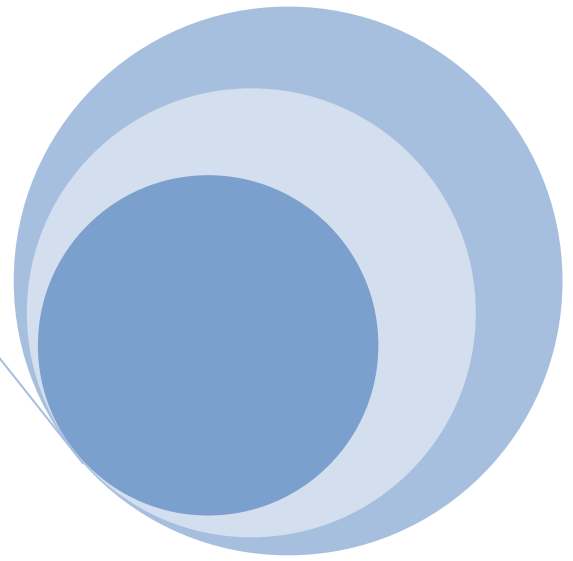
References:

1. Composite materials Hand Book (M .M.schwartz,ed). McGraw-Hill, New York , 1992, p. 2.112.

2. J . R. Stalder, in "Materials science and technology for Advanced Application", Prentice-Hall, Englewood Cliffs, N.J. 1962.

3. Baleman, L. (1963), The chemistry and physics of Rubber like subsatbnces.

4. Ferry , J.D (1980), viscoelastic properties of polymers, John Wiley and sons, New York , 3rd edition.

5. D.l. Schmidt , in "engineering Design for plastic" , Reinhold , New York; 1964.

6. Mallick , P.K and S.Newman 1990, "Composite Materials Technology ,Processing and Properties, 25-65.Hanser, munich.

7. Ward, I.M. (1971), mechanical properties of solid polymers, wiley interscience,London.

8. M.Arshad Bashir and M.B Khan .Synthesis and Mechanical Properties evaluation of ablative material.8th IBCAST, NCP, Islamabd, Pakistan. Jan 09

9. D.H Morton –Jones. Polymer Processing. Polymer Research Group, Chemistry Department, University of Lancaster (1989).

10. C.M. Bhuvaneswan .Ethalene- Propylene diene rubber as a futuristic elastomer for insulation of solid rocket moters. Defense Science Journal Vol.56, NO.3 July 2006,pp 309-302.

11. Composite .Elsevier, Composite Science and Technology 61 (2001) p, 260- 290.

12. Allen ,G and J.C.Bevington (1989), comprehensive polymer Science, Pergamon press, oxford vols 107.

13. Muraleekrishnan, R; Raghvan, A.J ; Rao, S.S & Nian, K.N. in HEMCE.. Development of EPDM rubber based low density insulator for solid propellant rocket motors. In proceedings of the 3rd international conference, 6-8 December 2000, Thiruvananthapuram. pp 245-289.

14. John W.Weeton, Dean M ,Peters, Karyn L. Thomas, Engineer's Guide to Composite Materials, ASM, World Publishing Corporation 1987.

15. Muraleekrishnan, R; Raghvan, A.J ; Rao, S.S & Nian, K.N. in MACRO. In Ethylene-propylene diene monomer (EPDM) –neoprene rubber blends: Evaluation as rocket motor insulation material. In processing of the international seminar ,9-11 december 2002, Kharagpur.

16. Krishna K. Chawla , Composite materials Science and Engineering .springer- Veralg, world publishing corporation 1987.

17. Stephen P.Timoshenko and D.H.Young, "Elements of Strength of materials" 5th edition, D . Van Nostrand Company, INC. Maruzen Company LTD,pp 204 – 324.

18. Broutman , L.J., and R.G. Krock (eds): Modern Composite Materials, addition. Wesley,reading, mass ,1967.

19. Piggott, M.R: Load Bearing fiber Commposite, Pergamon press, oxford, England 1980.

20. Rosen , B. W. : " Mechanics of Composite Strengthening" inn Fiber Composite Materials., American Socity for metals , Metals park ,Ohio, 1965,p.37.

21. McClintock ,Frank A., and Ali S .Argon (eds) : Mechanical Behavior of Materials, Addison Wesley, reading mass 1966.

22. Hertzberg, R.W : Deformation and fracture mechanics of Engineering Materials, Wiley, New York,1976.

23. Backofen , walter A,: Deformation processing , Addison –Wesley ,reading ,mass 1972.

24. Ralls , K.M ., T.H.Courtney and J.wulff: An Introduction of Materials Scirnce and Engineering, wiley, New York, 1976.

25. Thomas H.Courtney, "Mechanical Behavior of Materials" ,McGraw-Hill International Editions of Material Science Series.

26. S. Chocron Benloulo, J. Rodriguez and V. Shchez Galvez A Simple Analytical Model for Ballistic Impact in Composites *J. pHs IV* FRANCE 7 (1 997), Colloque C3, Supplement au Journal de Physique I11 d'aoiit 1997, *Ciencia de Materiales, ETSZ Caminos Canales y Puertos, Universidad Polittcnica de Madrid,28040 Madrid, Spain.*

27.	Departmeent Of Defense Handbook, Composite Material Handbook,Volune 2. Polymer Matrix Composite Material Properties.

28. **A** comparison of the shear strength of structural composite lumber using

29. torsion and shear block tests, Rakesh Gupta＊Tobias S. Siller.

30. Eduardo Batista FRANCO1, Patrícia Aleixo dos SANTOS2, Rafael Francisco Lia MONDELLI3, The Effect Of Different Light-Curing Units On Tensile Strength An Microhardness Of A Composite Resin, J Appl Oral Sci. *2007;15(6):470-4*

31. Álvaro Della Bona,Paula Benetti,,Márcia Borba,,Dileta Cecchetti, Flexural and diametral tensile strength of composite resins, Braz Oral Res 2008;22(1):84-9